Summer 7-16-2021

Effective Computational Cosmology

Eva Nesbit
Syracuse University

ABSTRACT

Effective Field Theories (EFTs) provide a unique framework in which to attempt to answer outstanding questions in cosmology (and all field of physics, for that matter). This work investigates how the use of both EFTs and computational tools can help us to advance our knowledge of how the universe evolved and formed over time. Specifically, we review the successful EFT of Inflation, the EFT of Dark Energy (EFTDE), and introduce the EFT of Reheating as a generalized model of particle formation after inflation. In this way, we show how effective EFTs are at quantifying physical phenomenology at many different energy scales. Additionally, we review some useful codes and numerical algorithms and apply them to the question of post-inflationary resonance and late-time cosmic acceleration. In the case of the latter, we use real data to constrain EFTDE theory, offering a map – the first of its kind – from EFT parameters to standard cosmological parameters.

EFFECTIVE COMPUTATIONAL COSMOLOGY

by

Eva Nesbit

B.A., Kenyon College, 2016

Dissertation

Submitted in partial fulfillment of the requirements for the degree of

Doctor of Philosophy in Physics

Syracuse University

July 2021

ACKNOWLEDGMENTS

First and foremost, I thank my graduate advisor, *Scott Watson*. Scott believed in me since we first started working together when I was an undergrad at Kenyon, and he has been my champion ever since. Not only did he teach me everything I know about Effective Field Theories, but he has also met me with a level of humanity and kindness that is somewhat rare in our field, and in the world in general. The care he takes in fostering a positive lab environment and his ever-present faith in me helped to mold me into the well-rounded physicist I am today.

I would also like to thank my undergraduate advisor, *Tom Giblin*, who recognized and fostered my nascent interest in cosmology. With Tom's help and unrelenting encouragement, I learned the basics of cosmology and numerical integration, and also what it means to be a research scientist. The skills I learned in his lab and the experiences he gave me propelled me to pursue graduate school and physics as a career. After graduating from Kenyon, Tom continued to be a sounding board for physics questions as well as life advice in general. I am thankful for his presence in my life as a mentor and also as a friend. Not to mention, he gave the world *Maribel*, for which we are all indebted!

Additionally, I thank the members of my physics cohort – from my time at both Syracuse and Kenyon – through which I have made life-long friends. The collaborative nature of our field and of reseach in general is something I continue to cherish. Specifically, I thank *Gizem Şengör* and *Ogan Özsoy* for their patience and assistance as I got my footing in grad school and in this field. I thank *Kenny Ratliff* for single-handedly helping me through QFT I and II and for being the best roommate and math enthusiast a girl could ask for. I thank *Brandon Melcher* for his presence and humor in our office, his thoughtful physics discussions, and his continued support of me with his willingness to answer any question I may have for him even after he graduated! I thank *Gabriele Rigo* for being an awesome office-mate, friend, and my go-to for discussing all things Italian food and culture. I thank

Lindsay DeMarchi, *Pinaki Yallappa Dombara*, *Ali Imran*, *Nick Didio*, *Elizabeth Lawson-Keister*, *Ohana Benevides Rodrigues*, *Kyungeun Kim*, and many more from my Syracuse cohort for the friendship and fun they brought to graduate school. Additionally, I am thankful to the friends I made in the physics department at Kenyon for their continued support, all these years later: *Avery Tishue*, *Zach Weiner*, *Aidan Lee*, *Furqan Dar*, and *Alan Li*. Learning and studying with you all comprise some of the happiest times I had doing physics over the past nine years.

I also express my deepest gratitude to the collaborators I worked with on the projects in this thesis. Those I have not already mentioned include *Yue Zhao*, *Gordon Kane*, *Dragan Huterer* and *Yuewei Wen*. I thoroughly enjoyed learning from and with you all. Most recently, the time I have spent working with Yuewei on the Effective Field Theory of Dark Energy project has been so, so rewarding. I found our discussions to be both fun and illuminating. I treasure both the professional relationship and the friendship we have built over the past couple of years through working – and sometimes struggling – together on this project. Dragan has, of course, been a guiding light in this work and taught me basically everything I know about observational surveys and the constraints they put on theory. My work with collaborators outside of my local departments has deeply changed me as a physicist and as a person, always for the better.

I also have many people to thank outside of the physics community. These people helped keep me sane during some very stressful times (which, as it turns out, was most of grad school). It truly took a village to propel me through some of the toughest academic years of my life. I thank my good friends *Katie Page* and *Alison Zarider* for taking all my phone calls, making me laugh, and always building me up when I felt down. I couldn't have done it without your unbridled support and love. I thank my boyfriend, *Vince Wells*, for always being a safe space to come home to. I have felt so lucky to have him as my most trusted companion, especially over the past year.

Finally, I would be remiss not to mention my most tried and true supporters – my family. To my mom, *Shannon*, my dad, *Mark*, and my sister, *Olivia*: I love you guys so much and it is practically impossible to put my gratitude and love for you into words, much less a single paragraph. My parents prioritized my education all throughout my life and nurtured my curiosity from a young age. For this, I am forever grateful. Additionally, growing up with a sister provided me with a best friend from the start. As we grow older, her support and wisdom have been invaluable. This dissertation is the culmination of five years of hard work, and I thank each and every person that helped me along the way and made it all possible.

TABLE OF CONTENTS

LIST OF FIGURES

ABBREVIATIONS

GR	**G**eneral **R**elativity
EFE	**E**instein **F**ield **E**quations
EFT	**E**ffective **F**ield **T**heory
CMB	**C**osmic **M**icrowave **B**ackground
GUT	**G**rand **U**nification **T**heory
QFT	**Q**uantum **F**ield **T**heory
EFTDE	**E**ffective **F**ield **T**heory of **D**ark **E**nergy
DE	**D**ark **E**nergy
MG	**M**odified **G**ravity
RK-2	Second Order **R**unge-**K**utta
LH	**L**atin **h**ypercube

SYMBOLS

$g_{\mu\nu}$	space-time metric
$G_{\mu\nu}$	Einstein tensor
$m_{\rm pl}$	reduced planck mass
ds^2	line element
a	scale factor
H_0	Hubble constant
H	Hubble parameter
c	speed of light
ρ	energy density
p	pressure
q	deceleration parameter
Ω_i	fractional energy density of species i
M	energy scale cut-off of an EFT (also denoted Λ)
w	equation of state parameter
N	number of e-folds during inflation (also denoted N_*)
d	space-time dimension
S	the action
$\mathcal{L}$	the Lagrangian
g_i	coupling constants in a generic EFT
$\mathcal{O}_i$	operators in a generic EFT
φ	inflaton field (also denoted ϕ)
k	wave number
R	Ricci scalar
$R_{\mu\nu}$	Ricci tensor
$R_{\mu\nu\rho\sigma}$	Reimann-Christoffel tensor

$C_{\mu\nu\rho\sigma}$	Weyl tensor
χ	generic reheat field
m_i	mass of field i
ω_k	frequency of field oscillation
π	goldstone boson
$V(\phi)$	potential energy function
L	size of one side of box in `GABE`
σ	modulus field (also standard deviation, depending on context)
A_i	gauge field
$Y_{\ell m}$	spherical harmonics
$\hat{C}_\ell$	angular power spectrum
$a_{\ell m}$	expansion coefficients
Cov_ℓ	coviariance matrix
f_{sky}	fraction of the sky surveyed
χ^2	chi-squared value
$\Omega_b h^2$	baryon density
$\Omega_c h^2$	dark matter density
A_s	perturbation amplitude
n_s	scalar spectral index
τ	reionization optical depth
L	likelihood

To my parents,

for instilling in me a love of learning

and for everything else.

CHAPTER 1

INTRODUCTION

Human beings have long sought to understand our place in the cosmos. From the early astronomers of Babylon to Galileo, Einstein, and present-day collaborations like LIGO and the LHC, we have grappled with the origins of the universe and our place in it. For a rather recent and significant part of history, however, humans were unaware of the dynamic nature of the universe. It was not until the work of Edwin Hubble in 1929 that we learned that our universe is not static, but rather, is dynamic and evolving. From there, we discovered that even the expansion of the universe is not decelerating – it is speeding up. Thus, both the size and rate of growth are quantities that have varied over the history of the universe. The most dramatic period of growth took place at about 10^{-36} seconds after its birth. In a small fraction of a second, space expanded by a factor of e^{60}. We refer to this exceptional period of exponential expansion as inflation, and the particle that facilitated it, the inflaton. Some time after inflation ends, matter particles begin to form, followed by small and large scale structures, and the universe that we observe begins to take shape.

The universe we observe is well-described by the ΛCDM model which states the universe is composed of 3 primary ingredients: baryonic matter, dark matter, and dark energy. Baryonic matter is the standard stuff we see all around us – the stuff we are made of. Dark matter and dark energy are something else completely – something unknown – and make up the majority of the stuff in our universe. In fact, baryonic matter makes up just 5% of our universe.

In the late 1970s, astronomer Vera Rubin observed the kinematics of the rotating galaxy Andrometa and noticed that the matter at the edges of the galaxy had the same velocity as the matter at the center. This behavior apparently violated Newton's Laws of motion, which predicted matter at the outer edges to rotate slower. There must be some other form of matter holding the galaxy together. This was the first observational evidence of dark

matter, a mysterious substance we now know to make up close to 25% of our observable universe. As it turns out, without the presence of dark matter, galaxy formation in our universe would have taken much longer, and a universe such as we see it today would have been impossible. The evidence for dark matter is compelling, though detecting it directly is rather elusive. Dark matter is hard to see: it does not absorb, emit, or reflect light and, as far as we can tell, only interacts standard model particles via gravity.

The second elusive substance, and one that makes up the remaining 70% of our universe, is dark energy. It's presence was originally postulated by Einstein with the addition of the cosmological constant to his theory of General Relativity. The presence of dark energy was confirmed through observation in 1998 using measurements of Type 1A supernovae. Supernova act as "standard candles" in the universe and offer a way to measure the expansion rate. This work in high-red shift supernovae searches was so significant it won the Nobel Prize in Physics in 2011. The existence of dark energy has been further confirmed by other observational endeavors, though the fundamental theory behind it remains an open question.

In this thesis, we explore mechanisms driving the evolution of the universe ranging from first particle formation and (p)reheating, to late-time structure formation and theories of dark energy and modified gravity. Studying the dynamics of the early universe is experimentally tough (to say the least). Technological advances over the last couple of decades have made it possible for scientists to experimentally study the nature of fundamental particles at colliders like the LHC in Switzerland. These particle colliders, however, are only able to probe at energies up to about 6TeV. The energy scale at the beginning of the universe was upwards of 10^{12}TeV. Even if collider technology continues to improve, we will never be able to recreate conditions like those at the birth of the universe. We must, therefore, pursue another method of investigation into our cosmic origins.

This thesis uses computational methods to accomplish said investigations. These numerical simulations allow us to study physics at energy scales far beyond the reach of any particle

collider, presently or in the future. Additionally, many cosmological models are highly non-linear and non-analytic, deepening our need for numerical tools to investigate some of these models. Models of primary focus in this work include those described by an Effective Field Theory (EFT) – a mathematical construct that allows us to study phenomenological physics at energy scales higher than those described by the Standard Model. This allows us to parameterize what we do not know while giving us access to a more fundamental understanding of the underlying physics. In this work, we use computational tools to investigate the highly non-linear models that arise from the use of the EFT framework to describe both reheating and first particle formation as well as theories of dark energy and modified gravity. Although separated by a large period of time, both models of interest – the EFT of Reheating and the EFT of Dark Energy – lend themselves to computational exploration, the primary focus of this thesis.

In Chapter 2, we begin by familiarizing ourselves with the fundamentals of modern cosmology. We summarize the standard cosmological model, called ΛCDM, and introduce places where this model fails to accurately describe the universe we live in. We then briefly propose solutions to the aforementioned problems plaguing ΛCDM cosmology.

In Chapter 3, we introduce Effective Field Theories, a mathematical framework originally used in particle physics and the isolation of the weak force. We discuss their utility in cosmology. Specifically, their ability to describe the inflationary epoch, (p)Reheating and particle formation, and late-time acceleration (DE/MG).

In Chapter 4, we use `GABE` to investigate the question of if the universe was actually radiation dominated prior to Nucleosynthesis. String theory approaches to both beyond the Standard Model and Inflationary model building generically predict the existence of scalars (moduli) that are light compared to the scale of quantum gravity. These moduli become displaced from their low energy minima in the early universe and lead to a prolonged matter-dominated epoch prior to BBN. In this chapter, we examine whether non-perturbative

effects such as parametric resonance or tachyonic instabilities can shorten, or even eliminate, the moduli condensate and matter-dominated epoch. Such effects depend crucially on the strength of the couplings, and we find that unless the moduli become strongly coupled the matter-dominated epoch is unavoidable. In particular, we find that in string and M-theory compactifications where the lightest moduli are near the TeV-scale that a matter-dominated epoch will persist until the time of Big Bang Nucleosynthesis.

In the appendix of Chapter 4, we review the computational tools used in this work – namely, `GABE`. The "Grid and Bubble Evolver" evolves scalar fields over an expanding background, thus modeling the evolution of the universe. The inflaton – the particle driving the period of exponential expansion at the very beginning of the universe, inflation – can be modeled as a simple scalar field, making `GABE` a prime candidate for the study of inflationary cosmology and (p)reheating.

In Chapter 5, we tackle the question of how to constrain EFTDE models with observational data. The EFT framework allows us to elegantly describe large classes of models of cosmic acceleration. However, prior to this thesis work, there was no good way to systematically rule these models in or out. We present a computational pipeline to do just this. We introduce codes like `EFTCAMB` and `EFTCosmoMC` which offer insight into the physics at times closer to recombination – when the universe first became transparent to light and the CMB formed. Additionally, we introduce a numerical tool called an emulator that can be used to speed up computation time. We focus our study on Horndeski models, as these are perhaps the most preferred models under the EFTDE umbrella. We find that models of Horndeski can produce unique, distinguishable features possibly detectable in the future observational surveys. We specifically study how these modes would look in the $w_0 - w_a$ plane where w_0 and w_a are the coefficients in the CPL parameterization of the equation of state parameter of the universe, w.

CHAPTER 2

CONCORDANCE COSMOLOGY

Our best working understanding of the universe is thanks, in most part, to Albert Einstein and his 1917 publication of *Cosmological Considerations of the General Theory of Relativity* [1]. In it, he equates the "stuff" in the universe with the curvature of space-time - the four-dimensional manifold in which our universe lives. This idea is encapsulated in Einstein's Field Equations,

$$G_{\mu\nu} = \frac{T_{\mu\nu}}{m_{\rm pl}^2} + \Lambda g_{\mu\nu}. \tag{2.1}$$

The Einstein tensor, $G_{\mu\nu}$, is a function of the metric and accounts for how space-time is curved. $T_{\mu\nu}$ is the stress-energy tensor and accounts for the aforementioned "stuff" in the universe – namely, the energy density, ρ, and pressure, p. The cosmological constant, Λ, is the so-called "vaccuum energy" of space that is responsible for the observed accelerated expansion of the universe. This last term has a rather storied history and a controversial present that will be discussed further in Section 2.1.4.

The solutions to Einstein's field equations comprise the components of the metric, and therefore, factors of the line element, ds^2. The line element (also referred to as the space-time interval) tells us the distance between two events in space-time. The simplest solution to the EFE is known as the Minkoski metric, and it describes a flat, static universe [2]. Unfortunately, a flat, static universe is the solution to Einstein's field equations for just one trivial case — only an empty universe.

In 1922, Alexander Friedman, Georges Lemaître, Howard P. Robertson and Arthur Geoffrey Walker worked to simultaneously show that a universe with *stuff* in it must *necessarily* be expanding [3; 4; 5; 6]. This revelation that our universe could not be static, in combination with the cosmological principle that says the universe is homogeneous and isotropic, implies that all of space is expanding at the same rate. Therefore, Friedman, Lemaître, Robertson,

and Walker were able to parameterize the expansion of the universe by one number dependent on only time, called the scale factor, $a(t)$. This solution to the EFE is called the FLRW metric,

$$ds^2 = -c^2dt^2 + a(t)^2\left[\frac{dr^2}{1-kr^2} + r^2(d\theta^2 + \sin^2\theta\, d\phi^2)\right], \tag{2.2}$$

and is the most general metric that is invariant under spatial translations and rotations. The constant k encodes information about the geometry of the universe and can take values 0 (Euclidean geometry), 1 (closed geometry), or -1 (open geometry). It is customary to take $c = 1$. Under this metric and the continued assumption that our universe is homogeneous and isotropic, the EFE reduce to a set of differential equations describing the evolution of the scale factor,

$$\left(\frac{\dot{a}}{a}\right)^2 = \frac{\rho}{3m_{\text{pl}}^2} + \frac{\Lambda}{3} - \frac{k}{a^2} \tag{2.3}$$

$$\frac{\ddot{a}}{a} = -\frac{1}{6m_{\text{pl}}^2}(\rho + 3p) + \frac{\Lambda}{3}. \tag{2.4}$$

This revolutionary idea of an expanding universe was observationally confirmed just a few years later by Edwin Hubble [7]. By taking precise measurements of the speed of various galaxies relative to Earth, Hubble determined that most of them were red shifted. This lead him to deduce that the universe is expanding. A plot of Hubble's original data is seen in Figure 2.1. Additionally, Hubble realized a correlation between galaxy distance and associated red shift: galaxies farther away from us were moving away at a faster rate. This came to be known, aptly, as Hubble's law,

$$v = H_0 r \tag{2.5}$$

where H_0, Hubble's constant,

$$H_0 = \left.\frac{\dot{a}}{a}\right|_{\text{t=today}} \tag{2.6}$$

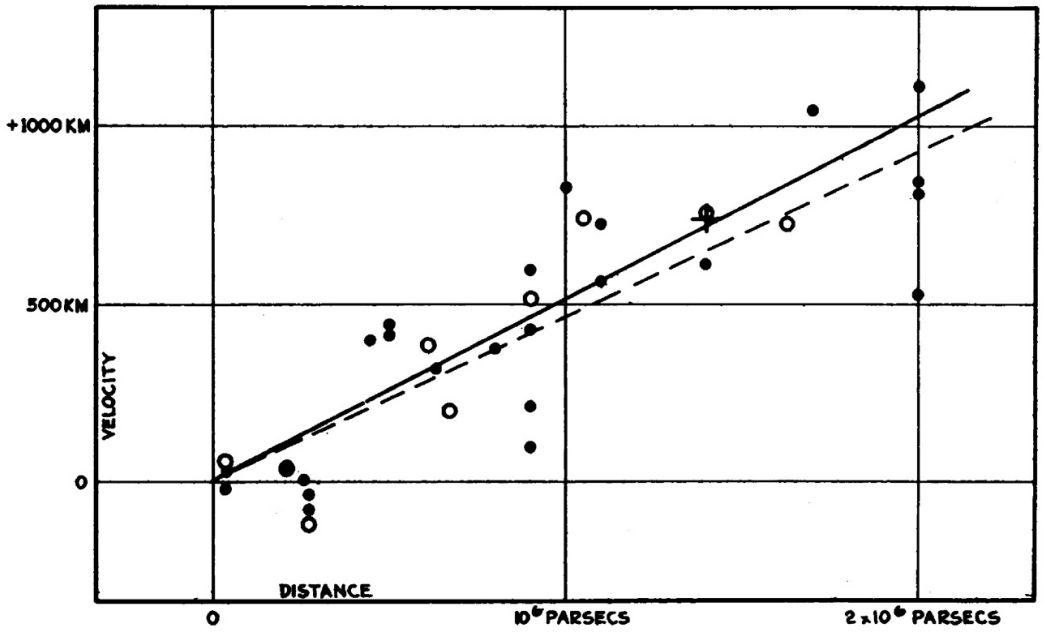

Figure 2.1: Hubble's original data, displaying a linear relation (at small redshifts) between a galaxy's receding velocity and distance from the observer. This experimentally confirmed an expanding universe for the first time.

is the present-day rate of expansion of the universe.

2.1 Problems with Concordance Cosmology

2.1.1 Horizon

The cosmic microwave background (CMB) offers insight into what the universe looked like at the time of recombination, when the universe first became transparent to light. Precise measurements of the CMB tell us that the universe is exactly 2.73K to one part in 10^5 [11; 12]. This observationally confirms half of the cosmological principle – the universe is indubitably homogeneous. Homogeneity on CMB scales requires a causal connection between all parts of the observable universe. The horizon problem addresses standard cosmology's inability to predict this causal connection.

For simplicity, consider just time and one spatial dimension. Causal connection requires

a null space-time interval. Thus, the line element in Equation 2.2 becomes,

$$ds^2 = 0 = -dt^2 + a(t)dx^2, \tag{2.7}$$

and we have $dx = dta(t)^{-1}$. We can integrate this equation over a designated period of time, t_1 to t_2, to find the maximum distance between two causally connected points. We are interested in the value of this integral for two scenarios: $t_1 = 0$ to $t_2 = t_{rec}$, the forward-propagating light cone, and $t_1 = t_{rec}$ to $t_2 = t_0$, the backward-propagating light cone. Here, t_0 is present day.

In order to calculate this interval, we need to know more about the evolution of the scale factor over the history of the universe. The early universe can be approximated as a perfect fluid and thus takes on the equation of state,

$$p = w\rho \tag{2.8}$$

where w is called the equation of state parameter and depends on the content of the universe. Each dominating substance takes a different equation of state parameter: $w = 1/3$, $w = 0$, and $w = -1$ for radiation, matter, and dark energy respectively. It can then be shown that, in this perfect fluid approximation, the evolution of the scale factor depends only on the equation of state parameter,

$$a(t) = \left(\frac{t}{t_0}\right)^{\frac{2}{3(1+w)}}. \tag{2.9}$$

We know the universe was matter dominated (and had been for a while) at the time of recombination. With $w = 0$, the integrals in question become

$$\int_0^{t_{rec}} a(t)^{-1}dt = 3t_0^{2/3}t_{rec}^{1/3} \tag{2.10}$$

$$\int_{t_{rec}}^{t_0} a(t)^{-1}dt = 3t_0\left[1 - \left(\frac{t_{rec}}{t_0}^{1/3}\right)\right]. \tag{2.11}$$

Taking $t_0 \gg t_{rec}$ we can see that the light cone calculated from t_{rec} to present day, t_0, is much larger than the same calculated from 0 to t_{rec}. In this way, we observe areas of causal connection that standard cosmology cannot not predict or explain. A visual representation of this mis-match is shown in Figure 2.2. Our universe is distinctly homogeneous yet our theory does not predict or explain this.

2.1.2 Flatness

Observationally, the universe appears to be completely spatially flat [8]. Our concordance model offers no explanation for why this might be. Considering a spatially flat universe, $k = 0$, and one without a cosmological constant, the critical density of such a universe is

$$\rho_c = 3m_{\text{pl}}^2 H^2. \tag{2.12}$$

Defining the dimensionless density parameter, $\Omega = \rho/\rho_c$, and dividing both sides of the first Friedman equation, equation 2.3, by H^2, we obtain

$$1 - \Omega(t) = -\frac{k}{a^2 H^2}. \tag{2.13}$$

We can use this equation to determine how much the dimensionless density parameter differs from 1. Since we observe $k = 0$, $\Omega(t)$ must be equal to 1 within one part in 10^{-60} at the Planck time, $10^{-44}s$. However, quantum mechanical perturbations are unavoidable and require variations much larger than 10^{-60}. Our inability to reconcile theory with observation here is known as the flatness problem.

2.1.3 Magnetic Monopoles

At some point towards the very beginning of the universe, the Grand Unification Theory tells us that the universe was upwards of 10^{27}K. This corresponds to energies around 10^{12}TeV.

This is referred to as the Grand Unification Energy, or the GUT scale. Above the GUT scale, three of the four fundamental forces (the electromagnetic, the strong, and the weak forces) acted as one single electronuclear force. This is the result of a larger gauge symmetry. The fourth fundamental force, gravity, decoupled at the Planck scale, prior to the Grand Unification epoch.

As the universe cooled and fell below the GUT scale, it underwent a phase transition in which the larger gauge symmetries broke and the strong force decoupled from the electroweak force. From QFT, we expect this phase transition to produce point-like topological defects in our fields, corresponding to the production of magnetic monopoles. We expect a *lot* of them. Despite our best efforts, however, we have yet to detect a single magnetic monopole. This paradox is known as the Magnetic Monopole Problem.

2.1.4 Cosmological Constant

Assuming conservation of the energy-momentum tensor, $\nabla_\mu T^{\mu\nu} = 0$, equations 2.3 and 2.4 can be written,

$$\Omega_m + \Omega_\Lambda + \Omega_k = 1 \tag{2.14}$$

$$q(1 - \Omega_m) = -\left(\Omega_\Lambda + \frac{\dot{\Omega}_m}{2H}\right) \tag{2.15}$$

where q is famously the deceleration parameter, $q = -\ddot{a}/aH^2$. Additionally, we have defined the fractional energy densities of matter, $\Omega_m = \rho/3m_{\rm pl}^2H^2$, the cosmological constant, $\Omega_\Lambda = \Lambda/2H^2$, and spatial curvature, $k/3a^2H^2$. Modern observational cosmologists have had a huge amount of success in measuring these parameters, leading to both understanding and also to the introduction of major scientific questions yet to be answered.

Most recent measurements of the deceleration parameter reveal $q = -0.55$ [9]. This means the universe is currently experiencing a period of accelerated expansion. Naively, we

expect the gravitational attraction of the matter in the universe to slow the expansion rate of the universe, resulting in a positive deceleration parameter. So, this result is itself surprising based on our concordance model.

Additionally, measurements of the fractional energy density of dark energy paint a surprising picture: $\Omega_\Lambda = 0.685$ [8]. Meaning, almost 70% of our universe is comprised of a yet unidentified substance described, in this model, by a non-vanishing cosmological constant. Assuming GR is a valid EFT up until it's cut-off scale, M, then naturalness leads us to expect $m_{\rm pl}^2\Lambda \sim M^4$ [10]. Choosing the Planck scale as the theory's cut-off, we should have $\Lambda \sim m_{\rm pl}^2$. Instead, observationally, we have $\Omega_\Lambda \sim 1$ which implies,

$$\Lambda \sim H_0^2 \sim m_{\rm pl}^2 \times 10^{-120}. \tag{2.16}$$

Thus, the observed value of the cosmological constant is 120 orders of magnitude smaller than expected. This major discrepancy between model and observations is known as the cosmological constant problem.

2.2 Proposed Solutions

2.2.1 Inflationary Cosmology

In the early 1980s, Alan Guth set out to find an explanation for the lack of magnetic monopoles present in our universe. He managed to answer not only this question but also two others: the horizon and flatness problems. His solution was the introduction of an inflationary epoch – a period of exponential expansion at the very beginning of our universe. This necessitated the evolution of the scale factor take exponential form, allowing the universe to grow by a factor of e^{60}, thereby achieving homogeneity on the order of CMB scales [13]. An illustration of how this solves the horizon problem can be see in Figure 2.3.

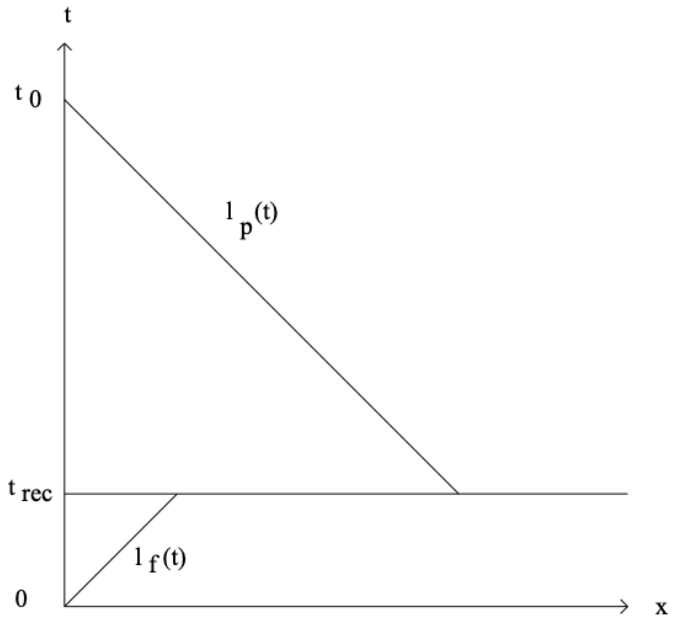

Figure 2.2: An illustration of the horizon problem. In this space-time diagram, we see that the backward-propagating light cone, $l_p(t)$, is much larger than the forward-propagating light cone $l_f(t)$ at the time of recombination, t_{rec} [2].

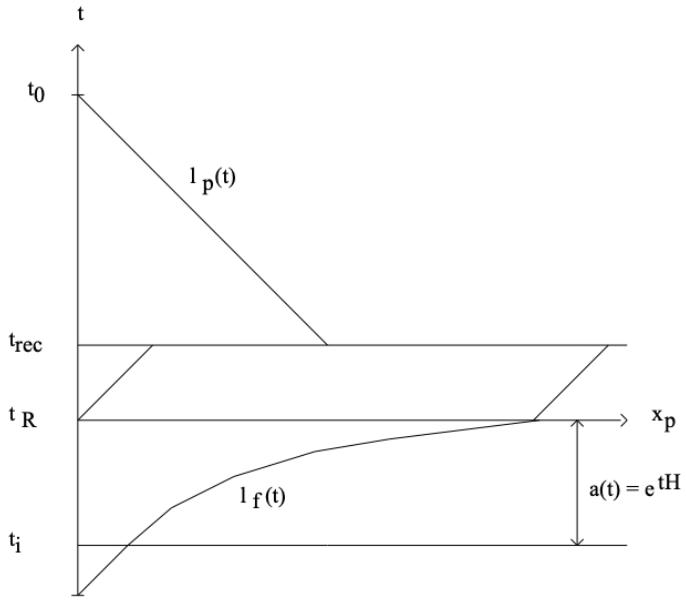

Figure 2.3: An illustration of Guth's solution to the horizon problem, where t_R is the reheat time. By introducing a period of exponential expansion at the beginning of the universe (inflation), our forward-propagating light cone, l_f, is now larger than the backward-propagating light cone, l_p, and we are able to achieve homogeneity and causality [2].

During the inflationary epoch, the evolution of the scale factor takes exponential form,

$$a(t) = a_i e^{H(t-t_i)} \tag{2.17}$$

where we mark the beginning and the end of the inflationary period as t_i and t respectively. We can then rewrite equation 2.13 as,

$$1 - \Omega(t) = -\frac{k}{H^2 e^{2Ht}}. \tag{2.18}$$

We can compare the flatness of a post-inflationary universe to its initial flatness,

$$\frac{1 - \Omega(t)}{1 - \Omega(t_i)} = e^{-2N} \tag{2.19}$$

where $N = H(t_f - t_i)$ is the number of e-folds that take place during inflation. If N is a very large number, the left side of the equation becomes very small. Therefore, no matter how bumpy the universe used to be, the inflationary period flattened it out so much that we observe a nearly perfectly (spatially) flat universe, $\Omega = 1$.

The question Guth initially set out to answer was with regard to the lack of magnetic monopoles in our universe. The inflationary epoch he introduced dilutes the density of monopoles significantly. Additionally, by the end of inflation, all of the energy in the universe would be distributed across incredibly vast distances. Hence, the energy density would be far too low to facilitate the production of magnetic monopoles. The probability of even one single monopole existing in our observable universe is highly unlikely.

2.2.2 Modified Gravity

The observed acceleration of the universe and its origins in an unnaturally tiny cosmological constant serves as fodder for much theoretical and observational discussion. There exist

many different theories offering their own explanations to the quandary, though none in particular stands out at the moment. A review of such theories can be found in [14]. Using data to differentiate between these models will be a large topic of this work (see Chapter 5). Regardless of the model, any alternative explanation for cosmic acceleration will include alterations to the EFE. The Effective Field Theory of Dark Energy/Modified Gravity (EFTDE for short) is an overarching theory that includes many of these alterations. Namely, those that include up to one new scalar degree of freedom. A table illustrating just how general the framework of the EFTDE is and how many different kinds of models it includes can be found in Figure 3.6.

CHAPTER 3

EFFECTIVE FIELD THEORIES

The Effective Field Theory framework is a mathematical tool that allows us to approximate underlying physical phenomena while still remaining consistent with known physics. The framework exploits the fact that different physics occurs at different energy scales. Meaning, physics at low energies (or long distances) is not affected by different physics at high energies (or short distances). Of course, "low" and "high" are relative – the energy of inflation is low compared to the Planck scale. As Baumann said is his notes on the subject, "Nature comes with many scales...[and] science progresses because we can treat one scale at a time" [15]. An illustration of this natural hierarchy is shown in Figure 3.1.

Within the EFT framework, we are able to integrate out the physics of the high energy degrees of freedom to derive an *effective* low energy theory suitable for comparison to observations in our low energy world. To do this, we include all low energy degrees of freedom allowed by the symmetries and specify the field content. In this way, we are able to parameterize our ignorance about fundamental physics [19]. The following summary of how this is done in practice is taken primarily from [17]. There is ample literature on the subject, with some of my favorite discussions located in [15; 16; 17; 18; 19; 20; 21].

Any effective action in d space-time dimensions can be written,

$$S = \int d^d x \sum_i g_i \mathcal{O}_i \tag{3.1}$$

in terms of the coupling constants, g_i and the operators, $\mathcal{O}_i$. These operators are invariant under the defined symmetries of the theory and depend on the specified fields and their derivatives at a single point in space-time. If a specified operators has units E^{δ_i} then the dimension of the operator is defined to be δ_i and the couplings, g_i, have units $E^{d-\delta_i}$. We can define a dimensionless coupling $\bar{g}_i = g_i M^{\delta_i - d}$ where M is the characteristic mass scale

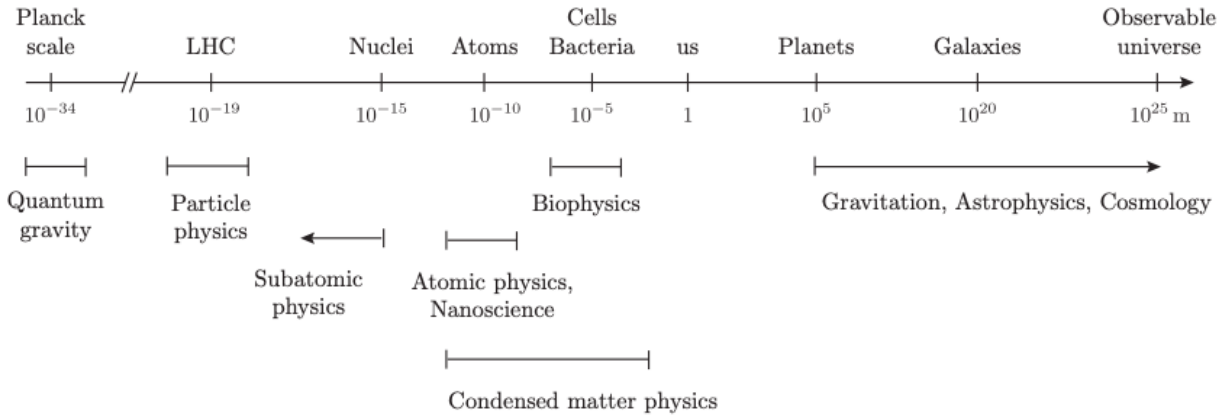

Figure 3.1: An illustration of physical scales as they appear naturally [15]. It is this hierarchy that enables us to treat one scale at a time with an EFT and thus parameterize our ignorance about the more fundamental physics.

known as the *cut-off* of the EFT. It is chosen such that $\bar{g}_i \lesssim 1$. Then, it follows that the the order of the i^{th} term is,

$$\int d^d x \, g_i \mathcal{O}_i \sim \bar{g}_i \left(\frac{E}{M}\right)^{\delta_i - d} \tag{3.2}$$

where the energy scale E is larger than any other mass scale in the theory except M. We are now able to group operators into three distinct categories based on their contributions to the action: *relevant*, *marginal*, and *irrelevant*. If $\delta_i > d$, the term becomes less important at low energies, and therefore deemed irrelevant (nonrenormalizable). If $\delta_i < d$, the term is more important at lower energies and is deemed relevant (superrenormalizable). An operator with $\delta_i = d$ is equally important at all scales and is marginal (strictly renormalizable).

Thus, the low-energy phenomenology of the EFT is encoded in the relevant operators and small corrections due to physics at higher energy scales is encoded in the irrelevant operators. In most cases, there is a finite number of relevant and marginal terms, so the low energy physics depends on a finite number of parameters. This convenient fact – essential to our ability to craft EFTs – is summarized well by Weinberg when he said, "Any effective field theory necessarily includes an infinite number of non-renormalizable interactions. Nev-

ertheless...we expect that at sufficiently low energy all the non-renormalizable interactions in such effective field theories are highly suppressed" [16].

As you can see, the framework of EFTs is very general, making it applicable to many different kinds of science. EFTs have been used across all areas of physics to help us better understand our world. Famously, Enrico Fermi used an EFT to describe beta decay wherein the force mediators, the W^- bosons, are integrated out of the theory. Fermi's low-energy approximation of the decay ultimately lead to the isolation of the electroweak force. In the sections that follow I summarize multiple applications of EFTs to the field of cosmology.

3.1 EFT of Inflation

As introduced in Section 2.1, standard cosmology is plagued by several problems, including the horizon, flatness, and monopole problems. The introduction of a period of accelerated expansion – called inflation – offers a solution to all of these [13]. In cosmology, an EFT approach has been used to investigate the phenomenology of inflation in a couple different ways. Initially, Weinberg applied the EFT framework to the inflationary background [40]. This methodology is covered in 3.1.1. In contrast, Cheung et al. realized that Weinberg's EFT of Inflation fell short in describing nonlinear backgrounds and thus focused on the EFT of perturbations around an assumed background [43]. This methodology is covered in 3.1.2.

3.1.1 EFT of the Background

The simplest model of inflation is one with a single canonically normalized inflaton field, $\varphi_c(x)$, described by the Lagrangian,

$$\mathcal{L}_0 = \sqrt{-g}\left[\frac{1}{2}m_{\rm pl}^2 R - \frac{1}{2}(\partial\varphi_c)^2 - V(\varphi_c)\right]. \tag{3.3}$$

Here, R is the Ricci scalar, and $V(\varphi_c)$ is a potential down which the inflaton rolls slowly. The scale of observed fluctuations is $H = k/a \approx \sqrt{\epsilon} \times 10^{14}\,\mathrm{GeV}$ where k/a is the physical wave number. This is much lower than the Planck scale, $m_{\mathrm{pl}} \approx 10^{18}\,\mathrm{GeV}$, leading Weinberg to argue that Equation 3.3 can be treated as the first term in a generic EFT. Terms with higher derivatives are suppressed by negative powers of some large mass, M, the cut-off scale of the theory. Having an observation scale much lower than the cut-off scale justifies this approach.

We can get a better idea for the size of M by considering the time derivative of the unperturbed canonically normalized inflaton field, $\bar{\varphi}_c$,

$$\dot{\bar{\varphi}}_c = \sqrt{2\epsilon}\, m_{\mathrm{pl}} H, \tag{3.4}$$

where ϵ is the value of $-\dot{H}/H^2$ at the time of evaluation. So, the change in the inflaton field during one Hubble time at the time the inflaton modes exit the horizon is of the order $\dot{\bar{\varphi}}_c/H = \sqrt{2\epsilon}\, m_{\mathrm{pl}}$. Hence, the cut-off scale, M, cannot be much smaller than $\sqrt{2\epsilon}\, m_{\mathrm{pl}}$. We move forward with the tentative assumption that M is on the order of $\sqrt{2\epsilon}\, m_{\mathrm{pl}}$.

The leading correction to $\mathcal{L}_0$ (Equation 3.3) will consist of a sum of all generally covariant terms with four space-time derivatives and dimensionless functions, $f_n(\varphi)$, taken to be of order unity as coefficients,

$$\begin{aligned}
\Delta\mathcal{L} = \ \sqrt{-g}\ \Big[& f_1(\varphi)\big(\partial\varphi\big)^4 + f_2(\varphi)\big(\partial\varphi\big)^2\Box\varphi + f_3(\varphi)\big(\Box\varphi\big)^2 \\
+ \ & f_4(\varphi)R^{\mu\nu}\partial_\mu\varphi\partial_\nu\varphi + f_5(\varphi)R\big(\partial\varphi\big)^2 + f_6(\varphi)R\Box\varphi + f_7(\varphi)R^2 \\
+ \ & f_8(\varphi)R^{\mu\nu}R_{\mu\nu} + f_9(\varphi)C^{\mu\nu\rho\sigma}C_{\mu\nu\rho\sigma} + f_{10}(\varphi)\epsilon^{\mu\nu\rho\sigma}C_{\mu\nu}{}^{\kappa\lambda}C_{\rho\sigma\kappa\lambda}\Big],
\end{aligned} \tag{3.5}$$

where $\Box\varphi \equiv g^{\mu\nu}\varphi_{,\mu;\nu}$ is the invariant d'Alembertian of φ; $\epsilon^{\mu\nu\rho\sigma}$ is the totally antisymmetric tensor density with $\epsilon^{1230} \equiv +1$; and $C_{\mu\nu\rho\sigma}$, the Weyl tensor, is used instead of the

Riemann–Christoffel tensor, $R_{\mu\nu\rho\sigma}$,

$$C_{\mu\nu\rho\sigma} \equiv R_{\mu\nu\rho\sigma} - \frac{1}{2}\Big(g_{\mu\rho}R_{\nu\sigma} - g_{\mu\sigma}R_{\nu\rho} - g_{\nu\rho}R_{\mu\sigma} + g_{\nu\sigma}R_{\mu\rho}\Big) + \frac{R}{6}\Big(g_{\mu\rho}g_{\nu\sigma} - g_{\nu\rho}g_{\mu\sigma}\Big). \quad (3.6)$$

There are a cumbersome amount of terms in Equation 3.6. Luckily, we can use the equations of motion resulting from this theory to trade derivatives of φ with functions of φ along with some field redefinitions and eliminate all but three terms,

$$\Delta\mathcal{L} = \sqrt{-g}\Big(f_1(\varphi)\big(\partial\varphi\big)^4 + f_9(\varphi)C^{\mu\nu\rho\sigma}C_{\mu\nu\rho\sigma} + f_{10}(\varphi)\epsilon^{\mu\nu\rho\sigma}C_{\mu\nu}{}^{\kappa\lambda}C_{\rho\sigma\kappa\lambda}\Big). \quad (3.7)$$

And with this, we obtain Weinberg's EFT of the inflationary background. Unfortunately, this method falls short in its (in)ability to describe nonlinear backgrounds, such as those seen in DBI inflation – an inflationary model arising from string theory. The following approach outline in 3.1.2, pioneered by Cheung et al. in [43], *assumes* a background and does the EFT of the fluctuations around that background. This way, the background can be anything we define it to be (even nonlinear).

3.1.2 EFT of the Perturbations

What follows is a summary of the most general theory of a single field model and describing the *fluctuations* around a quasi de Sitter background [43]. This theory of the perturbations around the time evolving solution differs dramatically from Weinberg's theory of the background. Although φ is a scalar under all diffeomorphisms, the perturbation, $\delta\varphi$, is a scalar only under spatial diffeomorphisms and transforms non-linearly with respect to time diffeomorphisms,

$$t \longrightarrow t + \xi^0(t,\vec{x}) \quad \delta\varphi \longrightarrow \delta\varphi + \dot{\varphi}_0(t)\xi^0. \quad (3.8)$$

We choose a gauge where there are no inflaton perturbations – namely, unitary gauge, $\varphi(t,\vec{x}) = \varphi_0(t)$ – and all degrees of freedom are in the metric. The scalar variable $\delta\varphi$ has been "eaten" by the metric (or, graviton). The graviton itself now has three degrees of freedom: the scalar mode and the two tensor helicities. As spatial diffeomorphisms remain unbroken, the most general Lagrangian in this gauge will contain operators that are functions of the metric, $g_{\mu\nu}$ and invariant under the time dependent spatial diffeomorphisms, $x^i \longrightarrow x^i + \xi(t,\vec{x})$. Thus, the most generic action that can be written under these conditions looks like,

$$\begin{aligned} S &= \int d^4x\sqrt{-g}\Big[\frac{1}{2}m_{\rm pl}^2 R - c(t)g^{00} - \Lambda(t) + \frac{1}{2!}M_2(t)^4(g^{00}+1)^2 + \frac{1}{3!}M_3(t)^4(g^{00}+1)^3 \\ &- \frac{1}{2}\bar{M}_1(t)^3(g^{00}+1)\delta K^\mu{}_\mu - \frac{1}{2}\bar{M}_2(t)^2\delta K^\mu{}_\mu{}^2 - \frac{1}{2}\bar{M}_3(t)^2\delta K^\mu{}_\nu\delta K^\nu{}_\mu + ...\Big], \end{aligned} \tag{3.9}$$

where $\delta K_{\mu\nu}$ is the variation of the extrinsic curvature of constant time surfaces with respect to the unperturbed FLRW solution, $\delta K_{\mu\nu} = K_{\mu\nu} - a^2 H h_{\mu\nu}$ and $h_{\mu\nu}$ is the induced spatial metric. The ellipsis represents terms that are of higher order in the fluctuations or with more derivatives.

The unperturbed FLRW history fixes $c(t)$ and $\Lambda(t)$ and differences among models are encoded in the higher order terms. In other words, $c(t)$ and $\Lambda(t)$ are the background terms and can be mapped to energy density and pressure,

$$H^2 = \frac{1}{3m_{\rm pl}^2}\Big[c(t) + \Lambda(t)\Big] \tag{3.10}$$

$$\dot{H} + H^2 = -\frac{1}{3m_{\rm pl}^2}\Big[2c(t) - \Lambda(t)\Big]. \tag{3.11}$$

Solving for $c(t)$ and $\Lambda(t)$ explicitly and plugging the results back into the action, Equation

3.9, gives

$$\begin{aligned} S &= \int d^4x\sqrt{-g}\Big[\frac{1}{2}m_{\rm pl}^2 R + m_{\rm pl}^2\dot{H}g^{00} - m_{\rm pl}^2(3H^2+\dot{H}) + \frac{1}{2!}M_2(t)^4(g^{00}+1)^2 \\ &+ \frac{1}{3!}M_3(t)^4(g^{00}+1)^3 - \frac{1}{2}\bar{M}_1(t)^3(g^{00}+1)\delta K^\mu{}_\mu - \frac{1}{2}\bar{M}_2(t)^2\delta K^\mu{}_\mu{}^2 \\ &- \frac{1}{2}\bar{M}_3(t)^2\delta K^\mu{}_\nu\delta K^\nu{}_\mu + ...\Big]. \end{aligned} \tag{3.12}$$

This is the most generic Lagrangian for the scalar mode as well as for gravity. Since we are interested in solutions over which H and $\dot{H}$ do not change very much (in one Hubble time), it is safe to assume the same is true of the time-dependent coefficients. These EFT coefficients are therefore often taken to be constants. Additionally, unlike Weinberg's EFT, we have the freedom to choose any expansion history – we can choose any function of time for $c(t)$ and $\Lambda(t)$.

We are now caught up on the historical foundation of EFTs in cosmology and have seen how they can successfully describe the inflationary epoch. In the following section, we present original research into extending both Weinberg's EFT of Inflation as well as Cheung et. al.'s rendition to include the period of (p)reheating after inflation.

3.2 EFT of Reheating

If inflation occurred in the early universe it must have eventually ended resulting in a hot, thermal universe by the time of Big Bang Nucleosynthesis (BBN). The process by which the inflaton's energy is transferred into other particles – which hopefully, eventually, gave rise to Standard Model particles – is known as inflationary reheating. Reheating can occur perturbatively [23; 24; 25], or non-perturbatively in a process known as preheating [26; 27; 28] (see [29; 30] for recent reviews).

Existing investigations into reheating have been rather model dependent, often focusing on constraining the precise regions of the parameter space that lead to successful reheat-

ing. Analytic methods for exploring the dynamics still rely on the earliest works mentioned above, and the non-linearities and complexity of the reheating process still require invoking numeric/lattice methods [31; 32; 33; 34; 35; 36; 37; 29; 30]. Moreover, the wealth of cosmological observations from the Cosmic Microwave Background (CMB) and Large Scale Structure (LSS) relate to the physics of inflation far before reheating, and so the lack of observational windows on (p)reheating has also made its study far less compelling than inflation – with the prediction of gravitational waves providing a possible exception.

In this work, we take steps to address the model dependence of (p)reheating building on motivation from recent works [38; 39; 22]. Our approach is to use the Effective Field Theory (EFT) approach to cosmology, which at this point has been applied to all cosmic epochs except for (p)reheating. We will first consider the EFT of the background as developed by Weinberg for inflation in [40] and later adapted to studies of dark energy in [41]. Ultimately, we will find that this approach is not completely satisfactory in generalizing studies of reheating. Instead we find that the different approach of the EFT of cosmological perturbations is more promising.

The EFT of Inflation [42; 43; 44] and generalizations to dark energy [45; 46; 47; 48] and structure formation [49] are based on the idea that there is a physical clock corresponding to the Goldstone boson that non-linearly realizes the spontaneously broken time diffeomorphism invariance of the background. In unitary gauge – where the clock is homogeneous – the matter perturbations are encoded within the metric, *i.e.* the would-be Goldstone boson is 'eaten' by the metric, since gravity is a gauge theory. After we establish the limitations of the EFT background approach, we then present an EFT of reheating using this EFT of perturbations to develop a more robust approach to studying the end of inflation and reheating.

The rest of our discussion on the EFT of Reheating is as follows. In Section 3.2.1, we review some of the important issues and constraints surrounding particular examples of (p)reheating models. In Section 3.2.2, we consider Weinberg's approach to the EFT of

Inflation, and consider how inflation might end and (p)reheating would proceed. We find that the perturbative approach to the background presents a substantial challenge to this approach, along with the usual problem of knowing the complete inflationary potential. This motivates us to construct an EFT of reheating in Section 3.2.3 – focusing on the EFT of the perturbations. We analyze the process of particle production, demonstrate how our approach connects to existing preheating models, and discuss ways in which our EFT can be used to connect to both inflation (and its end) and observations. In Section 3.2.4, we conclude and discuss the challenges facing our approach and future directions.

3.2.1 Challenges for Inflationary Reheating

Model dependent studies of (p)reheating have raised a number of important questions and issues. From the perspective of inflationary model building within string theory, the requirement to isolate the inflationary sector to achieve an adequate duration of inflation can result in challenges in transferring the energy density to other fields, and eventually the Standard model sector following inflation [50]. The complexity of the string landscape and the large number of moduli fields can exacerbate this problem [51]. In bottom-up approaches, toy models often demonstrate a conflict between the need for the inflaton to have feeble interactions during inflation (so as to be consistent with both successful inflation and constraints on non-Gaussianity), and later having strong enough couplings for the complete decay of the inflaton and the (eventual) successful reheating of the Standard Model. Perturbative decay can also present a challenge depending on the effective mass of the decay channels and the time dependence of the inflaton decay rate [52].

As an example, consider Chaotic inflation with $V \sim m_\phi^2 \phi^2$ and reheating with a renormalizable coupling to a reheat field, χ. We note that this model is in tension with existing CMB constraints, but it presents a simple example of the more general problems one might

anticipate with (p)reheating. The Lagrangian we consider is[1]

$$\mathcal{L} = -\frac{1}{2}(\partial\phi)^2 - \frac{1}{2}m_\phi^2\phi^2 - \frac{1}{2}(\partial\chi)^2 - U(\chi) - \frac{g^2}{2}\phi^2\chi^2, \tag{3.13}$$

where we assume that initially the reheat field is fixed by its $U(\chi)$ and remains in its vacuum during inflation. The mass of the inflaton is fixed by the power spectrum [53],

$$\Delta^2_{\mathcal{R}} = \frac{1}{96\pi^2}\left(\frac{m_\phi}{m_{\rm pl}}\right)^2 (4N_*)^2 \equiv 2.2\times 10^{-9} \tag{3.14}$$

where N_* is the number of e-folds before the end of inflation and with $N_* = 60$ we have $m_\phi \simeq 6.4\times 10^{-6}\, m_{\rm pl}$. The inflaton will begin to oscillate around the minimum of its potential when its mass becomes comparable to the Hubble scale, $m_\phi \approx H(t_{\rm osc})$, with a profile given by the expression $\phi_0(t) = \Phi(t)\sin(m_\phi t)$ [28]. The amplitude of the oscillations, $\Phi(t)$, is a monotonic function of cosmic time given by $\Phi = \sqrt{8/3}\ (m_{\rm pl}/2\pi N_{\rm osc})$, where $N_{\rm osc}$ is the number of oscillations after the end of inflation. Setting $N_{\rm osc} = 1$ gives $\Phi \approx 0.3\, m_{\rm pl}$, which we take as the initial amplitude of the inflaton oscillations.

If the direct coupling in (3.13) presents the only decay channel for the inflaton the expansion of the universe will prevent the complete perturbative decay of the inflaton [28]. This is because the decay rate, Γ, scales as $\Gamma \propto \Phi^2 \sim 1/t^2$ whereas the expansion rate during reheating scales as $H \sim 1/t$. Instead, in this case decay must proceed non-perturbatively through preheating [26; 27; 28], where parametric resonance can lead to enhanced decay of the inflaton condensate. The mode equation for χ fluctuations resulting from (3.13) in the presence of the oscillating condensate $\phi_0(t)$ is

$$\ddot{\chi}_k + \left[k^2 + m_\chi^2 + g^2\phi_0^2\right]\chi_k = 0, \tag{3.15}$$

1. We work in reduced Planck units $m_{\rm pl} = 1/\sqrt{8\pi G} = 2.4\times 10^{18}\,\text{GeV}$ with $\hbar = c = 1$ and with a 'mostly plus' $(-,+,+,+)$ sign convention for the metric. Our conventions for curvature tensors are those of Weinberg.

where we have neglected the expansion of the universe ($a = 1$) and note that including gravitational effects would act to strengthen the main conclusion below. If the field begins in its Bunch-Davies vacuum the corresponding WKB solution is $\chi_k \sim \exp(-i \int \omega_k(t')dt')$, where ω_k is time-dependent frequency corresponding to the terms inside the brackets in (3.15). Particle production occurs if the adiabatic conditions fail corresponding to $\dot{\omega}_k \gg \omega_k^2$ or $\ddot{\omega}_k \gg \omega_k^3$, etc... Thus, a necessary condition for preheating is

$$\frac{\dot{\omega}_k}{\omega_k^2} \simeq \frac{g^2\phi\dot{\phi}}{\left(k^2 + m_\chi^2 + g^2\phi^2\right)^{3/2}} > 1, \tag{3.16}$$

corresponding to the production of modes with their momenta satisfying

$$k^2 \lesssim \left(g^2\phi\dot{\phi}\right)^{2/3} - g^2\phi^2 - m_\chi^2. \tag{3.17}$$

The ratio in (3.16) is maximal when the inflaton is near the bottom of the potential, where we can approximate $\dot{\phi}_0 \simeq m_\phi\Phi$. Broad resonance [28] will assure us that preheating is successful. This corresponds to a restriction on the range of wave numbers in the resonance band $\Delta k \gg m_\phi$. Maximizing the right side of (3.17) with respect to ϕ, we find the maximum value of $\phi_*^2 \simeq 0.2\,\dot{\phi}/g$ corresponding to a maximum value of resonant momentum $k_*^2 = 0.4\,g\dot{\phi} - m_\chi^2$. Therefore the condition for broad resonance $\Delta k \simeq k_* \gg m_\phi$ can be written as a condition on the coupling constant g,

$$g \gg \frac{m_\phi^2 + m_\chi^2}{\dot{\phi}} \simeq \frac{m_\phi^2 + m_\chi^2}{m_\phi\Phi}. \tag{3.18}$$

Taking $\Phi \simeq 0.3\,m_{\rm pl}$ and assuming $m_\chi \ll m_\phi$ we find $g \gg 3.8 \times 10^{-5}$ for efficient preheating in the broad resonance regime.

On the other hand, we can obtain a lower bound on the strength of the coupling by requiring the one-loop correction induced by the $g^2\phi^2\chi^2$ interaction to not to spoil the flat-

ness of the potential during inflation. That is, we require $\delta m_\phi \lesssim m_\phi \simeq 6.4 \times 10^{-6}\, m_{\rm pl}$, whereas the loop correction is $\delta m_\phi^2 = (g^2 \Lambda_{\rm uv}^2)/(16\pi^2)$. The cut-off is expected to be Planckian $\Lambda_{\rm uv} \approx m_{\rm pl}$, implying $g < 10^{-5}$. Clearly, this result implies that the required value of the coupling, g, to obtain efficient preheating is inconsistent with having a naturally light inflaton during inflation. In other words, in general it is expected that heavy χ fields running in the loops induced by the direct coupling $g^2\phi^2\chi^2$ tends to de-stabilize parameters of the inflationary sector if we insist on the effective particle production at the end of inflation.

We have a good understanding of the limitations to the approximations we have used above to constrain preheating in chaotic inflation models, especially since these toy models have been well-studied over the years to establish when they lead to successful reheating. At the same time, it is clear that we are seeing tension in analytic expectations for finding reliable preheating models. It is also clear that doing a full non-linear analyses for all parameters in all models of preheating is not an efficient way to do model analysis. Can one always establish a connection between the parameters during inflation and those same parameters during reheating? What is the expected mass of the reheat fields during inflation? Can't the inflaton just decay through higher dimensional operators present at the time of reheating? These are some of the questions we hope to address by developing a more systematic approach to reheating below.

3.2.2 Reheating in Weinberg's Covariant Formulation of the EFT of Inflation

In this section, we extend Weinberg's EFT approach to inflation [40] to include the end of inflation and the beginning of (p)reheating. Focusing on a two-field scalar field model for simplicity, we present both analytic and numeric results from our investigation into the background evolution and the resulting particle production. We find that consistency of the background EFT within this approach limits its applicability and how well it can be used to

successfully describe (p)reheating. This will motivate us to consider a different approach in Section 3.2.3.

3.2.2.1 Construction of the EFT

Following [40] we consider the most general EFT of a scalar field in General Relativity which can be written as

$$\mathcal{L}_{\rm inf} = -\frac{1}{2}m_{\rm pl}^2 R - \frac{1}{2}\left(\partial\phi\right)^2 - V(\phi) + \frac{c_1}{\Lambda^4}\left(\partial\phi\right)^4, \tag{3.19}$$

where Λ is the UV cutoff of the theory, in general $c_1 = c_1(\phi)$ is an arbitrary function of the scalar, and we have neglected terms involving the Weyl tensor which are suppressed relative to the leading correction [40]. Assuming that the equations of motion admit inflationary solutions it was shown in [40] that this is also the most general EFT for the inflationary background (to be contrasted to the EFT for the perturbations which we will discuss in Section 3.2.3).

CMB observations imply that the power spectrum of scalar fluctuations is nearly scale-invariant, which can be realized through an approximate shift symmetry for the inflaton. This allows us to approximate $c_1(\phi)$ as nearly constant during inflation (its time evolution is slow-roll suppressed). When the EFT expansion is applicable, *i.e.* $\Lambda > \dot{\phi}^{1/2}$, self-interactions of the inflaton are small and non-Gaussianity is negligible [54].

We now introduce an additional scalar that will play the role of the reheat field after inflation. For simplicity, we will focus on the situation where the reheat field has an effective mass of at least the Hubble-scale during inflation to avoid considering multi-field inflation. However, the reheat field's mass during inflation is an important consideration which we comment on later. Given these assumptions the starting point of our analysis is similar in spirit to that of [55], where those authors considered the EFT of the inflationary background coupled to an additional scalar sector during inflation. Again working to next-to-leading order in the derivative expansion we can introduce the Lagrangian for the additional scalar

χ,

$$\mathcal{L}_\chi = -\frac{1}{2}(\partial\chi)^2 - U(\chi) + \frac{c_2}{\Lambda^4}(\partial\chi)^4\,, \tag{3.20}$$

where c_2 and $U(\chi)$ are arbitrary functions of χ, but can not contain the inflaton due to its approximate shift symmetry[2].

Finally, we can introduce the interactions between the two sectors that respect the inflaton's shift symmetry – implying that terms of the form $\phi^p\chi^q$ are forbidden. At the level of dimension five operators it was shown in [55] that the shift symmetry can be used to forbid the operators $\partial_\mu\phi\partial^\mu\chi$ and $\chi\partial_\mu\phi\partial^\mu\chi$. Similar arguments can be used at the level of dimension six operators and we find the two leading interactions[3]

$$\mathcal{L}_{\rm mix} = -c_3(\partial\phi)^2\frac{\chi}{\Lambda} - c_4(\partial\phi)^2\frac{\chi^2}{\Lambda^2} + \mathcal{O}\left(\frac{1}{\Lambda^3}\right), \tag{3.21}$$

where c_3 and c_4 are expected to be order one constants and positive (for a UV completable EFT [56] and to avoid pathological instabilities [57]). Given our discussion and assumptions above, the EFT of Inflation with an additional to-be reheat field is then given by, $\mathcal{L} = \mathcal{L}_{\rm inf} + \mathcal{L}_\chi + \mathcal{L}_{\rm mix}$. Focusing on the leading interactions we have

$$\mathcal{L} = \frac{1}{2}m_{\rm pl}^2 R - \frac{1}{2}f\left(\frac{\chi}{\Lambda}\right)(\partial\phi)^2 - \frac{1}{2}(\partial\chi)^2 - V(\phi) - U(\chi), \tag{3.22}$$

where

$$f\left(\frac{\chi}{\Lambda}\right) = 1 + 2c_3\frac{\chi}{\Lambda} + 2c_4\frac{\chi^2}{\Lambda^2}. \tag{3.23}$$

The dynamics of fluctuations that arise from (3.22) have been studied extensively in the context of inflation. In particular, there can be interesting signatures for both the power

2. The spontaneous or explicit breaking of the shift symmetry at the time of reheating can be important and creates an additional limitation of this approach.

3. We have taken the cutoff of the EFT to be the same for both the inflationary and hidden sector for simplicity, although this need not be the case. We expect our main conclusions in this section to be insensitive to this assumption.

spectrum and higher point correlation functions (*e.g.* non-gaussianity) depending on the mass of χ [58], its stabilization [59; 60; 61; 62; 63; 64], and whether the χ and ϕ sectors are strongly or weakly mixed [65].

In this work we are interested in connecting this system to the end of inflation and reheating. In particular, we would like to investigate if (p)reheating of the χ sector can be achieved through the derivative couplings in (3.23) as these are the leading interactions allowed by the shift symmetry of the inflaton.

We note that (p)reheating with derivative couplings has been considered before. The authors of [66] have studied a particular realization of the EFT we are considering in this work. In their case the approximate shift symmetry of the EFT resulted from a specific UV completion motivated by Natural Inflation [67], where the spontaneous (and explicit) breaking of a $U(1)$ symmetry of a complex scalar resulted in an inflaton associated with the pseudo-Nambu-Goldstone Boson (pNGB) and the reheat field corresponded to the excitation of the radial direction. The UV theory took the form

$$\mathcal{L} = -(\partial_\mu \Phi)(\partial^\mu \Phi^*) - \lambda(F^2 - \Phi^* \Phi), \tag{3.24}$$

where the $U(1)$ symmetry is broken by the vacuum solution $\langle|\Phi|\rangle = F$. The inflaton potential results from the explicit breaking term

$$V(\phi) = \mu^4 \left[1 - \cos\left(\frac{\phi}{F}\right)\right]. \tag{3.25}$$

Expanding around the vacuum solution using

$$\Phi = (F + \chi)\ e^{i\phi/F}, \tag{3.26}$$

one can easily see that this particular model can be recast as the EFT of the matter sector

given by the Lagrangian (3.22) with the replacement $\Lambda \to F$. We note that in this particular class of models, adequate inflation unfortunately requires $F \gg m_{\rm pl}$, which seems to be at odds with additional non-perturbative corrections and expectations from quantum gravity [68; 69]. However, we emphasize that the (bottom-up) EFT approach we are taking here is more general than this particular class of models. In particular, we emphasize (see also [55]) that the symmetries resulting in (3.22) may be the result of a fundamental symmetry of the UV theory (as in the example of [66]), but they can also be the result of an accidental symmetry in the IR, or the result of fine-tuning of the effective potential. In this way, the model of [66] provides a particular UV completion of the more general EFT approach we consider here. This is analogous to the way in which EFT methods can capture phenomenology near the scale of Electroweak symmetry breaking, without one having a precise description of the UV physics and mechanism responsible for breaking Electroweak symmetry.

In general, the inflaton potential $V(\phi)$ in our EFT is arbitrary and does not need to take the specific form given in (3.25). We also have that the scale Λ can be taken as $\Lambda < m_{\rm pl}$ without raising any immediate issues about the consistency of inflation. We will see the importance of this observation when we consider the dynamics of the background and fluctuations in the following sections.

3.2.2.2 Analysis of Reheating in the EFT

To justify using an EFT at the end of inflation, we need to ensure that the model is self-consistent, i.e. we have to check that there is a consistent background solution to the equations of motion for the fields,

$$\ddot{\phi} + 3H\dot{\phi} + \partial_\chi \left(\ln f\right) \dot{\phi}\dot{\chi} + f^{-1}\partial_\phi V = 0, \tag{3.27}$$

and

$$\ddot{\chi} + 3H\dot{\chi} - \frac{1}{2}(\partial_\chi f)\ \dot{\phi}^2 + \partial_\chi U = 0, \tag{3.28}$$

and that the background also admits a perturbative description. This procedure will allow us to study the existence (or non-existence) of resonant phenomena, and establish when viable preheating occurs.

We begin by studying the behavior of the background fields ϕ_0 and χ_0. These are described by the following equations of motion,

$$\ddot{\phi}_0 + 3H\dot{\phi}_0 + \partial_\chi\left(\ln f\right)\dot{\phi}_0\dot{\chi}_0 + f^{-1}\partial_\phi V = 0, \tag{3.29}$$

and

$$\ddot{\chi}_0 + 3H\dot{\chi}_0 - \frac{1}{2}(\partial_\chi f)\ \dot{\phi}_0^2 + \partial_\chi U = 0. \tag{3.30}$$

If we further assume that the zero-mode dominates the energy density (and pressure) of the universe in the linear regime, then we can write down the evolution equations for the scale factor,

$$H^2 = \frac{1}{3m_{\rm pl}^2}\left(\frac{1}{2}f\dot{\phi}_0^2 + \frac{1}{2}\dot{\chi}_0^2 + V(\phi_0) + U(\chi_0)\right), \tag{3.31}$$

and the Hubble parameter,

$$\dot{H} = -\frac{1}{2m_{\rm pl}^2}\left(f\dot{\phi}_0^2 + \dot{\chi}_0^2\right). \tag{3.32}$$

The first question that we need to address is whether the zero-mode of the reheat field acquires a significant displacement from zero. Using (3.23), and taking c_3 and c_4 to be order-one constants then (3.30) becomes

$$\ddot{\chi}_0 \quad + \quad 3H\dot{\chi}_0 + \partial_\chi U - \frac{\dot{\phi}_0^2}{\Lambda^2}\chi_0 - \frac{\dot{\phi}_0^2}{\Lambda} = 0, \tag{3.33}$$

The last two terms in (3.33) come from the EFT expansion – *i.e.* we have dropped terms in

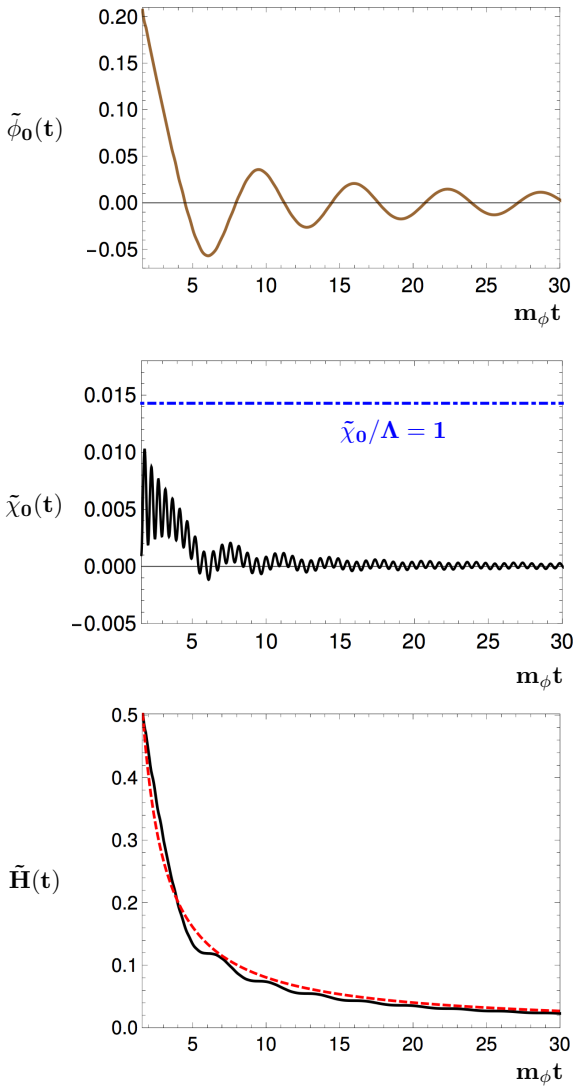

Figure 3.2: The evolution of the background fields and Hubble parameter, where tildes imply we have normalized these quantities by $\sqrt{8\pi}m_{\rm pl}$, and time is in units of the inflaton mass. For this realization we take $m_\chi/m_\phi = 10$, $m_{\rm pl}/\Lambda = 14$ and initial conditions $\phi_0 = 1.038\ m_{\rm pl}$, $\dot{\phi}_0 = -0.662\ m_{\rm pl}$, $\chi_0 = \dot{\chi}_0 = 0.005\ m_{\rm pl}$. The top panel gives the evolution of the inflaton. In the middle panel the solid black curve is $\tilde{\chi}_0(t)$ and below the dot-dashed blue horizontal line marks the region where the EFT of the background is valid. The bottom plot gives the Hubble rate where the red-dashed line represents a strictly matter dominated evolution.

the Lagrangian of order $\sim \dot{\phi}_0^2\chi_0^3/\Lambda^3$ and higher. Therefore, if either of these terms become large (e.g. if $\chi_0/\Lambda > 1$) then the EFT expansion of the background is not justified. Equation

(3.33) is that of a harmonic oscillator with time-dependent frequency, where the last term resembles an external force, which we also require to be small compared to the restoring force from the effective potential. Assuming that $U(\chi_0) \approx m_\chi^2 \chi_0^2/2$, which is self consistent with our small-displacement assumption, we can find the stable minimum of the effective potential,

$$U_{\rm eff} = U(\chi_0) - \frac{1}{2}\dot{\phi}_0^2 f\left(\frac{\chi}{\Lambda}\right). \tag{3.34}$$

to be

$$\chi_0(t) \simeq \frac{\dot{\phi}_0^2}{m_\chi^2 \Lambda} + \mathcal{O}\left(\frac{\dot{\phi}_0^4}{m_\chi^4 \Lambda^2}\right). \tag{3.35}$$

The velocity of the inflaton at the end of inflation is roughly $\dot{\phi} \sim m_\phi m_{\rm pl}$, which allows us to write down an approximate condition on the size of χ_0,

$$\frac{\chi_0}{\Lambda} < 1 \tag{3.36}$$

implies that

$$\frac{m_\phi^2}{m_\chi^2} < \left(\frac{\Lambda}{m_{\rm pl}}\right)^2 \tag{3.37}$$

That is, we find that we are free to lower the cutoff of the EFT below the Planck scale ($\Lambda \ll m_{\rm pl}$), but at the cost of increasing the mass of the reheat field above that of the inflaton. The fact that particle production is still possible in the $m_\chi \gg m_\phi$ regime emphasizes the importance of preheating versus reheating, since in this situation perturbative decays are kinematically forbidden. It is also interesting that this condition is *independently* required so that the reheat field does not interfere with the the inflationary dynamics prior to reheating (constraints from non-Gaussianity could also be imposed). That is, even for $m_\phi < m_\chi \simeq 3H_I$ such heavy fields can have a dramatic impact on inflation [58; 59; 60; 61; 62; 63; 64; 65]. We also note that the presence of a discrete Z_2 symmetry could be used to forbid the dimension five operator leading to the tadpole in (3.33), and our stability condition (3.37) would still

hold due to the presence of the dimension six operator.

We have numerically verified the result (3.37) by solving the system (3.29)-(3.31) for a range of masses, initial conditions, and the cutoff Λ. In Figure 3.2, we plot a particular realization of a consistent configuration for the background fields together with the evolution of the cosmological background. In the plot, we take $m_{\rm pl}/\Lambda = 14$ and $m_\chi/m_\phi = 10$ consistent with (3.37). We see that the background value χ_0 stays consistent within the EFT regime, while inflaton oscillations proceed as in the case of a quadratic potential. On the other hand, it can be seen that the expansion of the universe is slightly faster than $H(t) \propto t^{-1}$ initially, and then asymptotes to this behavior at late times $m_\phi t \gg 1$. We conclude this section by emphasizing that in order to have a stable, well-behaved background solution within the regime of validity of the EFT, one requires the condition, (3.37) to be satisfied.

1. Non-perturbative Dynamics and Limitations of the Background EFT

We now consider whether resonant particle production is possible around the background we analyzed in the previous section. Expanding both scalar fields to first order around their background values, $\phi = \phi_0 + \delta\phi$, $\chi = \chi_0 + \delta\chi$ in the Lagrangian (3.22), we write the equation of motion for the linearized fluctuations of the reheat field in Fourier space as

$$\delta\ddot{\chi}_k + 3H\delta\dot{\chi}_k + \left[\left(\frac{k}{a}\right)^2 + m_\chi^2 - \frac{\dot{\phi}_0^2}{\Lambda^2}\right]\delta\chi_k = 2\frac{\dot{\phi}_0}{\Lambda}\left[1 + \frac{\chi_0}{\Lambda}\right]\delta\dot{\phi}_k, \tag{3.38}$$

where the terms on the right side are due to the mixing with inflaton fluctuations. These terms can source $\delta\chi_k$ fluctuations whenever $\delta\dot{\phi}_k$ is large. In the initial stage of (p)reheating the effect of this term will be negligible. Neglecting these terms, we focus on sub-Hubble scales first neglecting the cosmological expansion (we take $a(t) \to 1$, $H(t) \to 0$). In this

approximation, (3.38) becomes

$$\delta\ddot{\chi}_k + \left[k^2 + m_\chi^2 - \frac{\dot{\phi}_0^2}{\Lambda^2}\right]\delta\chi_k = 0, \tag{3.39}$$

where we define the frequency of the modes as $\omega_k^2(t) = k^2 + m_\chi^2 - \dot{\phi}_0^2/\Lambda^2$. Given a coherently oscillating inflaton, $\phi_0 = \Phi(t)\sin(m_\phi t)$, we can map this mode equation to the Mathieu equation

$$\delta\chi_k'' + [A_k - 2q\cos(2z)]\,\delta\chi_k = 0, \tag{3.40}$$

where we have defined the dimensionless time $z = m_\phi t$ and $A_k = (k^2 + m_\chi^2)/m_\phi^2 - 2q$ with $q = \Phi^2/4\Lambda^2$. Floquet's theorem [70] states that for a given wave-number, (3.38) has solutions of the form

$$\delta\chi_k = e^{\mu_k z} g_1(z) + e^{-\mu_k z} g_2(z), \tag{3.41}$$

where g_1 and g_2 are periodic functions and μ_k is the Floquet exponent. In general, the Floquet exponent μ_k depends on the wave number k, the mass of the reheat field m_χ, and the ratio Φ/Λ. For cases where the real part of the exponent is non-zero, we have exponentially growing modes of $\delta\chi_k$.

The structure of (3.40) tells us that the resonant momenta are grouped into bands in parameter space. Since $k^2 > 0$, and hence, $A_k > -2q$, there are also meaningful statements one can make about the regions of the Mathieu parameter space that are probed by our reheating models. One interesting case is when some modes satisfy $-2q < A_k < 0$; in this case, (3.40) assures us that there's a time when the mass-squared of the these modes is negative (analogous to the cases explored in [71]) and the Floquet exponent can be very large, $\mu_k \simeq (4/\pi)\ q^{1/2}$ for $q \gg 1$. There's another case in which $0 < A_k < 2q$, where the mass-squared of some of the $\delta\chi_k$ modes become tachyonic for certain time intervals and is also very efficient (analogous to [34].)

On the other hand, A_k is frequently larger than $2q$. While these models have parametric

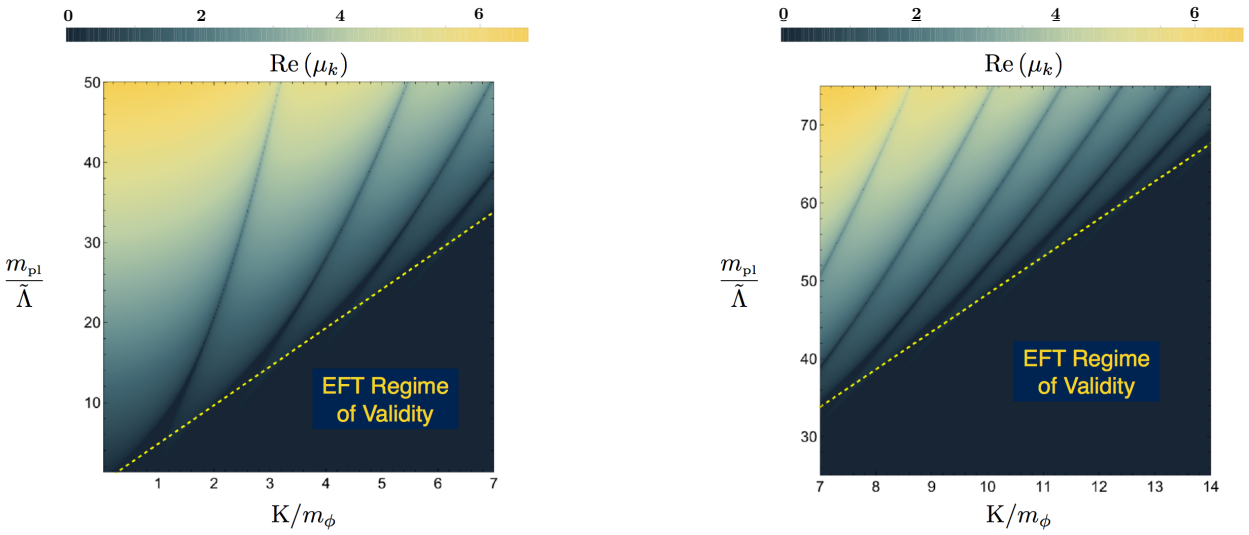

Figure 3.3: Instability band structure for the model $V_{\rm tot} = \frac{1}{2}m_\phi^2\phi^2 + \frac{1}{2}m_\chi^2\chi^2 - \frac{1}{2}\dot{\phi}_0^2 f\left(\frac{\chi}{\Lambda}\right)$, where f is given by (3.23). This density plot represents the real part of the scaled Floquet exponent, $\mathrm{Re}(\mu_k)$, where lighter regions represent larger values. The y-axis is the hierarchy between the Planck mass and the rescaled cut-off of the EFT, $\tilde{\Lambda} = \Lambda/\sqrt{8\pi}$, while the x-axis corresponds to $K = \sqrt{k^2 + m_\chi^2}$ in units of m_ϕ.

instabilities, the resonance structure requires us to be more careful. For our purposes here, the consistency of the background EFT requires the mass of the reheat field to satisfy $m_\chi^2 > \dot{\phi}_0^2/\Lambda^2$, which requires avoiding the regions of the parameter space that guarantee strong, broad, resonance. While the inflaton undergoes periodic oscillations this condition implies

$$m_\chi^2 > m_\phi^2 \frac{\Phi^2}{\Lambda^2}, \tag{3.42}$$

which is exactly what we have found in equation (3.37) with $\Phi = m_{\rm pl}$. Here, we have used $\phi(t) = \Phi \sin(m_\phi t)$ considering the maximum value of $\dot{\phi}_0^2/\Lambda^2$. We have also studied this system numerically, using FloqEx [72], with our results appearing in Figure 3.3. The figure shows the magnitude of the Floquet exponent as a function of cutoff and wave number. One can see the broad (and tachyonic) resonance regimes mostly live outside of those probed by the EFT. We must keep in mind, though, that these estimates could still produce some

particles through parametric resonance, and should be studied through full lattice methods – we leave this to future work.

Our main conclusion thus far is that if we require the reheat field to respect the shift symmetry of the inflationary sector (implying adequate inflation consistent with CMB observations), successful reheating suggests considering an EFT cutoff far below the Planck scale $\Lambda \ll m_{\rm pl}$. We saw that having such a sub-Planckian cutoff can quickly lead to the breakdown of the background EFT expansion when we require efficient reheating in the EFT.

As another example of when the EFT expansion may breakdown, consider the corrections we have thus far neglected in (3.19). When evaluated on the background the operator contains a term

$$\frac{c_1}{\Lambda^4}\left(\partial\phi\right)^4 \supset \frac{c_1}{\Lambda^4}\dot{\phi}_0^2\left(\partial\phi\right)^2 . \tag{3.43}$$

During inflation this term will be slow-roll suppressed $\dot{\phi}_0^2/\Lambda^4 \sim \epsilon\, H^2 m_{\rm pl}^2/\Lambda^4$ and higher order terms will be even further suppressed as long as Λ is not far below $m_{\rm pl}$ during inflation[4]. However, for smaller values of the cutoff this corresponds to strong coupling of the background and our EFT approach breaks down – this would also lead to a large level of non-Gaussianity [65]. Assuming the background remains weakly coupled at the end of inflation we have

$$\frac{c_1}{\Lambda^4}\dot{\phi}_0^2 \sim \frac{m_\phi^2\phi_e^2}{\Lambda^4} \sim \left(\frac{m_\phi}{m_{\rm pl}}\right)^2\left(\frac{\phi_e}{m_{\rm pl}}\right)^2\left(\frac{m_{\rm pl}}{\Lambda}\right)^4, \tag{3.44}$$

so for Λ far below the Planck scale the EFT would again fail as this term would be as important as the kinetic term (and terms even higher in derivatives that we neglected would also be important). For example, in chaotic inflation where the inflaton mass is fixed by the COBE normalization this implies $\Lambda \gtrsim 10^{-3}\, m_{\rm pl}$. We emphasize that this constraint has nothing to do with requiring adequate inflation and is an added constraint for the consistency of the derivative expansion of the EFT during reheating. We now turn to a different EFT

4. Using the power spectrum normalization one can also show the condition $\dot{\phi}_0^2/\Lambda^4 < 1$ implies a lower bound $\Lambda/m_{\rm pl} \gtrsim \sqrt{\epsilon}\, 10^{-2}$, where $\epsilon = d(H^{-1})/dt$ is the slow-roll parameter.

approach where the challenges discussed in this section can be addressed.

3.2.3 The EFT of (p)Reheating

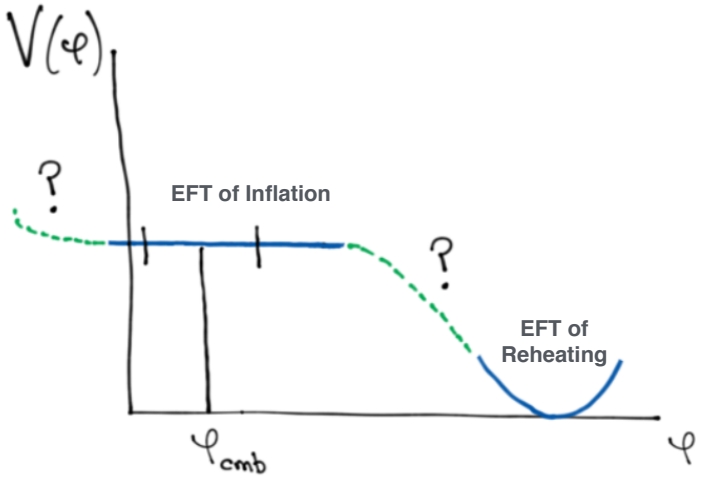

Figure 3.4: Obtaining adequate inflation, ending inflation and then successful reheating in the EFT requires a complete knowledge of the inflationary potential. This presents a challenge when using Weinberg's EFT approach to capture reheating in many classes of models.

We have seen that using an EFT approach to the background has limited utility in simultaneously describing inflation and reheating. Indeed, in addition to the challenges discussed at the end of Section 3.2.2, an additional concern is that there could be terms that badly break the shift symmetry at the time of reheating. Such terms could be small during inflation (suppressed by the breaking scale), but could be important at the time of reheating. Alternatively, there are many reheating models in which the shape of the potential during inflation is vastly different than it is during reheating (and could include additional fields like in hybrid models) and the background EFT approach requires a knowledge of the complete potential. This is illustrated in Figure 3.4.

In particular, the terms arising from the breaking of the shift symmetry of the inflaton (which would include thus far forbidden terms of the form $g_i \phi^p \chi^q$) could become as important

as the other terms we have considered in (3.38). As another example consider the potential

$$V = \frac{m^2 M^2}{2\alpha}\left[\left(1+\frac{\phi^2}{M^2}\right)^{\alpha} - 1\right]. \tag{3.45}$$

where $\alpha < 1$. This toy model captures many important inflationary models including axion monodromy [73]. During the inflationary phase this potential scales as $V \sim \phi^{2\alpha}$ and is sensitive to the scale M, whereas the behavior during reheating ($\phi < M$) is independent of M and $V \sim m^2\phi^2$. So in our EFT approach expanding the field in powers of ϕ/Λ is causing us to miss these types of theories.

In addition, new degrees of freedom could appear at the time of reheating that were heavy during inflation and could have been integrated out – in other words the EFT during inflation and the EFT during reheating can correspond to two distinct EFTs. This is not to say our approach doesn't capture many models. In particular, we've seen that the model of [66] is captured by our approach, and most chaotic inflation models would be as well. But even focusing only on the inflationary epoch we know that Weinberg's EFT is not capable of capturing a large number of interesting models. For example, in DBI type models where the background is in some sense strongly coupled one needs a non-perturbative expression for the background as it is a resummed expression where each derivative in the derivative expansion must be kept, e.g. $V \sim \sqrt{1-\dot{\phi}^2/\Lambda^4}$. Such models are not captured by the Lagrangian of (3.19). One may also anticipate reheating models where the background of the reheat field could also exhibit such non-linear behavior and then the derivative expansion of the Lagrangian (3.20) would be inadequate – as well as the expansion of the mixing terms stopping at dimension six in (3.21). One final objection is that we have only concentrated on scalar reheat fields. Reheating to fermions and gauge fields is also important, and the way in which this proceeds is not only model dependent, but the spin statistics can also make important differences in the efficiency of reheating [74].

Given these shortcomings of the EFT of the background we now turn to construct an

EFT for reheating along the lines of the EFT of Inflation [43]. As we will discuss, this approach can overcome many of the obstacles established in this Section. In the remainder of this section, we first begin by constructing an EFT focusing on the fluctuations directly at the end of inflation. This theory will share many similarities with the EFT of multi-field inflation [65; 44]. However there will be important differences which we will discuss. We then demonstrate how the approach can reproduce both the results of self resonant reheating and multi-field reheating. We also discuss some new models that arise from considering the symmetries of the EFT.

3.2.3.1 Construction of the EFT of Fluctuations

The EFT expansion in fluctuations (rather than the background) relies on the fact that the background expansion of the universe spontaneously breaks time-translation invariance. Over the history of the universe there have been many different dominant forms of matter and energy, and so many different sources of time-translation breaking including; inflatons, post-inflation / pre-BBN fields, radiation, dark matter, and eventually dark energy today. As the universe passed through these phases the energy density changed its composition many times, but the scale factor continued to monotonically increase. The EFT approach takes this background evolution as given *a priori* (as specified by the background functions $a(t)$, $H(t)$, and $\dot{H}(t)$) and focuses directly on the most general EFT for the fluctuations around this background.

In taking this approach we give up on realizing explicit models for the background, and instead focus on implications and observations associated with the fluctuations. In regards to connecting with observations this approach is adequate[5], since physical observables correspond to fluctuations and not background quantities [76]. The approach also has the advantage that the underlying physics responsible for driving the background expansion can

5. Although the connection to observables is not necessarily always straightforward [75].

be non-perturbative, in the sense that the background doesn't need to admit an EFT expansion (as we required in Section 3.2.2). Instead, this EFT approach is more general and models are classified by their symmetry breaking properties and the allowed operators in the Lagrangian correspond to cosmological perturbations. In many cases the symmetries alone can be used to establish rigid constraints on the theory of the fluctuations and associated observables. For example, it is well known that inflation requires that de Sitter symmetry must be non-linearly realized and this leads to constraints on inflaton correlation functions. This fact is manifest in the EFT of Inflation approach using the corresponding Goldstone boson [76]. This EFT approach has also been shown to be useful when the cosmological background changes its behavior, e.g. in the EFT of Dark Energy [47; 46; 48], where one is primarily interested in observations during matter domination, but also must account for observations during dark energy domination.

The generality of the EFT approach when applied to cosmological backgrounds was first established in [42], where the authors were investigating violations of the Null Energy Condition in non-standard cosmologies. In that paper, referencing earlier work of Weinberg [77], it was pointed out that on long wavelengths there is always an adiabatic mode corresponding to the Goldstone boson of spontaneously broken time diffeomorphism invariance. Whenever a decoupling limit exists – in which the Goldstone decouples from gravity – this broken symmetry is then realized as spontaneously broken time translation invariance (the gauge symmetry effectively becomes a global symmetry). Thus, for any FRW spacetime it is possible to utilize the EFT approach and it is in this vain that we will construct our EFT for reheating following the initial ideas presented in [22].

As an example, suitable for studying the dynamics at the end of inflation, we can consider a decelerated FRW expansion with the background metric

$$ds^2 = -dt^2 + a^2(t)\delta_{ij}dx^i dx^j, \quad \ddot{a}(t) < 0. \tag{3.46}$$

We can think of this background as generated by the evolution of a set of homogeneous scalars[6] fields, *i.e.* $\{\phi_0, \chi_0, \dots\}$. In this work, to study dynamics at the end of inflation, we may consider only one of the scalars, *e.g.* the inflaton ϕ_0, that contributes significantly to the evolution of scale factor, $a(t)$. This FRW evolution has a preferred time slicing described by the homogeneous scalar which can also be considered a clock. In order to describe the theory of fluctuations around this background, we can go to a co-moving frame (unitary gauge) where the vacuum expectation value of the scalar coincides with this privileged time slicing, corresponding to distinct values of $\langle\phi\rangle = \phi_0$. As we have fixed the slicing of space-time, general time diffs[7] are no longer a symmetry and the fluctuations of the scalar are hidden in the metric perturbations, which now describe three degrees of freedom: two transverse for the graviton and one for the scalar. We can always re-introduce inflaton fluctuations by a common local shift in time, *i.e.* $t \to t + \pi(x)$. By definition, such a fluctuation corresponds to an adiabatic fluctuation, proportional to Goldstone mode $\delta\phi = \dot{\phi}_0\pi$ associated with the broken symmetry. In this work, apart from the adiabatic fluctuations, we will consider an additional degree of freedom $X(t,x) = \chi_0(t) + \chi(t,x)$, which will play the role of the (p)reheat field. As is standard in the literature we will take this field to be a subdominant source of background evolution during the first stages of preheating (*i.e.* $\rho_\phi \gg \rho_\chi$) since before particle creation $\langle X\rangle \simeq 0$.

1. The Action in Unitary Gauge

The procedure for constructing the EFT of fluctuations for the inflationary sector coupled to a reheat field *at the time of reheating* is similar to the case of quasi-single field inflation considered in [79]. Those authors considered the effects of particle production during inflation, whereas here we consider reheating and important differences will be discussed below.

6. In general, we are not restricted to scalar fields, *e.g.* another example can be a set of perfect fluids.

7. As we mentioned before our main interest is the global part of time diffs, *i.e.* time translations. See [78] for more discussion on this matter.

Nevertheless, the action can be constructed analogously and working in unitary gauge the action for the fluctuations is

$$S = \int d^4x\sqrt{-g}\left[\frac{m_{\rm pl}^2}{2}R - f_1(t) - f_2(t)g^{00} + F^{(2)}(\delta g^{00}, \chi, \delta R_{\mu\nu\rho\sigma}, \delta K_{\mu\nu}; \nabla_\mu; t)\right], \quad (3.47)$$

where f_1 and f_2 are arbitrary functions of time, $F^{(2)}$ starts quadratic in operators which must be covariant in spatial indices but not in time, ∇_μ is the covariant derivative, and $\delta R_{\mu\nu\rho\sigma}$ and $\delta K_{\mu\nu}$ are the fluctuations in the Riemann tensor and extrinsic curvature, respectively. Note that the second and third terms in the above action are the only ones that contain linear perturbations. Requiring that terms linear in the fluctuations vanish (*i.e.* tadpole cancelation) follows from enforcing the background equations of motion in an FRW background [43],

$$3H^2m_{\rm pl}^2 = f_1(t) + f_2(t), \quad (3.48)$$

and

$$-2\dot{H}m_{\rm pl}^2 = 2f_2(t). \quad (3.49)$$

As a simple example of tadpole cancelation, consider the end of inflation where the inflaton begins oscillating with a potential $V(\phi)$ and where derivative interactions and the density of other fields are negligible. In this case the functions in (3.49) are given by $f_1 = V(\phi_0)$ and $f_2 = \dot{\phi}_0^2/2$. However, more generally, f_1 and f_2 can take any form as long as the background corresponds to the (p)reheating period, *i.e.* an FRW universe with possibly small corrections due to oscillations. For example, we could have a preheating model corresponding to DBI-like models of inflation where a large number of derivative self-interactions could play an important role [80]. In that case the functions f_1 and f_2 would contain terms with an infinite number of derivatives at the level of the background. The key is that the behavior of the matter sector will be captured by the functions f_1 and f_2, and once we cancel the tadpoles, the background is then given (by the equations of motion) by $H(t)$ and its derivatives. Then,

we can focus on the EFT of the fluctuations about this background – just as in the case of the EFT of Inflation or DE [43; 46; 47]. Thus, the problem we encountered in the previous section, where we would need to keep all the terms in the χ/Λ expansion is not an issue here. Instead, these terms are captured by H and $\dot{H}$ and could represent re-summed, non-perturbative expressions for the background[8]. Moreover, because we are *not* performing a perturbative expansion of the background, we work under the assumption that we have a complete knowledge of the potential overcoming the problems associated with Figure 3.4.

The most general action is found by expanding the function $F^{(2)}$ in (3.47) in terms of fluctuations $\{\delta g^{00}, \chi, \delta K_{\mu\nu}, \delta R_{\mu\nu\rho\sigma}\}$ and their derivatives. We emphasize that this EFT expansion is one in perturbations and derivatives. During reheating, the fluctuations are also assumed to be initially small, however significant particle production can change this (as we will discuss). Whereas the derivative expansion follows from locality, causality and unitarity in an FRW universe. In the gravity sector, δg^{00} is a zero derivative object, whereas $\delta K_{\mu\nu}$ corresponds to one derivative and $\delta R_{\mu\nu\rho\sigma}$ to two, as they contain first and second order derivatives of the metric, respectively. When we introduce the Goldstone boson in the next section, it will be clear that terms with δK and δR will include higher derivatives of the Goldstone boson. Finally, we find it convenient to split the action in (3.47) into three parts

$$S = S_{\rm g} + S_{\chi} + S_{{\rm g}\chi}, \tag{3.50}$$

where the action $S_{\rm g}$ contains only terms build out of $\{\delta g^{00}, \delta K_{\mu\nu}, \delta R_{\mu\nu\rho\sigma}\}$, S_{χ} contains those purely from χ and the action $S_{{\rm g}\chi}$ is due to mixing between gravity sector and χ.

8. The importance of strong coupling and resummation appears in many areas of physics including QCD and theories of modified gravity. See e.g. [81].

Following our discussion above, we then have

$$S_{\rm g} = \int d^4x\sqrt{-g}\left[\frac{m_{\rm pl}^2}{2}R - m_{\rm pl}^2\left(3H^2(t)+\dot{H}(t)\right) + m_{\rm pl}^2\dot{H}(t)g^{00} + \frac{m_2^4(t)}{2!}\left(\delta g^{00}\right)^2 + \ldots\right], \tag{3.51}$$

$$S_\chi = \int d^4x\sqrt{-g}\left[-\frac{\alpha_1(t)}{2}g^{\mu\nu}\partial_\mu\chi\partial_\nu\chi + \frac{\alpha_2(t)}{2}(\partial^0\chi)^2 - \frac{\alpha_3(t)}{2}\chi^2 + \alpha_4(t)\chi\partial^0\chi\right], \tag{3.52}$$

$$S_{{\rm g}\chi} = \int d^4x\sqrt{-g}\left[\beta_1(t)\delta g^{00}\chi + \beta_2(t)\delta g^{00}\partial^0\chi + \beta_3(t)\partial^0\chi - (\dot{\beta}_3(t) + 3H(t)\beta_3(t))\chi\right], \tag{3.53}$$

where $g^{00} = -1 + \delta g^{00}$ and the dots represent terms higher order in fluctuations and derivatives. Here, $\{m_2(t), \alpha_i(t), \beta_i(t)\}$ are thus far arbitrary functions of time that are permitted in the unitary gauge as time diffs have been spontaneously broken by the background. We note that the coefficient of the δg^{00} operator is fixed by the background, implying that it is *universal* in the sense that all preheating models with the same background evolution will have the same coefficient (specified by $H(t)$ and its derivatives). Whereas, the operator $\left(\delta g^{00}\right)^2$ is an example of a *non-universal* operator, because m_2 is not fixed by the symmetries of the FRW background. Instead its value corresponds to a specific class of models (those with a non-unity sound speed). Similarly, broken time diffs generally allow for a term proportional to α_2 that leads to non-trivial sound speed $c_\chi = \alpha_1/(\alpha_1+\alpha_2)$ in the reheat sector χ. In (3.53), the functions β_i can be seen as a measure of the strength of mixing with gravitational fluctuations (including one scalar d.o.f). At this stage, the usefulness of this approach might be in question, given the large number of free parameters. However, as we will see in the following sections, even though this is the most general theory to quadratic order, in practice many of the terms in (3.51)-(3.53) are not important for elementary processes within reheating. Finally, we can further simplify the action by performing a field re-definition of χ, using that $\chi = 0$ on the background trajectory and using time reparametrization invariance to set $\alpha_4 = \beta_3 = 0$ in the actions (3.52) and (3.53).

The form of (3.51), (3.52) and (3.53) are not particularly useful in studying the dynamics

as the scalar fluctuation representing inflaton is not manifest. We can re-introduce diffeomorphism invariance and the Goldstone mode related to inflaton by the Stückelberg trick, which will be our main focus in the following section.

2. Introducing the Goldstone Boson

To introduce the Goldstone boson along with time diffs, we first perform the broken time diffs $t \to t + \xi^0(t, \vec{x})$ in the actions (3.51)-(3.53). Since the cosmological background (*i.e.* $H, \dot{H}$) as well as the free functions $\{\alpha_i, \beta_i\}$ depend on cosmic time, t. The gauge function, ξ^0, will appear explicitly in the actions for the perturbations. We then replace $\xi^0 \to \pi(t, \vec{x})$ everywhere it appears in the action and require that the Goldstone transforms non-linearly, $\pi \to \pi - \xi^0$ under diffs. In this way, clearly full diffeomorphism invariance can be restored in (3.51)-(3.53). In order to find the explicit form of the actions including the Goldstone π, we need to know the transformation rule for the remaining operators appearing in (3.51)-(3.53) under $t \to t + \pi$. Under the transformation we have

$$\begin{aligned}
g^{00} &\to g^{00} + 2g^{0\mu}\partial_\mu\pi + g^{\mu\nu}\partial_\mu\pi\partial_\nu\pi, \\
g^{i0} &\to g^{i0} + g^{i\nu}\partial_\nu\pi, \\
\partial^0\chi &\to \partial^0\chi + g^{\mu\nu}\partial_\mu\chi\partial_\nu\pi, \\
f(t) &\to f(t+\pi) \qquad (3.54) \\
R_{\mu\nu\lambda\sigma} &\to R_{\mu\nu\lambda\sigma} \qquad (3.55) \\
\int d^4x\sqrt{-g} &\to \int d^4x\sqrt{-g}
\end{aligned}$$

where $f(t)$ represents any time-dependent function appearing in the action. Carrying out this procedure on the action (3.51) we find

$$S_{\rm g} = \int d^4x\sqrt{-g}\Bigg[\frac{m_{\rm pl}^2}{2}R - m_{\rm pl}^2\left(3H(t+\pi)^2 + \dot{H}(t+\pi)\right) + m_{\rm pl}^2\dot{H}(t+\pi)(g^{00} + 2g^{0\mu}\partial_\mu\pi + g^{\mu\nu}\partial_\mu\pi\partial_\nu\pi) + \frac{m_2^4(t+\pi)}{2!}(\delta g^{00} + 2g^{0\mu}\partial_\mu\pi + g^{\mu\nu}\partial_\mu\pi\partial_\nu\pi)^2\Bigg]\,. \tag{3.56}$$

We see that this action is invariant under time diffs if we require the Goldstone to transform as $\pi \to \pi - \xi^0(t,\vec{x})$, *i.e.* the symmetry is non-linearly realized [44]. We also note that requiring the symmetry be realized in the UV has forced relationships between the various operators (all the terms in parentheses must have the same coefficients). Following the same steps, (3.52) and (3.53) become

$$S_\chi = \int d^4x\sqrt{-g}\left[-\frac{\alpha_1(t+\pi)}{2}g^{\mu\nu}\partial_\mu\chi\partial_\nu\chi + \frac{\alpha_2(t+\pi)}{2}(\partial^0\chi + \partial_\mu\pi\partial^\mu\chi)^2 - \frac{\alpha_3(t+\pi)}{2}\chi^2\right], \tag{3.57}$$

$$S_{{\rm g}\chi} = \int d^4x\sqrt{-g}\Big[\beta_1(t+\pi)(\delta g^{00} + 2\partial^0\pi + \partial_\mu\pi\partial^\mu\pi)\chi + \beta_2(t+\pi)(\delta g^{00} + 2\partial^0\pi + \partial_\mu\pi\partial^\mu\pi)(\partial^0\chi + \partial_\mu\pi\partial^\mu\chi)\Big]. \tag{3.58}$$

Similar to the discussion above, the non-linearly realized symmetry introduces interactions between χ and the Goldstone, π.

To describe the dynamics at the end of inflation, working with the full action given by $S_{\rm g} + S_\chi + S_{{\rm g}\chi}$ in complete generality is a difficult task. First of all, we need to have some input for the time-dependent functions, *i.e.* $\{H(t), \alpha_i(t), \beta_i(t)\}$ appearing in the Lagrangian. However, as we will see, an investigation on the background dynamics during reheating along with the associated symmetries and scales of interest will allow us to obtain generic

information on the form of these functions. This will be our main focus in the next section.

3.2.3.2 Background Evolution During Reheating and Symmetries of the Action

1. Background Evolution and Symmetries

In parametrizing the background expansion we have assumed a decelerating FRW universe. A simple example is provided by a perfect fluid with an equation of state w and with corresponding scale factor $a(t) \propto t^{2/3(1+w)}$ and expansion rate $H(t) = \dot{a}/a \propto t^{-1}$ with H^{-1} setting the cosmic time scale. On the other hand, in studies of the dynamics at the end of inflation the frequency of inflaton oscillations introduce another important time scale. For example, if the inflaton oscillates in a power-law potential, $V \propto \phi_0^n$, the period of oscillations will be $2\pi\omega^{-1} = 4\int_0^{\phi_i} \mathrm{d}\phi_0 \ (V(\phi_i) - V(\phi_0))^{-1/2}$, which for general n depends on the initial amplitude, ϕ_i [82]. In the limit that the period of oscillations is much smaller than the expansion time scale, $\omega^{-1} \ll H^{-1}$, coherent scalar field oscillations behave like a perfect fluid with an average equation of state, $\langle w \rangle_{\mathrm{a}} = (n-2)/(n+2)$ [83].

The presence of two different time scales leads to interesting symmetry breaking patterns within the EFT, and whether a symmetry is realized will depend on the dynamics under investigation. At high energies (or small wavelengths) the energy being probed E_{probed} exceeds both the oscillation and expansion energy *i.e.* $E_{\mathrm{probed}} \gg \omega \gg H$ and so the time evolution of the oscillator and the cosmic expansion is negligible – time-translations are a good symmetry. As we lower the energy scale to $E_{\mathrm{probed}} \lesssim \omega$ we first break time-translation invariance down to a discrete symmetry $t \to t + 2\pi\omega^{-1}$. Then as we further lower the energy to $E_{\mathrm{probed}} \lesssim H \ll \omega$ this discrete symmetry is further broken by the cosmic expansion. This symmetry breaking reflects that on large scales (low-energy) we have an expanding universe, but on sub-Hubble scales the only time dependence results from the oscillating

scalar field and the effect of the expansion can be ignored. And at even higher energies (smaller distances / faster time scales) the scalar oscillations would not be probed.

This hierarchy in scales can be captured by parameterizing the background behavior by a Hubble rate that is a sum of a monotonically evolving part and a small rapidly oscillating component,

$$H(t) = H_{\rm FRW}(t) + H_{\rm osc}(t)P(\omega t), \tag{3.59}$$

where the first term is adiabatically evolving $H_{\rm FRW}(t) \propto t^{-1}$ and monotonically decreasing, whereas the second term leads to an oscillatory correction described by a general periodic function $P(\omega t)$ with period $T = 2\pi\omega^{-1}$. In order to ensure an overall monotonic FRW evolution we take the first term to be dominant, $H_{\rm FRW} \gg H_{\rm osc}$. This implies our clock is always monotonically increasing – as exemplified by the monotonic evolution of the scale factor $a(t)$ in an FRW universe. This situation is to be contrasted with models where the universe itself is oscillating [84], which can exhibit a number of pathologies [57]. We also note that the time dependence of $H_{\rm FRW}$ and $H_{\rm osc}$ is slow compared with the time scale of oscillations ω^{-1}, *i.e.* $\dot{H}_{\rm FRW}/(H_{\rm FRW}\omega) \sim \dot{H}_{\rm osc}/(H_{\rm osc}\omega) \ll 1$. This corresponds to our earlier statement that on short time scales (larger energies) there is an approximate discrete symmetry.

An important question is whether we can generalize the symmetry arguments above for the time-dependent functions associated with the non-universal operators in (3.56)-(3.58), *i.e.* $\{m_2, \alpha_i, \beta_i\}$. On general grounds, in an FRW background described by (3.59) we expect that the functions m_2, α_i, β_i – which describe the self-couplings, and couplings/mixings between the Goldstone and the reheat sector χ – to be a generic function of the Hubble rate in (3.59) and its derivatives. Depending on the couplings between these sectors this suggests that in general we can write these functions in the form

$$F_i(t) = M_i^p(t)P'(\omega' t), \tag{3.60}$$

where in general the periodic function P' is different from the one in (3.59) as is the frequency $\omega' \neq \omega$. Here, the index i collectively represents time-dependent functions $\{m_2, \alpha_i, \beta_i\}$ and p denotes the mass dimension of these functions. Suggested by the symmetry breaking pattern we discussed above, we can similarly take $\dot{M}_i/(M_i\omega) \ll 1$.

2. Symmetries of the Action and Implications

An important consequence of the discrete symmetry of the Goldstone is that non-derivative interactions can appear in the action. When this is a good symmetry we can expand the background and non-universal parameters $\{H, \dot{H}, m_2, \alpha_i, \beta_i\}$ in the form

$$F_i(t+\pi) = F_i(t) + \dot{F}_i(t)\pi + \frac{1}{2}\ddot{F}_i(t)\pi^2 + \dots \ . \tag{3.61}$$

This breaking is similar in spirit to the work of [85], where those authors considered resonant non-Gaussianity induced through small-scale oscillations in H and $\dot{H}$ during single-field inflation. In the two-sector EFT we are considering here we can extend that study to dynamics that arise in the presence of interactions between the Goldstone π and reheating χ sectors. Moreover, contrary to the situation during inflation, where there is a fixed energy scale corresponding to horizon crossing, [43], to study dynamics at the *end* of inflation we are often interested in the dynamics at sub-Hubble scales. For sub-Hubble scales with $E_{\rm probe} > \omega$ we expect interactions induced by expanding the time-dependent functions in (3.61), which parametrize important contributions to the dynamics. Such interactions can induce large loop corrections for the parameters of the EFT, and additionally back-reaction effects can become large and the perturbative expansion of the EFT of fluctuations will fail. In typical studies of preheating, the importance of such contributions correspond to the end of 'stage one', which can be followed by turbulence and chaotic behavior [28]. We leave an investigation of these stages to future work. In the following, we will focus on the

first stages of preheating and establish how our framework captures existing models. We will also explore new models and their connection to observations during the first stages of preheating.

3.2.3.3 Capturing Existing Models

1. Reheating Through Self-Resonance

In this section, we focus on the Goldstone sector in (3.56) to construct models of reheating through self-resonance. That is, we want to establish how the EFT reproduces self-resonant models of reheating where inflaton 'particles' (here corresponding to the Goldstone $\pi \sim \delta\phi$) are created from oscillations of the background condensate $\phi_0(t)$. We will also consider when gravitational fluctuations can be shown to decouple. To begin we expand the time-dependent functions in (3.56) and use the ADM decomposition[9] of the metric in spatially flat gauge working to second order in fluctuations $\delta N, N^i$ and π. We have

$$\begin{aligned}\mathcal{L}_{\pi_c} &= \frac{1}{2}\left(\dot{\pi}_c^2 - c_\pi^2\frac{(\partial_i\pi_c)^2}{a^2}\right) - \frac{1}{2}m_\pi^2(t)\pi_c^2 - \frac{(-2\dot{H})^{1/2}}{c_\pi}\left(\dot{\pi}_c\delta N_c - \frac{1}{2}\left(\frac{\ddot{H}}{\dot{H}} - 2\frac{\dot{c}_\pi}{c_\pi}\right)\pi_c\delta N_c\right) \\ &+ (-2\dot{H})^{1/2}c_\pi\left(3H\delta N_c + \partial_i N_c^i\right)\pi_c + \ldots \end{aligned} \tag{3.62}$$

where we introduced the canonical fields $\pi_c = \sqrt{-2\dot{H}m_{\rm pl}^2}\, c_\pi^{-1}\pi$, $\delta N_c = m_{\rm pl}\delta N, N_c^i = m_{\rm pl}N^i$, the sound speed of the fluctuations is $c_\pi^2 = m_{\rm pl}^2\dot{H}/(m_{\rm pl}^2\dot{H} - m_2^4)$, and we neglect terms involving the scalar curvature as they are sub-leading.

An important consequence of the background evolution and time-dependent sound speed

9. Details appear in Appendix A

is that it induces a time-dependent mass[10] for the Goldstone

$$m_\pi^2 = -3\dot{H}c_\pi^2 - \frac{1}{4}\left(\frac{\ddot{H}}{\dot{H}} - 2\frac{\dot{c}_\pi}{c_\pi}\right)^2 - \frac{3H}{2}\left(\frac{\ddot{H}}{\dot{H}} - 2\frac{\dot{c}_\pi}{c_\pi}\right) - \frac{1}{2}\partial_t\left(\frac{\ddot{H}}{\dot{H}} - 2\frac{\dot{c}_\pi}{c_\pi}\right), \tag{3.63}$$

which we note would vanish in a strictly de Sitter limit with constant sound speed (familiar from the EFT of Inflation). Resonant effects induced by such time dependence of c_π is an interesting possibility that we will explore in future work. For simplicity, here we will focus on the time-dependence of the background and assume that the time dependence of the sound speed is negligible.

To understand the Goldstone dynamics we first identify the energy scales at which different phenomena become important. An important scale is the symmetry breaking scale below which we are able to focus on the EFT of the perturbations (we can 'integrate out the background') and the Goldstone description can be useful. Following closely the example of [65], we can identify the Noether current associated with the broken symmetry by introducing 'fake' Lorentz invariance in (3.62) by rescaling the spatial coordinates

$$\tilde{\mathcal{L}}_{\rm g} = -\frac{1}{2}(\tilde{\partial}\tilde{\pi}_c)^2 + \ldots, \tag{3.64}$$

where $\tilde{x} \equiv c_\pi^{-1}x$, $\tilde{\mathcal{L}}_{\rm g} \equiv c_\pi^3\mathcal{L}_{\rm g}$ and $\tilde{\pi}_c = (-2\dot{H}m_{\rm pl}^2c_\pi)^{1/2}\pi_c$. The Noether current associated with (3.64) is then $\tilde{J}^\mu = -\Lambda_{\rm sb}^2\partial^\mu\tilde{\pi}_c$, and the symmetry breaking scale is given by[11] $\Lambda_{\rm sb}^2 = (-2\dot{H}m_{\rm pl}^2c_\pi)^{1/2}$.

For the simplest models, with unity sound speed, we have $\Lambda_{\rm sb}^2 = (-2\dot{H}m_{\rm pl}^2)^{1/2}$, and this agrees with expectations that the time evolution of the background is responsible for breaking the time translation symmetry ($H(t)$ is changing in time). In particular, given the background evolution in (3.59) we are interested in the time averaged value $\Lambda_{\rm sb}^2 \equiv$

10. This is the mass term in the absence of mixing terms given in the second and third lines of (3.62).

11. We present the scale in terms of energy, but it is important to remember that since Lorentz invariance is spontaneously broken energy scales do not necessarily coincide with momenta [43].

$\langle(-2\dot{H}m_{\rm pl}^2 c_\pi)^{1/2}\rangle_T \approx H_{\rm FRW} m_{\rm pl}\ c_\pi^{1/2}$. For energy scales where $E < \Lambda_{\rm sb}$ the Goldstone description of (3.62) is valid. We emphasize that we are focusing on fluctuations around a decelerating FRW background, and so the symmetry breaking scale is more dependent on time[12] than the inflationary case *i.e.* $\Lambda_{\rm sb}^2 \propto t^{-1}$. However, in the presence of resonance and with strong enough couplings to the reheating sector to make reheating efficient, it is justified to take a decoupling limit $H_{\rm FRW} \to 0$ and $m_{\rm pl} \to \infty$, such that the combination $H_{\rm FRW} m_{\rm pl}$ remains fixed. In this case, an evolving symmetry breaking scale is unimportant for the validity of the Goldstone description – all that is required is a hierarchy of scales $\Lambda_{\rm sb} \gg \omega$ where ω is the oscillation time scale associated with the background evolution that appeared in (3.59).

Another important scale in understanding the Goldstone dynamics is the energy scale where mixing with gravitational fluctuations becomes important ($E_{\rm mix}$). Consider the frequency of the Goldstone π_c in Fourier space and in the absence of mixing terms

$$\omega_\pi^2 = \frac{c_\pi^2 k^2}{a^2} + m_\pi^2(t) + \ldots, \tag{3.65}$$

where dots represent sub-leading contributions of order H^2. We emphasize that ω_π is the frequency of the Goldstone, whereas the inflaton oscillations have a frequency we continue to denote by ω which is often comparable to the Goldstone mass $\omega \sim m_\pi$ as follows from (3.59) and (3.63). Remembering this distinction, we note that contrary to the inflationary case, we are not interested in the dynamics at a fixed energy scale, and in general whether mixing with gravity is important will depend on the scales one is interested in. For example, we can separate the Goldstone modes into relativistic $\omega \lesssim c_\pi k/a$ (or equivalently $m_\pi \lesssim c_\pi k/a$) and non-relativistic $\omega > (c_\pi k)/a$ modes. For relativistic modes, time derivatives scale the same as spatial ones in (3.62), *i.e.* $\dot{\pi}_c^2 \sim c_\pi^2(\partial_i \pi_c/a)^2 \sim \omega_\pi^2 \pi_c$. On the other hand, for non-relativistic

12. This raises the interesting issue of 'level crossing', which is ubiquitous when applying EFT to gravitational systems [86].

modes, spatial derivatives are less important than time derivatives and terms involving the spatial kinetic terms can be compared with the mixing terms in (3.62). The most relevant mixing term[13] between π_c and gravitational fluctuations is given by

$$\mathcal{L}_{\rm mix} \supset \frac{(-2\dot{H})^{1/2}}{2c_\pi}\frac{\ddot{H}}{\dot{H}}\pi_c\delta N_c. \tag{3.66}$$

From Appendix A, we use the solution $\delta N_c \approx c_\pi\pi_c$ in (3.66) and note that $\dot{H} \approx H^2$, $\ddot{H} \approx \omega H^2$ (where we keep the leading terms). This leads to $\mathcal{L}_{\rm mix} \approx \omega H\pi_c^2$ from which we can see the energy scale at which mixing with gravity becomes important is $E_{\rm mix} \approx (\omega H)^{1/2}$. For relativistic modes, mixing with gravity is always irrelevant as $\omega_\pi^2 > \omega^2 \gg \omega H$. For non-relativistic modes, we compare the mixing term with the spatial kinetic term in (3.62). This leads to the conclusion that mixing with gravity will be important for modes with momenta satisfying the following condition,

$$\frac{k}{a} \lesssim \frac{\sqrt{\omega H}}{c_\pi} \tag{3.67}$$

An explicit example: The generic construction above is useful in studying models of inflaton self-resonance. Consider an example where mixing with gravity at the end of inflation leads to resonant effects for π_c. For this purpose, we consider a simple limit of the unitary gauge action in (3.51) where $m_2 = 0$, $m_{\rm pl}^2(3H^2 + \dot{H}) = V(\phi_0) = m_\phi^2\phi_0^2/2$, and $\dot{H}m_{\rm pl}^2 = -\dot{\phi}_0^2/2$. These choices correspond to a cosmology dominated by a single scalar field – the inflaton. In the regime where $m_\phi \gg H$, the background condensate oscillates around the minimum of its potential $V = m_\phi^2\phi_0^2/2$, and in this case we can solve for the background evolution [87]

$$H(t) \;=\; H_{\rm FRW}(t) - \frac{3H_{\rm FRW}(t)^2}{4m_\phi}\sin(2m_\phi t) + \ldots, \tag{3.68}$$

13. Another equally important term is the one proportional to $\dot{\pi}_c\delta N_c$. When we solve for δN_c in terms of π_c and use this solution in (3.62), we can integrate by parts the time derivative on π_c leading to a term comparable to (3.66).

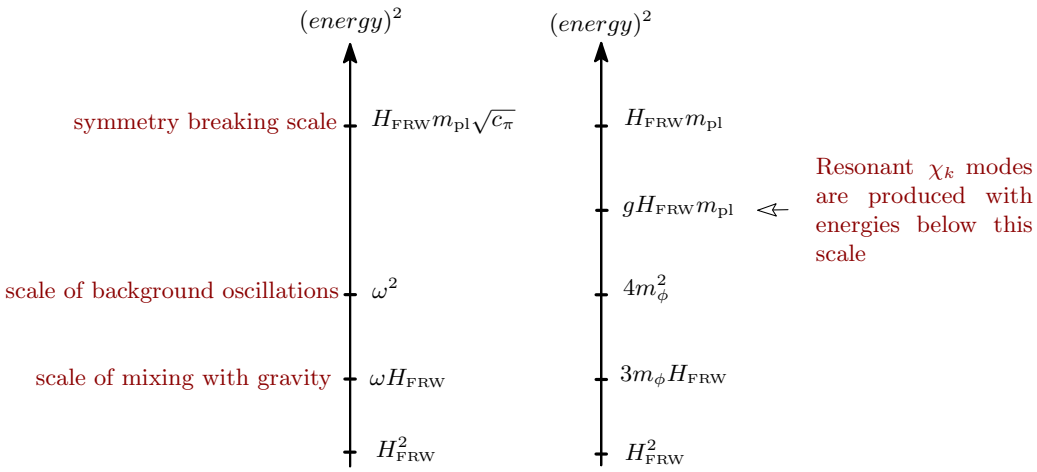

Figure 3.5: Relevant energy scales for the preheating models considered in Section 3.2.3.3. On the left, we have the hierarchy in energy scales associated with the dynamics of the Goldstone boson with a sound speed c_π following our general discussion of self-resonant models. The right diagram shows the hierarchy of scales for the example of canonical two-field preheating models.

where $H_{\rm FRW} = 2/(3t)$ is the Hubble rate in a matter dominated universe with scale factor $a(t) \propto t^{2/3}$ and dots represent terms suppressed by higher powers of H_m/m_ϕ. This solution has exactly the form proposed in (3.59) with $H_{\rm osc} \equiv -3H^2_{\rm FRW}/4m_\phi$, $\omega \equiv 2m_\phi$, and we also have $H_{\rm FRW} \ll m_\phi$.

Given the background evolution in (3.68), we can now consider the dynamics of π_c. To reproduce this class of models we take the $c_\pi \to 1$ limit, and solve for the constraints δN_c and N_c^i. Using our results from Appendix A, along with (3.62) we have

$$\mathcal{L}_{\pi_c} = -\frac{1}{2}(\partial\pi_c)^2 - \frac{1}{2}\Big(m_\pi^2(t) + m^2_{\rm mix}(t)\Big)\pi_c^2, \tag{3.69}$$

where the mass mixing induced by δN_c and N_c^i is

$$m^2_{\rm mix} = 6\dot{H} + 2\frac{\ddot{H}}{H} - 2\frac{\dot{H}^2}{H^2}. \tag{3.70}$$

Using the background evolution given by (3.68) and (3.70) the mode equation for the re-

scaled field variable $\tilde{\pi}_c = a^{3/2}\pi_c$ can be written as

$$\ddot{\tilde{\pi}}_c + \left[\frac{k^2}{a^2} + m_\phi^2\left(1 + 6\frac{H_{\rm FRW}}{m_\phi}\sin(2m_\phi t)\right)\right]\tilde{\pi}_c = 0, \tag{3.71}$$

where we have dropped additional terms further suppressed by $H^2_{\rm FRW}/m^2_\phi$ and $m^2_\pi \to V''(\phi_0) = m^2_\phi$ which follows from relating derivatives of the potential to the time derivatives of the Hubble rate given in (3.68) (See Appendix B).

To establish whether self-resonance results in particle production we can recast (3.71) in the form of a Mathieu equation by re-defining the time variable $z = m_\phi t + \pi/4$ with $A_k = 1 + k^2/(a^2 m^2_\phi)$ and $q = 3H_{\rm FRW}/m_\phi$. As the background evolution implies the hierarchy $H_{\rm FRW} \ll m_\phi$, this implies modes in equation (3.71) will be in the narrow resonance regime, $q \ll 1$. The first instability corresponds to the condition $A_k < 1 + q$ implying modes with momenta

$$\frac{k}{a} < \sqrt{3H_{\rm FRW}m_\phi} \tag{3.72}$$

will be amplified [28]. This result matches well with our previous estimate on the momentum scales where mixing with gravitational fluctuations is important in (3.67) (recalling we have $c_\pi = 1$ here).

Such resonant effects due to mixing with gravity have been considered previously in the literature [88; 89], where those authors studied the growth of the density perturbations and the onset of non-linear effects arising during oscillations of the background. Here, we can use the EFT to reproduce their results

$$\delta_k \equiv \frac{\delta\rho_k}{\bar{\rho}(t)} = \frac{\delta\rho_k}{3H^2 m^2_{\rm pl}} \propto \left(\frac{k}{aH_{\rm FRW}}\right)^2, \quad \text{for} \quad \frac{k}{a} < \sqrt{3H_{\rm FRW}m_\phi}, \tag{3.73}$$

where $\delta\rho_k$ is defined as

$$\delta\rho_k = (-2\dot{H})^{1/2} m_{\rm pl} \left[\dot{\pi}_c - \frac{1}{2}\left(3 + \frac{\ddot{H}}{\dot{H}} - 2\frac{\dot{H}}{H}\right)\pi_c \right]. \tag{3.74}$$

We now consider how the EFT captures models where the reheat sector results from the inflaton resonance given by the time-dependent functions in (3.57) and (3.58). If any of these couplings are stronger than gravitational strength the resonance in the reheat sector will typically dominate over the gravitationally induced effects discussed above.

2. Reheating in a Two-Field Model

In this section, we explicitly demonstrate how the EFT approach reproduces models of two-field reheating, taking as a concrete example the specific class of models given by (3.13). In the early stages of preheating the inflaton will dominate the energy density. We take the reheat field to be initially in its vacuum[14] with $\chi_0 = 0$, and we consider production of χ quanta in the presence of the oscillating inflaton condensate $\phi_0(t)$. In the unitary gauge with $\phi = \phi_0(t)$ and $\chi_0 = 0$, we have the following matter Lagrangian

$$S_m = \int d^4x\sqrt{-g}\left[-\frac{1}{2}\dot{\phi}_0^2 g^{00} - V(\phi_0) - \frac{1}{2}g^{\mu\nu}\partial_\mu\chi\partial_\nu\chi - \frac{1}{2}(U''(\chi_0) + g^2\phi_0^2)\chi^2 \right]. \tag{3.75}$$

Using the background equations of motion we can cancel the tadpole terms, $m_{\rm pl}^2(3H^2+\dot{H}) = V(\phi_0) = m_\phi^2\phi_0^2/2$, $\dot{H}m_{\rm pl}^2 = -\dot{\phi}_0^2/2$, and the unitary gauge matter Lagrangian is then given by

$$\mathcal{L}_m = m_{\rm pl}^2\dot{H}g^{00} - m_{\rm pl}^2(3H^2+\dot{H}) - \frac{1}{2}g^{\mu\nu}\partial_\mu\chi\partial_\nu\chi - \frac{1}{2}\left(m_\chi^2 + 2\frac{g^2 m_{\rm pl}^2}{m_\phi^2}(3H^2+\dot{H})\right)\chi^2, \tag{3.76}$$

14. We saw in Section 3.2.2 that it was a challenge for the background EFT model, but this is natural here as the shift symmetry of the background has been badly broken by the interactions.

where we defined $U''(\chi_0) \equiv m_\chi^2$. Comparing with the unitary gauge action (3.51) – (3.53), the matter Lagrangian (3.76) corresponds to the following choice for non-universal parameters in the EFT framework,

$$\alpha_1 = 1, \quad \alpha_3 = m_\chi^2 + 2\frac{g^2 m_{\rm pl}^2}{m_\phi^2}(3H^2 + \dot{H}), \quad \{m_2, \alpha_2, \alpha_4, \beta_1, \beta_2\} = 0. \tag{3.77}$$

We emphasize that in this model the linear mixing between the χ sector and gravitational sector (which includes the Goldstone in the unitary gauge) vanishes automatically since $\beta_1, \beta_2 = 0$ in (3.53). As before, we can introduce the Goldstone sector in (3.76) following the transformation[15] rules in (3.54). However, in the presence of strong resonance in the χ sector, *i.e.* if $\dot{\alpha_3}/\alpha_3^2 > \mathcal{O}(1)$ during any time in the linear stage of preheating, Goldstone fluctuations will be negligible compared to the χ's that are amplified through the strong resonance. In general, the validity of this argument relies on the strength of the coupling between the background and the χ sector through the mass term. For example, in the model we are considering here, introducing π via $t \to t + \pi$ (See also (3.54)) will lead to the Goldstone sector we have discussed in the previous section, where mixing with gravity leads to weak resonance $q \approx H_{\rm FRW}/m_\phi \ll 1$ (*c.f.* (3.71) and the discussion that follows). On the other hand, the strength of the resonance in the χ sector depends on the ratio $gm_{\rm pl}/m_\phi$ which can be quite large unless $g \ll 1$. Too see this in detail, it is enough to compare the scales in our EFT. The strength of the resonance in χ can be read from (3.77) and compared to the strength $\approx m_\phi H_{\rm FRW}$ of the resonance in the Goldstone sector in equation (3.71). The following condition is sufficient to neglect the Goldstone dynamics

$$g^2 \left(\frac{m_{\rm pl}}{m_\phi}\right) \left(\frac{\Lambda_{\rm sb}}{m_\phi}\right)^2 > 1. \tag{3.78}$$

15. It is important to note that the transformation $t \to t + \pi$ that introduces the Goldstone also induces non-linear interactions between the Goldstone and reheat sectors – we will elaborate on this below.

It is clear from this expression that unless the coupling constant is tiny $g \ll 1$ we can neglect the mild amplification of Goldstone due to mixing with gravity.

Another simplification we can make in this case is to consider the decoupling limit in the EFT where $|\dot{H}| \approx H^2_{\rm FRW} \to 0$ and $m^2_{\rm pl} \to \infty$, while keeping the combinations $\dot{H}m^2_{\rm pl}$ and $H^2 m^2_{\rm pl}$ as constant. In this limit, it is clear that π fluctuations will stay in their vacuum as the terms leading to narrow resonance vanishes ($H_{\rm FRW} \to 0$). We also note that the decoupling limit corresponds to taking the rigid space-time limit, $a \to 1$ that is commonly discussed in the preheating literature[16] [28; 29].

To study particle production, we can focus on the decoupling limit of the Lagrangian (3.76), and consider the mode equation for χ as,

$$\ddot{\chi}_k + \omega^2_\chi(t)\chi_k = 0 \tag{3.79}$$

where the time dependent frequency is given by

$$\omega^2_\chi = k^2 + m^2_\chi + \frac{g^2 m^2_{\rm pl}}{m^2_\phi}(3H^2 + \dot{H}). \tag{3.80}$$

In the decoupling limit, the time dependent mass induced by the background evolution stays intact, which is crucial for particle production. As we have mentioned before, particle production corresponds to the breakdown of the adiabaticity in the frequency, *i.e.* $|\dot{\omega}_\chi/\omega^2_\chi| > \mathcal{O}(1)$. Using (3.68) and the relations with the potential and Hubble rate in Appendix B, this condition translates into

$$K^2 \lesssim g\ H_{\rm FRW} m_{\rm pl} \approx g\Lambda^2_{\rm sb}, \tag{3.81}$$

where $K = \sqrt{k^2 + m^2_\chi}$ is the rescaled momenta. In the example we are considering, we

16. An additional and important point on the decoupling limit is that in this limit the time-dependent functions such as α_3 we are considering will be purely periodic functions. This can be seen by using (3.68) in equation (3.77) and taking the decoupling limit. This implies that EFT should respect an exact discrete symmetry in this limit.

see that this condition justifies the use of the EFT formalism as the resonant modes have a momenta much smaller than the symmetry breaking scale for small enough coupling, *i.e.* $H_{\rm FRW} m_{\rm pl} \equiv \Lambda_{\rm sb}^2 \gg g\Lambda_{\rm sb}^2$ for $g \ll 1$. The structure of the instability band along with the exponentially growing solutions in the χ sector have been studied many times in the literature [29]. Here, our main purpose is to show the connection of the EFT approach to well established two-field reheating models.

Another potential use of EFT formalism is to capture the effects of backreaction. This can be achieved by realizing that once we introduce the Goldstone mode in the unitary gauge Lagrangian (3.76) the time dependent mass (and for general models other time dependent functions) of χ becomes $\alpha_3(t+\pi)$. As α_3 is a rapidly varying function of time in the presence of particle production in the χ sector, this term will induce higher order interactions between π and χ upon expanding the function,

$$\mathcal{L}_{int} = -\frac{1}{2}\left(\dot{\alpha}_3\pi + \frac{1}{2}\ddot{\alpha}_3\pi^2\right)\chi^2. \tag{3.82}$$

In particular, in the current example the first term in (3.82) will lead to a tadpole term for $\pi_c = (-2\dot{H})^{1/2} m_{\rm pl}\pi$. In the Hartree approximation [28] this gives

$$\mathcal{L}_{int} \supset -\frac{1}{2}\frac{\dot{\alpha}_3}{(-2\dot{H}m_{\rm pl}^2)^{1/2}}\langle\chi^2\rangle\pi_c, \tag{3.83}$$

where

$$\langle\chi^2(t)\rangle = \frac{1}{2\pi^2}\int_0^\infty dk\ k^2\ |\chi_k(t)|^2. \tag{3.84}$$

The existence of such a tadpole term can be considered as an indication of backreaction effects. For example, as we produce χ particles the coefficient in front of π_c will grow and may eventually disturb the background evolution. In particular they can increase the

frequency of the background oscillations of the condensate [28],

$$m_\phi^2 \to m_\phi^2 + \frac{\dot{\alpha}_3}{(-2\dot{H}m_{\rm pl}^2)^{1/2}}\langle\chi^2\rangle \tag{3.85}$$

In order to understand the onset of the backreaction effects in the presence of particle production, we can compare the second term in (3.85) with m_ϕ^2. We refer to this time where the backreaction becomes important as t_b and the condition reads

$$m_\phi^2 = \frac{\dot{\alpha}_3(t_b)}{(-2\dot{H}(t_b)m_{\rm pl}^2)^{1/2}}\langle\chi^2(t_b)\rangle \tag{3.86}$$

Knowing the solutions for χ_k, the background evolution (3.68) and the couplings α_3 one can calculate t_b.

We emphasize that our discussion in this section is not limited to the example given by (3.77). Using the EFT formalism, we can in principle capture models that belong to the same "universality class", *i.e.* direct coupling models with interactions including $\mathcal{L}_m \propto \mu\phi\chi^2$ and non-renormalizable couplings $\mathcal{L}_m \propto \phi^n\chi^2/M^{n-2}$ where $n > 2$ and M, μ are energy scales [90].

3.2.3.4 A New Class of Reheating Models

In the previous section, we showed how the EFT captures resonance effects in two-field reheating models. We now reconsider particle production in the presence of a reduced sound speed for the reheat field, $c_\chi \neq 1$. Familiar from the EFT of Inflation and Dark Energy, there is no symmetry protecting $c_\chi = 1$ in the EFT of reheating. This gives rise to a new class of models for preheating where the produced particles can have $c_\chi \ll 1$.

We follow our previous discussion in Section 3.2.3.2 and consider the time-dependent functions associated with the reheat sector $\{\alpha_i, \beta_i\}$. The terms proportional to β_1 and β_2 in (3.58) lead to mixing of χ with both gravity and the Goldstone sector. We will ignore

these terms here, leaving a discussion of them to Appendix A. In the absence of these mixing terms we focus on the action (3.57). Defining the canonical field $\chi_c = \alpha_\chi(t)\chi$ where $\alpha_\chi^2(t) = \alpha_1(t)+\alpha_2(t)$, we have the following second order Lagrangian for the canonical reheat field

$$\mathcal{L}_{\chi_c} = \frac{1}{2}\left[\dot{\chi}_c^2 - c_\chi^2(t)\frac{(\partial_i\chi_c)^2}{a^2}\right] - \frac{1}{2}m_\chi^2(t)\chi_c^2, \tag{3.87}$$

where we have defined the sound speed $c_\chi^2 = \alpha_1/(\alpha_1+\alpha_2)$ and the time-dependent mass term is

$$m_\chi^2(t) = \frac{\alpha_3(t)}{\alpha_\chi^2(t)} - \left(\frac{\dot{\alpha_\chi}}{\alpha_\chi}\right)^2 + 3H\left(\frac{\dot{\alpha_\chi}}{\alpha_\chi}\right) + \partial_t\left(\frac{\dot{\alpha_\chi}}{\alpha_\chi}\right). \tag{3.88}$$

Similar to the Goldstone case in Section 3.2.3.3, we have a time-dependent mass $m_\chi(t)$ induced by the time dependence of the sound speed c_χ and α_1 [17]. We will concentrate on strong resonant effects due to non-adiabaticity in the time-dependent coefficient α_3 and assume that the time variation of α_χ is slow compared to α_3, so that the sound speed is nearly constant[18] (where $\alpha_1, \alpha_2 \approx$ *constant*). We can then neglect the last three terms in (3.88) and the mode equation for the re-scaled field variable $\tilde{\chi}_c = a^{3/2}\chi_c$ in Fourier space is

$$\ddot{\tilde{\chi}}_c^k + \left[c_\chi^2\frac{k^2}{a^2} + \alpha_3 + \Delta\right]\tilde{\chi}_c^k = 0, \tag{3.89}$$

where $\Delta = -3(3H^2+2\dot{H})/4 \approx \mathcal{O}(H^2)$ are gravitational terms resulting from the rescaling $\chi_c \to \tilde{\chi}_c$ and we have absorbed the constants α_1, α_2 into the definition of α_3. Following our discussion in Section 3.2.3.2, it is convenient to parameterize α_3 as $\alpha_3 = M^2(t)F(\omega t)$, where $M(t)$ is always adiabatic so that $\dot{M}/M^2 \ll 1$ and F is a periodic function which must violate adiabaticity so that preheating occurs. That is, at some point adequate particle production requires the so-far arbitrary function to satisfy $\dot{F}/F^2 > 1$. In many models the periodicity of the function will be set by the background evolution in (3.59). We focus on

17. Recall that $c_\chi^2 = \alpha_1/\alpha_\chi^2$

18. Again, we leave the interesting case of strong time dependence of the sound speed to future work.

the strong resonance regime where $M \gg H$ and $M/\omega \gg 1$ and hence drop $\mathcal{O}(H^2)$ terms in the frequency ω_χ^2,

$$\omega_\chi^2 = c_\chi^2 \frac{k^2}{a^2} + M^2 F(\omega t). \tag{3.90}$$

The non-adiabaticity in α_3 will lead to non-adiabaticity in the frequency ω_χ^2, *i.e.* $\dot{\omega}_\chi/\omega_\chi^2 > \mathcal{O}(1)$. We take this to occur as times t_j when ω_χ^2 is at its minimum[19]. This suggests that we can expand the frequency around the times t_j as

$$\omega_\chi^2 \simeq c_\chi^2 \frac{k^2}{a^2} + \frac{1}{2} M^2 \omega^2 (t - t_j)^2 + \dots \tag{3.91}$$

where we have used $\ddot{F} \approx \omega^2 F$ and dots represent higher order terms in the $t - t_j$ expansion. This allows us to re-write the mode equation in a simpler form

$$\ddot{\tilde{\chi}}_c^k + \left[c_\chi^2 \frac{k^2}{a^2} + \frac{M^2 \omega^2}{2} (t - t_j)^2 \right] \tilde{\chi}_c^k = 0 \tag{3.92}$$

and the typical momenta when adiabaticity is violated $\dot{\omega}_\chi > \omega_\chi^2$ corresponds to

$$k_*^2 \equiv \frac{M\omega}{c_\chi^2} \gtrsim \frac{k^2}{a^2}, \tag{3.93}$$

We see that for $c_\chi < 1$, the physical wave numbers inside the resonant regime are further enhanced (the resonance band is broadened) compared to the standard cases that have been studied in the literature. It is customary to map the mode equation (3.92) to a scattering problem described by a Schrödinger equation with a negative parabolic potential by defining a new time variable $\tau \equiv c_\chi k_* (t - t_j)$ and a dimensionless physical momentum $\kappa \equiv k/(a k_*)$,

$$\frac{d^2 \tilde{\chi}_c^k}{d\tau^2} + \left(\kappa^2 + \tau^2 \right) \tilde{\chi}_c^k = 0. \tag{3.94}$$

19. Note that here we are focusing on non-tachyonic resonance, for tachyonic resonance this situation will be different, see *e.g.* [90].

The solution to the scattering problem and the resulting number density of particles between scattering events has appeared in the literature many times [28; 91] (See also [39]). In real space, the growth of the number density of particles can be described by the following expression [28],

$$n_\chi(t) = \frac{1}{2\pi a^3}\int d^3k\; n_\chi^k(t) \sim \frac{k_*^3}{\sqrt{\pi\mu m_\phi t}} e^{2\mu m_\phi t}, \tag{3.95}$$

where (for simplicity) we have assumed that the background is given by the quadratic potential we considered before, *i.e.* $\omega \sim m_\phi$. Here μ is the maximum value of the Floquet index at $k_{\rm max} \approx k_*/2$ [28]. It is clear from this expression that there will be an enhancement in the number of produced particles due to the small sound speed in the χ sector, $k_* \propto c_\chi^{-1}$. This also agrees with our intuition as equation (3.93) tells us that resonant bands are wider for $c_\chi < 1$ and thus the contribution to the integral in (3.95) over resonant modes will be enhanced by factors of c_χ^{-1}. In the next section we will consider observational consequences of the EFT of reheating, focusing on this new class of models with non-standard sound speed. We also discuss additional challenges and future directions for the approach.

3.2.4 Challenges and Outlook

In Section 3.2.3, we have presented an EFT approach to reheating that overcomes the challenges of the background evolution discussed in Section 3.2.2 and is adequate to capture all existing reheating models in the literature. Guided by symmetries, our approach is also useful for finding new models of reheating, *e.g.* we found a new class of models where the reheating sector has $c_\chi \neq 1$. However, there are many challenges remaining for our EFT approach.

One of the more serious concerns is the lack of a direct connection to observations. This problem is not specific to our approach, with the lack of direct observational constraints on reheating being an important reason that far less is known about this epoch than inflation. In our EFT framework, symmetries help to alleviate more of the theoretical uncertainties

associated with reheating than a toy model approach. For example, the need to non-linearly realize time translations demonstrated that many of the unknown coefficients are related, and the need to violate non-adiabaticity (required for particle production) also placed some level of theoretical constraint on the reheating sector. Nevertheless, we saw in Section 3.2.3 there are a large number of free functions that must be further restricted by observations. Unlike the situation for inflation, where non-Gaussianity and features in the primordial power spectrum are a rich source of observational constraints, direct observational constraints on reheating are lacking. One possibility to remedy this is gravitation wave (GW) signatures.

Once particles are produced during reheating[20] they can scatter off each other creating a background of GWs [32; 35]. The scattering leads to a transverse-traceless source for the gravitons

$$\ddot{h}_{ij} + 3H\dot{h}_{ij} - \frac{1}{a^2}\partial^2 h_{ij} = \frac{2}{m_{\rm pl}^2} T_{ij}^{TT} \tag{3.96}$$

Following the methods of [92] we can then estimate the critical density of gravitational waves today[21]

$$\Omega_{\rm gw} = \frac{S_k(t_f)}{a_J^4\ \rho_J}\ \left(\frac{a_J}{a_{\rm rh}}\right)^{1-3w} \left(\frac{g_{\rm rh}}{g_0}\right)^{-1/3} \Omega_{r,0}, \tag{3.97}$$

where subscript "0" denotes a quantity evaluated today, 'J ' represents the time when the universe becomes radiation dominated and 'rh' denotes the beginning of reheating. Here, ω is the average equation of state of the universe between the time interval $t_J < t < t_{\rm rh}$ and g_i is the effective relativistic degrees of freedom. Finally, the source term S_k encodes the predictions for different classes of models in the EFT.

For example, let us consider the new class of models discussed in Section 3.2.3.4. In that

20. This should not be confused with sourcing a gravity perturbation with a second order scalar perturbation. Here we are considering on-shell particles that are classically scattering off of each other and generating a GW spectrum. We refer the reader to [92] for more details.

21. For a different approach we refer the reader to [93].

case the source term S_k is given by

$$\begin{aligned} S_k(t_f) &= \frac{c_\chi^4\, k^3}{4\pi^2 m_{\rm pl}^2} \int dp \int_{-1}^{1} d(\cos\theta)\; p^6 \sin^4\theta \\ &\times \left[\left| \int_{t_i}^{t_f} dt \cos(kt)\, \chi_c(p,t)\chi_c(|\vec{k}-\vec{p}|,t) \right|^2 + \left| \int_{t_i}^{t_f} dt \sin(kt)\, \chi_c(p,t)\chi_c(|\vec{k}-\vec{p}|,t) \right|^2 \right] \end{aligned} \tag{3.98}$$

where we focus on two-body scattering, θ is the scattering angle, and we assume that scattering happens at a fast enough rate that we can neglect the Hubble expansion. To get an order of magnitude estimate we can focus on the low momenta. In this case, the contribution of the mode functions to time integrals will be maximal for $p_* = \sqrt{M\omega}/c_\chi$ and defining a dimensionless momentum $P = p/p_*$ we have

$$S_k^{j+1} \sim \frac{1}{c_\chi^3} \frac{(M\omega)^{3/2} k^3}{m_{\rm pl}^2} \int_{-1}^{1} d(\cos\theta) \sin^4\theta \int\; dP P^6 \times [Time\ integrals], \tag{3.99}$$

where we recall that α_3 is parameterized by M and ω as in (3.92), and so the EFT parameters are determining the strength of the GW signal. Moreover, the gravitational waves will be amplified by a factor of c_χ^{-3}. This scaling may be counter-intuitive to the reader. The prefactor in (3.98) results from the two-to-two scattering of the particles as their momenta is now $p \to c_\chi p$. However, the lower sound speed implies it costs less energy to produce the particles leading to an enhancement of the particle production rate, and more particles scattering leads to more gravity waves. Thus, the GW signal is enhanced compared to the $c_\chi = 1$ case. Assuming this signal survives the later stages of reheating the detectability will depend on the peak frequency [32; 35; 93]

$$f = \frac{\sqrt{M\omega}}{a_j \rho_j^{1/4} c_\chi}\, 4 \times 10^{10}\ \text{Hz}, \tag{3.100}$$

which again depends explicitly on the EFT parameters and the sound speed. We see that

by reducing the sound speed we can increase the frequency in the new class of reheating models.

GWs provide one way to constrain the EFT parameters. However, we leave a more complete analysis, which requires following the signal through all the stages of reheating[22], to future work. Primordial Black Hole constraints and the matching of inflationary perturbations to late time observables lead to additional ways in which the EFT parameters may be restricted. In regards to the latter, we have stressed that direct observables correspond to perturbations, however the subtle ways in which we match inflationary predictions to CMB and LSS observations does depend implicitly on the background dynamics, particularly through the equation of state. Recently, it has been shown that the physics of reheating (including non-linearities and back-reaction) can have subtle and interesting effects on the equation of state and the dynamics of thermalization [95]. We hope to return to these issues and interesting possibilities in future work.

In addition to the challenge to connect with observations, a number of theoretical issues remain to be addressed. In particular, in this work we have primarily focused on connecting the EFT to scalar field driven models of reheating. However, the spectator field χ can be thought of as an additional clock field, which can also represent reheat fields beyond spin zero. Extending our framework to other spins is an important consideration. We have also primarily focused on the first stage of reheating in the EFT. However, one of the most useful applications of our approach could be to gain a better understanding of the rescattering and back-reaction effects that happen following the first stage. These are stages that usually require lattice simulations, and the Goldstone approach could be a fruitful way to get a better analytical understanding. There is also the issue of when the produced particles become significant enough that they contribute to the energy density. At this point the Goldstone boson (related to the matter sector responsible for time-translations being broken) can change

22. One interesting approach would be to see if we could combine the EFT framework here with the recent fitting analysis of [94].

its nature from inflatons to the reheat field. How this transition proceeds is important for establishing the connection between the Goldstone and the background fields. This is similar to the situation in studies of dissipation in the EFT of Inflation (see *e.g.* [96]), and we expect many of the techniques there could prove useful for the case of reheating as well.

Appendix A: ADM Formalism and Mixing with Gravity

To account for gravitational fluctuations and discuss the regime where they are irrelevant to the dynamics of the Goldstone we decompose the metric in the ADM form. In the spatially flat gauge we have

$$ds^2 = -(N^2 - N_i N^i)dt^2 + 2N_i dx^i dt + \hat{g}_{ij}\, dx^i dx^j, \tag{3.101}$$

where $\hat{g}_{ij} = a^2(\delta_{ij} + h_{ij})$ is the spatial metric and our gauge choice implies $h_{ii} = \partial_i h_{ij} = 0$. Inverse metric elements can be written as

$$g^{00} = -\frac{1}{N^2}\,, \quad g^{0i} = g^{i0} = \frac{N^i}{N^2}\,, \quad g^{ij} = h^{ij} - \frac{N^i N^j}{N^2}\,. \tag{3.102}$$

To find the relevant terms in the gravitational sector, we expand the Einstein Hilbert term as

$$S_{\rm g} \supset \frac{m_{\rm pl}^2}{2}\int d^4x\,\sqrt{-g}\,R = \frac{m_{\rm pl}^2}{2}\int d^4x\,\sqrt{\hat{g}}\,\big[NR^{(3)} + \frac{1}{N}(E^{ij}E_{ij} - E^i{}_i{}^2)\big], \tag{3.103}$$

where $R^{(3)}$ is the three curvature associated with spatial metric $\hat{g}_{ij}$ and E_{ij} is related to the extrinsic curvature of constant time slices through

$$E_{ij} \equiv NK_{ij} = \frac{1}{2}[\partial_t \hat{g}_{ij} - \hat{\nabla}_i N_j - \hat{\nabla}_j N_i]\,, \tag{3.104}$$

where $\hat{\nabla}_i$ is the covariant derivative with respect to spatial metric $\hat{g}_{ij}$. Using the above

expressions, we can expand (3.56) up to second order in scalar fluctuations

$$S_{\rm g}=\int d^4x\,a^3\Bigg[\;-\;\frac{m_{\rm pl}^2\dot{H}}{c_\pi^2}\Big(\dot{\pi}^2-c_\pi^2\frac{(\partial_i\pi)^2}{a^2}\Big)-3m_{\rm pl}^2\dot{H}^2\pi^2+m_{\rm pl}^2(2c_\pi^{-2}\dot{H}\dot{\pi}-6H\dot{H}\pi)\delta N+2m_{\rm pl}^2\dot{H}N^i\partial_i\pi$$
$$-\;m_{\rm pl}^2(3H^2+c_\pi^{-2}\dot{H})\delta N^2-2m_{\rm pl}^2H\delta N\partial_iN^i\Bigg] \tag{3.105}$$

where the speed of sound is defined as $c_\pi^2=m_{\rm pl}^2\dot{H}/(m_{\rm pl}^2\dot{H}-m_2^4)$. Defining the canonical fields, $\pi_c=\sqrt{-2\dot{H}m_{\rm pl}^2}\;c_\pi^{-1}\pi,\delta N_c=m_{\rm pl}\delta N,N_c^i=m_{\rm pl}N^i$, one can re-write the Lagrangian as in (3.62).

Focusing on the Goldstone sector for now, we can solve for the Lagrange multipliers δN and N^i in terms of π. To linear order in π we have,

$$\delta N=-\frac{\dot{H}}{H}\pi,\qquad\partial_iN^i=c_\pi^{-2}\frac{\dot{H}}{H^2}\partial_t\left(H\pi\right). \tag{3.106}$$

Using the canonical field definitions above we may write

$$\delta N_c=\frac{(-2\dot{H})^{1/2}}{2H}\pi_c,\qquad\partial_iN_c^i=c_\pi^{-2}\frac{\dot{H}}{H^2}\partial_t\left(\frac{c_\pi H\pi_c}{(-2\dot{H})^{1/2}}\right). \tag{3.107}$$

Using these solutions for the gravitational fluctuations $\delta N_c\;N_c^i$ in (3.62) (while taking the $c_\pi\to1$ limit) we recover the result of (3.69).

In the presence of a reheat sector χ, we need to take into account the mixing between χ and gravitational fluctuations, as well as $\pi-\chi$ mixings. Considering the mixings at second order we need to take into account the action in (3.58). Expanding up to second order in δN, N^i, π and χ, we have

$$S_{\rm mix}^{(2)}=\int d^4x\,a^3\Big[2\beta_1\left(\delta N-\dot{\pi}\right)\chi-2\beta_2\left(\delta N-\dot{\pi}\right)\dot{\chi}\Big]. \tag{3.108}$$

We note that the action (3.57) does not lead to any second order mixing therefore it is

enough to consider the mixing action above. Combining (3.105) and (3.108) in the presence of mixing we have the following solutions for the constraints,

$$\delta N = -\frac{\dot{H}}{H}\pi, \qquad \partial_i N^i = c_\pi^{-2}\frac{\dot{H}}{H^2}\partial_t\left(H\pi\right) + \frac{\beta_1}{m_{\rm pl}^2 H}\chi - \frac{\beta_2}{m_{\rm pl}^2 H}\dot{\chi}. \tag{3.109}$$

We see that inclusion of reheat sector does not change the solution for δN, but we have additional contributions to N^i proportional to the time-dependent parameters β_1, β_2 . To illustrate the decoupling of χ, we consider a simple π_c sector with $c_\pi = 1$ and note that time derivatives of canonically normalized fields χ_c and π_c have the approximate scalings in the WKB approximation,

$$\dot{\pi}_c \approx \omega_\pi \pi_c \sim \omega \pi_c, \qquad \dot{\chi}_c \approx \omega_\chi \chi_c \sim \sqrt{\alpha_3}\chi_c \sim M\chi_c, \tag{3.110}$$

where we take $|\alpha_3| = M^2$ following our discussion in the main text and focused on the non-relativistic modes for both fields. Following our discussion in section 3.2.3.2, we assume that the strength of the couplings β_1 and β_2 is as strong as the time-dependent parameter α_3 responsible for the resonance. By dimensional analysis, we therefore take $|\beta_1| \sim M^3$ and $|\beta_2| \sim M^2$. Canonically normalizing the fields as before we find from (3.108) that for resonant modes mixing between χ_c and gravitational fluctuations can be neglected in the following range of momenta

$$\left(\frac{M}{\Lambda_{\rm sb}}\right)\sqrt{MH} < \frac{c_\chi k}{a} < \sqrt{M\omega}. \tag{3.111}$$

Similarly we have the following range where we can neglect direct mixing between π_c and χ_c,

$$\left(\frac{M}{\Lambda_{\rm sb}}\right)\sqrt{M\omega} < \frac{c_\chi k}{a} < \sqrt{M\omega}. \tag{3.112}$$

Consistency of the EFT picture requires $M/\Lambda_{\rm sb} \ll 1$ and we see that within this regime we

can neglect both types of mixing for a wide range of momenta. In particular, with some mild assumptions, we showed that in the presence of strong resonance, we can neglect the mixings between π_c and χ_c. This finding is similar in spirit to the discussion presented in the recent works [97; 39] where those authors pointed out that it is technically natural to assume a flat field space metric in the presence of strong disorder/resonance.

We conclude this appendix by giving the second order action for tensor perturbations and their interaction with π_c and χ_c that we used in the main text. Using the gravitational part of the action in (3.103) with (3.104) and noting the Ricci curvature $R^{(3)}$ on spatial hyper-surfaces,

$$R^{(3)} = \hat{g}^{ik}\partial_l\Gamma^l_{ik} - \hat{g}^{ik}\partial_k\Gamma^l_{il} + \hat{g}^{ik}\Gamma^l_{ik}\Gamma^m_{lm} - \hat{g}^{ik}\Gamma^m_{il}\Gamma^l_{km}, \tag{3.113}$$

$$\Gamma^k_{ij} = \frac{1}{2}\hat{g}^{kl}\left(\partial_i\hat{g}_{jl} + \partial_j\hat{g}_{il} - \partial_l\hat{g}_{ij}\right), \tag{3.114}$$

we have the following second order action for the tensor part of the metric fluctuations

$$S_{\rm g} = \frac{m_{\rm pl}^2}{8}\int d^4x\, a^3\left(\dot{h}_{ij}\dot{h}_{ij} - \frac{\partial_k h_{ij}\partial_k h_{ij}}{a^2}\right). \tag{3.115}$$

On the other hand, expanding the actions (3.56) and (3.57) we find the following cubic order interactions between π_c and χ_c

$$S_{hXX} \supset \int d^4x\, a^3\left(\frac{c_\chi^2}{2}h_{ij}\frac{\partial_i\chi_c\partial_j\chi_c}{a^2} + \frac{c_\pi^2}{2}h_{ij}\frac{\partial_i\pi_c\partial_j\pi_c}{a^2}\right). \tag{3.116}$$

Appendix B: Relating Unitary Gauge to the Scalar Potential

In cosmologies dominated by a scalar field, we can map the time-dependent background quantities in our Unitary gauge Lagrangian (3.51) to the explicit scalar field models with a

given potential $V(\phi_0)$. A simple example we provided in the main text was

$$V(\phi_0) = m_{\rm pl}^2(3H^2(t) + \dot{H}(t)), \qquad -2\dot{H}m_{\rm pl}^2 = \dot{\phi}_0^2 \tag{3.117}$$

Using $\mathrm{d}\phi_0 = \dot{\phi}_0 dt$ and time derivatives of expressions in (3.117), we can relate the derivatives of the potential with respect to ϕ to the time derivatives of the Hubble rate $H(t)$. Here, we list some of these expressions,

$$V'(\phi_0) = \frac{m_{\rm pl}}{(-2\dot{H})^{1/2}}\left(6H\dot{H} + \ddot{H}\right), \tag{3.118}$$

$$V''(\phi_0) = -3\dot{H} - \frac{1}{4}\left(\frac{\ddot{H}}{\dot{H}}\right)^2 - \frac{3H}{2}\left(\frac{\ddot{H}}{\dot{H}}\right) - \frac{1}{2}\partial_t\left(\frac{\ddot{H}}{\dot{H}}\right), \tag{3.119}$$

$$V'''(\phi_0) = \frac{1}{(-2\dot{H}m_{\rm pl}^2)^{1/2}}\left[-\frac{H^{(4)}}{2\dot{H}} - \frac{9\ddot{H}}{2} + \frac{\ddot{H}^3}{2\dot{H}^3} - \frac{3H}{2}\partial_t\left(\frac{\ddot{H}}{\dot{H}}\right) + \frac{1}{2}\partial_t\left(\frac{\ddot{H}^2}{\dot{H}^2}\right)\right] \tag{3.120}$$

3.3 EFT of Dark Energy and Modified Gravity

The EFT of Dark Energy and Modified Gravity (EFTDE for short) provides a universal description for all DE and MG models that include a single scalar degree of freedom. It does so by extending the formalism previously applied to inflation in the EFT of Inflation (Cheung et al.'s approach), summarized in Section 3.1.2 [46; 47; 75]. Unlike the EFT of Inflation, however, the EFT coefficients in the EFTDE are free to be entirely time-dependent and cannot be reduced to constants. As you can imagine, this results in a cumbersome amount of possible solutions – a practically infinite amount of time-dependent functions to pick from. We will spend a good amount of time discussing how models under this huge EFTDE umbrella can be ruled in or out using data in Chapter 5.

In order to write down the EFTDE, we must first assume the validity of the Weak Equivalence Principle. This allows us to write $S_m[g_{\mu\nu}; \psi_m]$ where the metric $g_{\mu\nu}$ is universally coupled to matter fields, ψ_m. Then, similar to the EFT of Inflation, we write the most

general gravitational action for such a metric compatible with the residual symmetries of unbroken spatial diffeomorphisms. This results in the presence of a scalar field, ϕ, in the DE sector. In unitary gauge, this scalar degree of freedom is "eaten" by the metric. It can be explicitly reintroduced by the so-called "Stückelberg Trick": performing an infinitesimal time diffeomorphism $t \longrightarrow t + \pi(x)$, where π is now its own field and encodes the scalar dynamics of DE. This form of the action with the π field explicitly realized will not be useful to us in this work, however. In unitary gauge, the EFTDE action takes the form,

$$\begin{aligned} S &= \int d^4x\sqrt{-g}\Big[\frac{1}{2}m_0^2\Omega(t)R - \Lambda(t) - c(t)g^{00} + \frac{M_2^4(t)}{2}(\delta g^{00})^2 - \frac{\bar{M}_1^3(t)}{2}\delta K\delta g^{00} \\ &- \frac{\bar{M}_2^2(t)}{2}\delta K^2 - \frac{\bar{M}_3^2(t)}{2}\delta K_\nu{}^\mu \delta K_\mu{}^\nu + \frac{\hat{M}^2(t)}{2}\delta R^{(3)}\delta g^{00} + m_2(t)\partial_i g^{00}\partial^i g^{00} \\ &+ \mathcal{L}_m\Big], \end{aligned} \tag{3.121}$$

where $\delta g^{00} = g^{00} + 1$ is the perturbation to the time component of the metric, $R^{(3)}$ is the perturbation to the spatial component, and $\delta K_{\mu\nu}$ is the perturbation of the extrinsic curvature.

Conveniently, the background evolution depends on just three parameters, $c(t)$, $\Lambda(t)$, and $\Omega(t)$. Two of the three, routinely $c(t)$ and $\Lambda(t)$, can be constrained using Friedman's equations. $\Omega(t)$ is therefore a free parameter. A choice of $\Omega = 1$ corresponds to a ΛCDM background. m_0 is the mass scale of the problem and takes the value $m_{\rm pl}^2$ when $\Omega(t) = 1$. The rest of the EFT functions describe perturbations about that background and their effects can be studied independently from the background. We therefore have seven free parameters that describe the most general theory of DE/MG:

$$\big[m_0(t)\Omega(t);\, \bar{M}_1^3(t);\, M_2(t);\, \bar{M}_2(t);\, \bar{M}_3(t);\, \hat{M}(t);\, m_2(t)\big]. \tag{3.122}$$

For a summary of all models included in this very general formalism, see Figure 3.6 [75].

Model parameter	Ω	Λ	c	M_2^4	$\bar{M}_1^3$	$\bar{M}_2^2$	$\bar{M}_3^2$	$\hat{M}^2$	m_2^2
Corresponding Operator	R		δg^{00}	$(\delta g^{00})^2$	$\delta g^{00}\delta K^\mu_\mu$	$(\delta K^\mu_\mu)^2$	$\delta K^\mu_\nu K^\nu_\mu$	$\delta g^{00}\delta R^{(3)}$	$\frac{\bar{g}^{ij}}{a^2}\partial_i g^{00}\partial_j g^{00}$
ΛCDM	1	✓	0	-	-	-	-	-	-
Quintessence	1/✓	✓	✓	-	-	-	-	-	-
$f(R)$	✓	✓	0	-	-	-	-	-	-
k-essence	1/✓	✓	✓	✓	-	-	-	-	-
Galileon (Kinetic Braiding)	1/✓	✓	✓	✓	✓	-	-	-	-
DGP	✓	✓†	✓†	✓†	✓	-	-	-	-
Ghost Condensate	1/✓	✓	0	-	-	✓	✓	-	-
Horndeski (Generalized Galileon)	✓	✓	✓	✓	✓	✓†	✓†	✓†	-
Hořava-Lifshitz	1	✓	0	-	-	✓	-	-	✓

Figure 3.6: This chart illustrates the operators necessary to describe the various models of DE/MG included in the EFTDE formalism.

✓ Operator is necessary
- Operator is not included
1,0 Coefficient is unity or exactly vanishing
1/✓ Minimally and non-minimally coupled versions of this model exist
† Coefficients are linearly related to other coefficients in that model

CHAPTER 4

SEARCHING FOR RESONANCE WITH GABE

4.1 Moduli Fields

Moduli are a generic prediction in string theoretic approaches to beyond the Standard Model [106] and inflationary model building [107]. It was noted long ago that these moduli could be displaced from their low-energy minima in the early universe, and their coherent oscillations lead to a period of matter domination [108; 109; 110; 111; 112]. This matter phase has important differences from a strictly thermal universe and is a rich source of dark matter phenomenology – for a review see [106]. The matter phase can also lead to enhanced growth of structure [113; 114; 115], changes in inflationary predictions for the cosmic microwave background [116], and also the formation of primordial black holes [117; 118]. These cosmological and phenomenological predictions depend on the duration of the matter phase, which is determined by the moduli mass and couplings to other fields.

It is expected that moduli couple gravitationally, and the matter phase will persist until the perturbative decay of the modulus completes which, for 50 TeV moduli, will be around the time of Big Bang Nucleosynthesis (BBN) [106]. In the following original work in this chapter, we want to revisit these assumptions and determine if effects such as parametric enhancement [28; 27] or tachyonic instabilities [34] can lead to an enhanced decay of the moduli. In the former case, as the field oscillates, particles are produced, and Bose-Einstein statistics can lead to a significant enhancement of the decay compared to the perturbative decay rate [27; 28] (for a review see [30; 29]). Whereas, in tachyonic resonance, if the mass squared of the field becomes negative due to the time and/or field dependence of the couplings this can lead to the efficient decay of the field in less than a single oscillation [34]. It has also been argued that the dynamics and backreaction of the produced particles could be used to 'trap' moduli [119; 120; 121; 122]. If these types of instabilities are present

they can significantly enhance the moduli decay rate resulting in less of a matter phase or even prevent the formation of the moduli condensate all together. For very light moduli – that would decay after BBN – this enhanced decay may lead to a new way to address the cosmological moduli problem [108; 109; 110; 111; 112].

4.2 Moduli Decay Through Parametric and Tachyonic Resonance

The moduli will typically couple to other fields with gravitationally suppressed couplings. This is the case in examples like KKLT [123], as well as the cases of Large Volume Compactifications in Type IIB [124] and G2 compactifications of M-theory [125]. The perturbative decay rate of the modulus is then $\Gamma \sim m_\sigma^3/\Lambda^2$, where m_σ is the mass of the modulus and Λ the suppression scale. Taking[1] $\Lambda \sim m_{\rm pl}$ the corresponding reheat temperature for a $m_\sigma = 50$ TeV scalar is around 5 MeV [106]. Here we would like to determine whether parametric or tachyonic instabilities in the moduli can result in a faster decay and so higher reheat temperature.

We are motivated by recent work on preheating and the production of gauge fields at the end of inflation [126; 127; 128]. In these papers it was found that a tachyonic instability to production of massless gauge fields from inflaton couplings $\sigma F_{\mu\nu}\tilde{F}^{\mu\nu}/\Lambda$ [127; 128] or $\sigma F_{\mu\nu}F^{\mu\nu}/\Lambda$ [126] can lead to explosive particle production and drain energy completely before the inflaton can complete a full oscillation. If this result were also true for moduli, then this could prevent the formation of the condensate and the matter-dominated phase.

4.2.1 Moduli Coupling to Gauge Fields

In all of the string constructions mentioned above there are moduli with masses generated by gravitationally mediated Supersymmetry (SUSY) breaking. The corresponding moduli mass

1. We work with sign convention $(-,+,+,+)$ and with the reduced Planck mass $m_{\rm pl} = 1/(8\pi G)^{1/2} = 2.4 \times 10^{18}$ GeV. We use Greek indices to denote space-time $\mu = 0, 1, 2, 3$ whereas latin indices imply spatial directions only $k = 1, 2, 3$.

is determined by the gravitino mass $m_{3/2}$ as $m_\sigma = c\, m_{3/2}$ where c is a constant determined by the particular string theory realization, e.g. in the G2 MSSM $c \simeq 2$.

We now consider the coupling of the moduli to a hidden sector gauge field

$$S = \int d^4x\sqrt{-g}\left(-\frac{1}{4}F_{\mu\nu}F^{\mu\nu} - \frac{c}{4\Lambda}\sigma\, F_{\mu\nu}F^{\mu\nu}\right), \tag{4.1}$$

where c is an order one constant (computable in a given string model) and consistency of the effective theory requires $\sigma < \Lambda$. The corresponding equations of motion are

$$\nabla_\mu F^{\mu\nu} + \frac{c}{\Lambda}\nabla_\mu\left(\sigma\, F^{\mu\nu}\right) = 0, \tag{4.2}$$

$$\Box\sigma = \frac{\partial V}{\partial\sigma} + \frac{c}{4\Lambda}F_{\mu\nu}F^{\mu\nu}. \tag{4.3}$$

Working in Coulomb gauge $A^0 = 0, \quad \partial_i A^i = 0$, neglecting the expansion of the background, and introducing the field redefinition $\tilde{A}_k = \left[a(t)\left(1 + c\,\sigma/\Lambda\right)\right]^{1/2} A_k$ the resulting equations of motion are

$$\begin{aligned} \ddot{\sigma} \;&+\; 3H\dot{\sigma} + m_\sigma^2\sigma \\ &=\; \frac{c}{2\Lambda}\left[\frac{\dot{A}_\mu\dot{A}^\mu}{a^2} + \epsilon_{\mu\nu\lambda}\epsilon^{\lambda}{}_{\alpha\beta}\nabla^\mu A^\nu\nabla^\alpha A^\beta\right] \end{aligned} \tag{4.4}$$

$$\begin{aligned} \ddot{\tilde{A}}_k \;&+\; \left[k^2 + \frac{1}{2}\left(\frac{1}{1 + c\,\sigma/\Lambda}\right)^2\right. \\ &\times\; \left.\left(\frac{1}{2}c^2\frac{\dot{\sigma}^2}{\Lambda^2} - c^2\frac{\sigma\ddot{\sigma}}{\Lambda^2} - c\frac{\ddot{\sigma}}{\Lambda}\right)\right]\tilde{A}_k = 0, \end{aligned} \tag{4.5}$$

The moduli will remain frozen in their false minimum until $H \simeq m_\sigma$ at which time the moduli begin oscillations and $\sigma(t) = \sigma_0\cos(mt)$ where the initial amplitude is typically $\sigma_0 \sim m_{\rm pl}$.

The gauge field equation can be put in the form of a Mathieu equation by introducing the time variable $z = mt/2$. Noting that consistency of the effective theory requires $\sigma_0 < \Lambda$ and keeping only the leading terms we have

$$\frac{d^2 A_k}{dz^2} + \left[4 \left(\frac{k}{m_\sigma} \right)^2 + 2c \left(\frac{\sigma_0}{\Lambda} \right) \cos(2z) \right] A_k = 0 \tag{4.6}$$

where we have dropped terms further suppressed by powers of σ_0/Λ and we note that the leading time-dependent mass term corresponds to the term $\sim \ddot{\sigma}/\Lambda$ in (4.5).

Comparing (4.6) to the usual Mathieu equation

$$\frac{d^2 u}{dz^2} + \left[\mathcal{A}_k + 2q \cos(2z) \right] u = 0, \tag{4.7}$$

suggests the identifications

$$\mathcal{A}_k \equiv 4 \left(\frac{k}{m_\sigma} \right)^2, \qquad q \equiv c \left(\frac{\sigma_0}{\Lambda} \right). \tag{4.8}$$

Tachyonic instability corresponds to the condition $\mathcal{A}_k < 2q$, broad resonance occurs for $q \gg 1$ and narrow resonance occurs for $q \lesssim 1$. We can immediately see that broad resonance is forbidden, since validity of the effective theory requires $\sigma_0 < \Lambda$ or $q < 1$. Moreover, although narrow resonance could play a role, it may not lead to significant enhancement of the production [28]. Thus, we focus on the case of tachyonic resonance.

4.2.2 Tachyonic Resonance: Analytic Treatment

The modes that will undergo tachyonic resonance correspond to $\mathcal{A}_k < 2q$ in (4.7), which for the identification (4.8) implies

$$k < \frac{1}{\sqrt{2}} \left(\frac{\sigma_0}{\Lambda} \right)^{1/2} m_\sigma. \tag{4.9}$$

However, for post-inflation we are interested in sub-Hubble modes[2] so we also require $k/H > 1$ implying the modes of interest lie in a band

$$1 < \frac{k}{H} < \frac{1}{\sqrt{2}} \left(\frac{\sigma_0}{\Lambda}\right)^{1/2} \left(\frac{m_\sigma}{H}\right). \tag{4.10}$$

Thus, for tachyonic production of modes we require

$$\frac{1}{\sqrt{2}} \left(\frac{\sigma_0}{\Lambda}\right)^{1/2} \left(\frac{m_\sigma}{H}\right) \gg 1, \tag{4.11}$$

so at the onset of the moduli phase, when $H \simeq m_\sigma$ perturbativity of the effective theory again seems to limit the level of enhancement in gauge field production, since we require $\sigma_0 < \Lambda$. However, although the initial moduli displacement is typically expected to be an order of magnitude or so below the cutoff, as the moduli oscillations continue the Hubble parameter will continue to decrease $H < m_\sigma$, and tachyonic resonance becomes possible. There is a competing effect that the amplitude of the moduli oscillations also decreases compared to its initial value σ_0. It is a quantitative question of how important tachyonic resonance is for moduli decay and the duration of the epoch. Moreover, during oscillations, creation of moduli (moduli particles, meaning $k \neq 0$ modes), particle scattering, and backreaction of both moduli and gauge fields can play an important role, as well as the expansion of the universe. To account for these complexities and non-linearities we perform a lattice treatment and present those results in the next section.

4.2.3 Tachyonic Resonance: Lattice Results

To determine whether tachyonic (or parametric) instabilities occur in the system (4.4) and (4.5) we perform fully non-linear lattice simulations. We build our simulations using the software `GABE` [80], which has been used previously to study the interactions of scalar fields

2. This is required by causality if the gauge modes begin in their vacuum state following inflation.

and U(1) Abelian gauge fields [126; 127; 128]. Our simulations allow us to account not only for gauge field production, but also the effects of scalar particle production, rescattering, backreaction, and the expansion of the universe.

There are several restrictions on the allowed values of the fields and parameters of our model. For example, although we perform a lattice simulation, validity of the effective Supergravity description requires that the non-renormalizable operator in (4.1) remain subdominant to the leading kinetic term. Since c is a dimensionless $\mathcal{O}(1)$ Wilson coefficient this requires that σ not exceed the UV cutoff Λ (which is typically order the Planck or string scale).

We note that our simulations are similar to those of [126], where the role of the inflaton there, is instead given by the moduli here. As we will see, a key difference in our results compared to those of [126] is that there the authors considered a toy model with a dilatonic type coupling that could enter a "strong coupling" regime. In this study, we are limited by the validity of the effective theory $\sigma < \Lambda$ and we'll see this limits our ability to establish a strong resonance behavior[3].

In order to establish as large a resonance as possible we will take the initial amplitude of the moduli to be near the Planck scale $\sigma_0 \simeq m_{\rm pl}$ (we take $\sigma_0 = 0.2\, m_{\rm pl}$ as a fiducial value). Then, given our discussion of the validity of the effective theory requires that we take $\Lambda \sim m_{\rm pl}$, and as the field can change sign this also ensures that the kinetic term of (4.1) retains the correct sign. This limits us to a maximum coupling $c/4\Lambda \approx 6.9\, m_{\rm pl}^{-1}$. Throughout this section we will use this maximum value as to make the potential tachyonic window as large as possible (we have checked that for lower values of the cutoff the resonance is even weaker than the results we present here). We are left with only one free parameter, m_σ, which also sets the Hubble scale at the beginning of coherent oscillations.

Using `GABE` we discretize space onto a grid of 128^3 points that are on a homogeneously

3. The result that validity of an effective field theory approach can limit the importance of parametric resonance was noted recently in [130].

expanding box. The box has initial size, $L = 4m_\sigma^{-1} \approx 2H_0^{-1}$. The simulations solve (4.4) and (4.5) along with the Friedman equations. For numerical simplicity, we employ the standard *unit-less conformal* time, $d\tau = a(t)\, m\, dt$. We use an adaptive time step, $\Delta\tau = 0.005/a(\tau)$ so that we resolve the co-moving modes throughout the simulation. We initialize the modulus field consistent with the expectations of a field that carries the "freeze out" power as modes re-enter the horizon[4],

$$\left\langle \delta\sigma(k)\delta\sigma(k')\right\rangle = \frac{\pi^2}{2}\left(\frac{\Delta_s^2\sigma_0^2}{H_0^3}\right)\,\delta\left(k-k'\right), \tag{4.12}$$

assuming that most modes have not grown much since horizon re-entry[5] and have recently re-entered ($k \approx H_0$). For the gauge fields we set the initial conditions consistent with the Bunch Davies vacuum [126],

$$\left\langle \left|A_i(k)A_j(k')\right|^2\right\rangle = \frac{\delta_{ij}\,\delta\left(k-k'\right)}{2a\left(1+c\sigma/\Lambda\right)}, \tag{4.13}$$

with zero homogenous mode (we comment on the robustness of this assumption shortly). We take the initial surface in Coulomb gauge, but the rest of the simulation is carried out in Lorenz gauge, $\partial^\mu A_\mu = 0$, where Gauss' constraint is treated as a dynamical degree of freedom (as the equation of motion for A_0) and we check that the gauge constraint is maintained throughout our simulations. As we increase the mass of the modulus field, we shrink the physical size of the Hubble patch at the beginning of the simulation. This is the best approach to resolving shorter wavelength modes of the gauge fields, and hence, a larger fraction of energy in the gauge sector. As we set the initial conditions, we impose a

4. We start our simulations at the beginning of moduli oscillations and we take adiabatic initial conditions so that the inflaton fluctuations will have been transferred to the moduli that come to dominate the energy density (we assume no isocurvature, however see [131]) and assume that $\Delta_s^2 \approx 10^{-10}$.

5. Prior to moduli domination we take the universe to be radiation dominated following inflationary reheating and sub-Hubble modes of the moduli will undergo very little growth (their perturbations grow logarithmically with the scale factor $\sim \log(a)$.

window function (as in [126]) that cuts off power to modes $k \gtrsim 90\, m_\sigma$ for numerical stability. However, this scale is above the scale at which we would expect to see tachyonic instabilities.

Following [126], we take the ratio of the gauge field energy density ($\rho_{\rm EM}$) to the total energy ($\rho_{\rm tot}$) as a figure of merit of the amplification of the gauge field and the effectiveness of the tachyonic (and parametric) instabilities. Figure 4.1 shows the evolution of this parameter as a function of time for a large range of moduli masses. We find the robust result that *regardless* of the (relative) amplitude of the initial fluctuations of the gauge fields, tachyonic (and parametric) instabilities are absent and do not lead to significant amplification of the gauge fields. The variation in the initial value of $\rho_{\rm EM}$ reflects that we allow for different values of the moduli mass as discussed above. Considering a pre-existing density of gauge modes (*e.g.* non-Bunch Davies initial conditions with modes that were classically or quantum mechanically excited during inflation[6]) would have a similar effect, amplifying the initial spectrum of the gauge field, and hence, raising $\rho_{\rm EM}/\rho_{\rm tot}$ on the initial surface.

An additional measure at which to look for instabilities is in the spectra of the coupled fields. In Figure 4.2, we see that there is very little change to the power spectra of the fields. In cases where instabilities exist, we can generally see these instabilities in the power spectra of the fields. In none of the cases we studied did we see any indication of tachyonic or parametric instabilities.

Although we have not found significant evidence for an increased decay of the moduli, this does not necessarily imply a matter-dominated epoch. Indeed, it was recently shown that the non-linear dynamics of the fields can have an important influence on the equation of state [95]. Thus, we must lastly ensure that the expansion mimics that of a matter-dominated single-component universe. To do this, we track the equation of state parameter, $w = p/\rho$, which is the usual ratio of the isotropic pressure to the energy density. Figure 4.3 shows this

6. Model independent bounds on the level of gauge field production during inflation was recently established in [129]. There it was shown that requiring successful inflation limits the amplification of gauge fields which here limits the size of the initial amplitude taken for the gauge fields, *i.e.* one can not take the initial amplitude to be arbitrarily large.

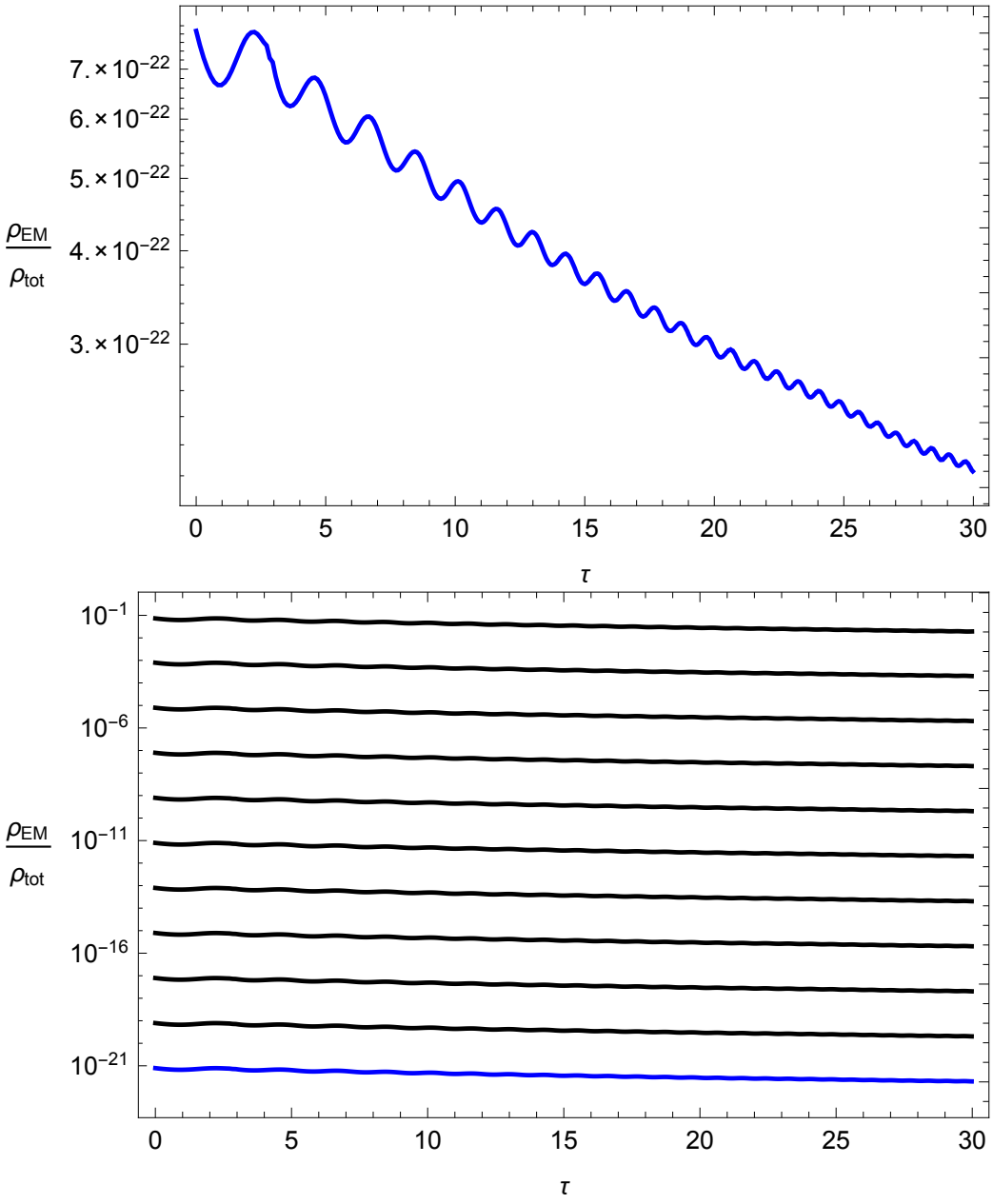

Figure 4.1: Plot of $\rho_{\rm EM}/\rho_{tot}$ vs. unit-less conformal time (see text) for a set of maximally coupled simulations, $c/\Lambda = 6.7\, m_{\rm pl}$. The top panel shows a simulation of the fiducial value of $m_\sigma = 50\,\text{TeV}$ and the bottom panel shows a range of masses, from $m_\sigma = 50\,\text{TeV}$ (bottom) to $m_\sigma = 5 \times 10^{11}\,\text{TeV}$, the 50 TeV case is labeled in blue in both plots. For each simulation $\rho_{tot}(t)$ is approximately the same, since the energy of the modulus is dominated by its homogeneous mode and is always the dominant component.

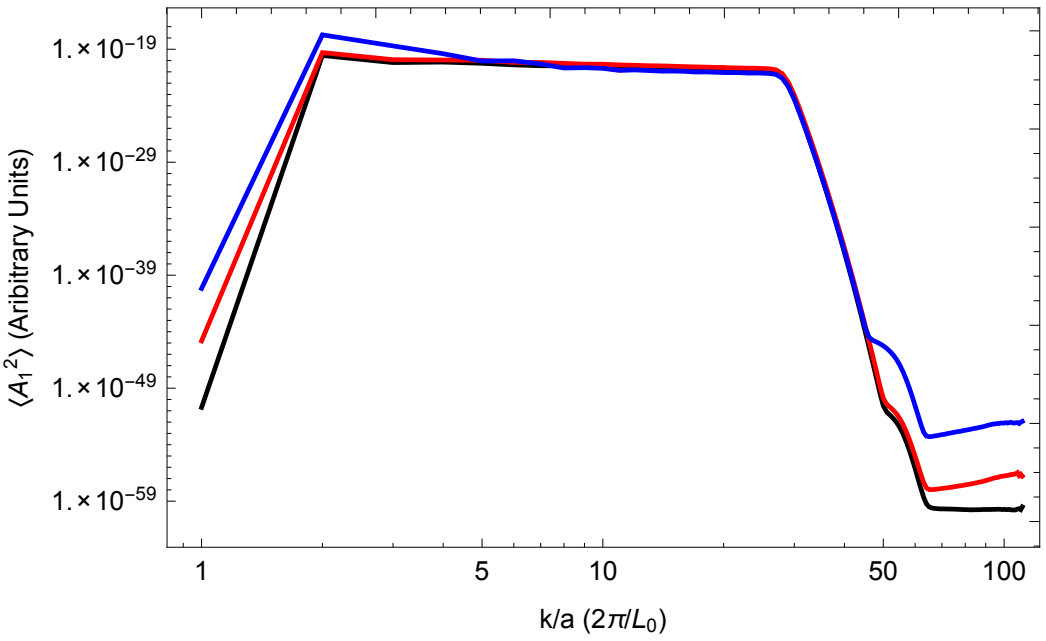

Figure 4.2: The power spectra of one component of the gauge field, A_1 at the beginning of the simulation (black), at the first zero crossing (red) and at the second zero crossing (blue) in a simulation where $m_\sigma = 50\,\text{TeV}$. At higher frequencies, the power is suppressed due to the window function imposed on the initial slice, the slight increases in these frequencies is not a physical response, but an accumulation of numerical truncation errors (and is still many orders of magnitude below the scales of interest). The increase in the zero-momentum bin is a consequence of the initial value being set to zero to machine-precision, with truncation errors making it drift away. The spectra undergo negligible amplification over the course of the simulation. The other spatial components of the field have identical behaviors, and similar results are seen in all simulations. We find no indication of tachyonic or parametric instabilities.

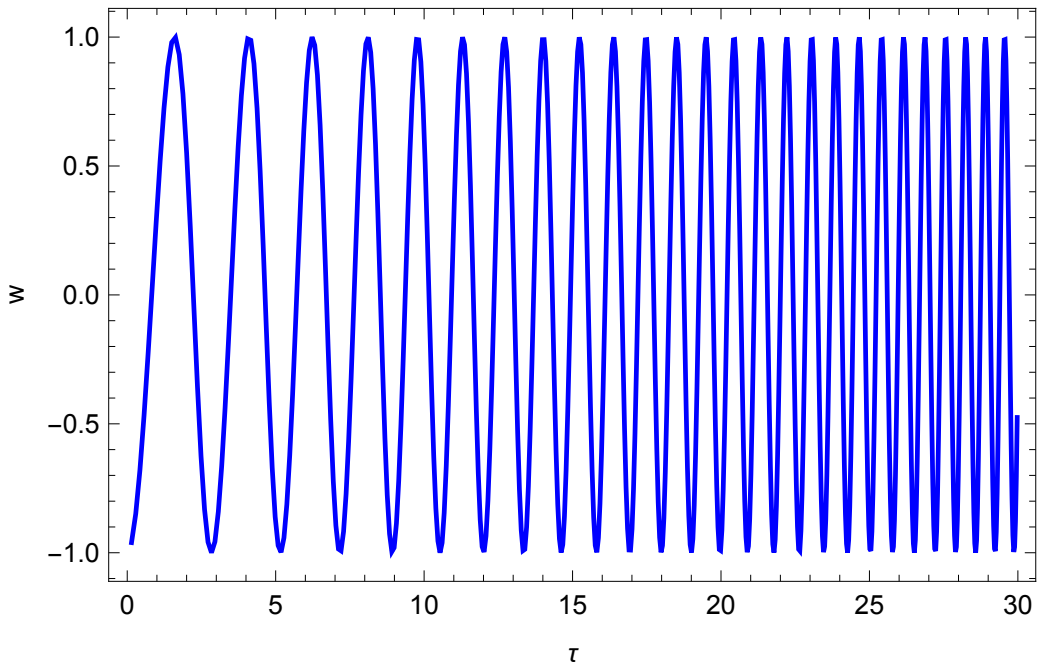

Figure 4.3: The equation of state for a simulation where $m_\sigma = 50\,\text{TeV}$ vs. unit-less conformal time (see text). We see that the average of the equation of state is that of a matter-dominated universe.

for the fiducial case, $m_\sigma = 50\,\text{TeV}$, and shows that w oscillates, as expected, between ± 1 as is the case of a massive scalar field dominated by its homogeneous value.

4.3 Discussion

In this work, we have considered the coupling of moduli to hidden sector gauge fields for a range of masses and initial values of the gauge fields. We found that even as we approach modestly strong coupling, tachyonic and parametric instabilities have no effect on the moduli decay rate. Moreover, we have seen that the equation of state during the moduli oscillations averages to the previously anticipated result of a matter-dominated universe. As gauge field production relies on the moduli dynamics breaking the conformal invariance of the gauge field sector [132], and in these string motivated models the source of this breaking comes from non-renormalizable operators, it may not be that surprising that this effect turned

out to be negligible. One reason for considering these operators was that such couplings generically appear in string theories, and are model independent in the sense that they arise strictly in the moduli sector and are typically independent of how one embeds the visible sector. This is indeed the case in examples like KKLT [123], as well as the cases of Large Volume Compactifications in Type IIB [124] and G2 compactifications of M-theory [125].

One may wonder if more model dependent couplings (arising from embedding the visible sector in a particular string construction) may alter our conclusions. For example, moduli couplings to the Higgs ($\sim \sigma H^\dagger H$) are relevant operators and the moduli might undergo enhanced decay to Higgs bosons. However, such couplings were already considered some time ago by Brandenberger and Shuhmaher in [133; 134]. They considered relevant operators arising from SUSY breaking for a range of moduli masses. Their results are similar to our findings for non-renormalizable operators. That is, if one requires a perturbative theory and consistency of the effective field theory then both parametric and tachyonic resonance does not significantly alter the moduli decay rate.

4.4 Appendix: Lattice Simulations and GABE

In Section 4.2.3 we used GABE, the grid and bubble evolver to obtain full numerical results for our model. Studying the dynamics of the early universe is experimentally tough. The energy scale at the beginning of the universe was upwards of 10^{12}TeV and collider energies reach just 6TeV at best. Even if collider technology continues to improve, we will never be able to recreate conditions like those at the birth of the universe. We must, therefore, pursue another method of investigation into our cosmic origins. We turn to computational tools to help us study this era of physics.

GABE is an open-source C++ code that models the evolution of scalar fields over an expanding background, thus modeling the evolution of the universe [98]. It is an excellent tool for the study of early universe physics. We use it in this thesis in both our study of the

EFT of reheating in Section 3.2 and in the study of oscillon production and self-resonance in moduli fields in Chapter 4.

The program employs the Second Order Runge-Kutta numerical integration method to evolve coupled differential equations on an N^3 lattice over an expanding background. The program outputs useful information at every time-step, including average field values, field variance, and the value of the scale factor. `GABE` is also designed to probe a wide variety of cosmological models. It can be modified to investigate canonical fields with a user-specified potential energy function, as well as, with changes to the kinetic terms in the Klein-Gordon equation, to evolve non-canonical, coupled scalar fields.

Rescalings

Computers can only keep track of raw numbers, so we must convert our physical variables into program variables stripped of units. Any rescaling can be used, but the default rescaling in `GABE` is defined by,

$$\varphi_{\rm pr} = \frac{\varphi}{m_{\rm pl}} \tag{4.14}$$

$$dx_{\rm pr} = m_\varphi dx \tag{4.15}$$

$$V_{\rm pr} = \frac{1}{m_\varphi^2 m_{\rm pl}^2} V(\varphi) \tag{4.16}$$

where the subscript 'pr' indicates a program variable.

Initialization

Numerical integration requires taking our fields, which are naturally continuous objects, and discretizing them to a lattice of a finite step size. By taking very small steps through program time, we can approximate the non-analytic solution to our system. When implemented correctly, numerical approximations techniques like RK-2 prove very reliable. A key part

of this implementation is the initialization of our fields. If we want to replicate the actual history of our universe, we must do our best to recreate a realistic starting condition.

Simulations with `GABE` begin at the end of inflation, when the universe assumes a state of Bunch-Davies vacuum [99]. In this state, the universe is devoid of particles and the inflaton field is *mostly* smooth – except for slight inhomogeneities due to quantum fluctuations. These fluctuations are on scales much smaller than the Hubble scale, and therefore cannot be neglected. We must initialize the mean value of the inflaton field as well as fluctuations on top of this mean value.

To construct a state of Bunch-Davies vacuum, we first evaluate the two-point correlation function of the field, φ, at two different points, $\vec{x}$ and $\vec{y}$. The power spectrum for a vacuum state is defined to be $1/2\omega_k$, and thus, the two-point function is

$$\langle \varphi(\vec{x})^\dagger \varphi(\vec{y}) \rangle = \int \frac{d^3k}{(2\pi)^3} \frac{1}{2\omega_k} e^{i\vec{k}\cdot(\vec{x}-\vec{y})}. \tag{4.17}$$

This calculation returns the amplitude for propagation of a particle of excitation between the two points specified. Taking the Fourier transform gives,

$$\langle \varphi(\vec{x})^\dagger \varphi(\vec{y}) \rangle = \left\langle \int \frac{d^3k_1}{(2\pi)^{3/2}} \frac{d^3k_2}{(2\pi)^{3/2}} \, \varphi^\dagger(\vec{k}_1) \, e^{i\vec{k}_1\cdot(\vec{x})} \, \varphi(\vec{k}_2) \, e^{i\vec{k}_2\cdot(\vec{y})} \right\rangle. \tag{4.18}$$

We must discretize both Equation 4.17 and Equation 4.18 to a box of length L and a step size of $dk = 2\pi/L$. Converting the two-point correlation function to a finite sum gives,

$$\int \frac{d^3k}{(2\pi)^3} \frac{1}{2\omega_k} e^{i\vec{k}\cdot(\vec{x}-\vec{y})} = \frac{1}{L^3} \sum_k \frac{1}{2\omega_k} e^{i\vec{k}\cdot(\vec{x}-\vec{y})}. \tag{4.19}$$

Similarly, discretizing the Fourier transform gives,

$$\frac{(2\pi)^3}{L^6} \sum_{\vec{k}_1,\vec{k}_2} \left\langle \varphi^\dagger(\vec{k}_1)\varphi(\vec{k}_2) \right\rangle e^{-i\vec{k}_1\cdot(\vec{x})} e^{i\vec{k}_2\cdot(\vec{y})}. \tag{4.20}$$

When $\vec{x} \neq \vec{y}$, Equation 4.19 is the integral over all space of a periodic function, $e^{i\vec{k}\cdot\vec{x}}$, and therefore evaluates to zero. In the special case where $\vec{x} = \vec{y}$, the argument of the exponential goes to zero and the integral evaluates to something nonzero. In other words, Equation 4.19 contains a delta function with the requirement that $\vec{x} = \vec{y}$,

$$\frac{1}{L^3}\sum_k \frac{1}{2\omega_k} e^{i\vec{k}\cdot(\vec{x}-\vec{y})} = \frac{1}{L^3}\sum_k \frac{1}{2\omega_k}. \tag{4.21}$$

Equating Equation 4.20 with Equation 4.21 gives,

$$\frac{(2\pi)^3}{L^6}\sum_{\vec{k}_1,\vec{k}_2} \left\langle \varphi^\dagger(\vec{k}_1)\varphi(\vec{k}_2) \right\rangle e^{-i\vec{k}_1\cdot(\vec{x})} e^{i\vec{k}_2\cdot(\vec{y})} = \frac{1}{L^3}\sum_k \frac{1}{2\omega_k}. \tag{4.22}$$

Recalling that we have imposed the $\vec{x} = \vec{y}$ condition, we can see another delta function on the left-hand side of this equation. Namely, $(\vec{k}_2 - \vec{k}_1)\cdot\vec{x}$ requires $\vec{k}_1 = \vec{k}_2$ to obtain something nonzero. Imposing this delta function, we get,

$$\sum_{\vec{k}} \left\langle |\varphi(\vec{k})|^2 \right\rangle = \left(\frac{L}{2\pi}\right)^3 \sum_k \frac{1}{2\omega_k}. \tag{4.23}$$

We conclude that the mean distribution of all the momentum modes is,

$$\left\langle |\varphi(\vec{k})|^2 \right\rangle = \left(\frac{L}{2\pi}\right)^3 \frac{1}{2\omega_k}. \tag{4.24}$$

The distribution of the each of the three components of the momentum, $\vec{k}$, must be gaussian. This leads to the choice of a Raleigh distribution with the average value defined by Equation 4.24,

$$P(\varphi_k) = \frac{\varphi_k}{\sigma^2} e^{-\varphi_k^2/2\sigma^2}, \tag{4.25}$$

where

$$\sigma^2 = \frac{L^3}{4\pi^4 \omega_k}. \tag{4.26}$$

In program variables, the probability distribution of field fluctuations is then,

$$P(|\varphi_{k,\mathrm{pr}}|) = \frac{2|\varphi_{k,\mathrm{pr}}|}{W^2_{k,\mathrm{pr}}} e^{-|\varphi_{k,\mathrm{pr}}|^2/W^2_{k,\mathrm{pr}}} \tag{4.27}$$

where $W_{k,\mathrm{pr}}$ is the root-mean-square amplitude in program units,

$$W_{k,\mathrm{pr}} = \sqrt{\frac{m^2 L^3_{\mathrm{pr}}}{2\,\omega_{k,\mathrm{pr}}\, dx^6_{\mathrm{pr}}}}. \tag{4.28}$$

Equation 4.28 depends on the wave number, k, which is specific to a given momentum mode. The angular frequency, $\omega_{k,\mathrm{pr}}$, also depends on wave number,

$$\omega^2_{k,\mathrm{pr}} = \left(\frac{2\pi}{L_{\mathrm{pr}}}\right)^2 |k|^2 + \frac{\partial^2 V_{\mathrm{pr}}}{\partial \varphi^2_{\mathrm{pr}}}. \tag{4.29}$$

In terms of initialization of `GABE`, we can use this Raleigh distribution to find the amplitude of each fluctuating mode on our initial field slice. We take the inverse Fourier transform of the result to obtain the position-space representation of the initial configuration of the field.

In practice, we aim to use a random number generator to pull values for the momentum modes, k, from a uniform distribution. In order to be physics, these modes we pull should follow a Rayleigh distribution. To construct such a distribution numerically, we define the magnitude of the intensity of a given mode, k, to be,

$$|\varphi_{k,\mathrm{pr}}| = \sqrt{-W^2_{k,\mathrm{pr}} \ln X} \tag{4.30}$$

where X is our random variable between 0 and 1. We rearrange to find the distribution for

X,

$$X = exp\left(-\frac{|\varphi_{k,\mathrm{pr}}|^2}{W_{k,\mathrm{pr}}^2}\right). \tag{4.31}$$

Our probability density must be a function of $|\varphi_{k,\mathrm{pr}}|$ rather than a function of X, so we use

$$p(y) = p(X(y))\left|\frac{dx}{dy}\right| \tag{4.32}$$

to convert. $X(y)$ follows a uniform distribution and thus, $P(X(y)) = 1$ for $0 \leq X \leq 1$. Then, Equation 4.32 evaluates to

$$\begin{aligned} P(|\varphi_{k,\mathrm{pr}}|) &= \frac{dX}{d|\varphi_{k,\mathrm{pr}}|} && (4.33)\\ &= \frac{2|\varphi_{k,\mathrm{pr}}|}{W_{k,\mathrm{pr}}}\exp\left(-\frac{|\varphi_{k,\mathrm{pr}}|^2}{W_{k,\mathrm{pr}}^2}\right), && (4.34) \end{aligned}$$

a Raleigh distribution.

We have now successfully enforced a Raleigh distribution for the amplitude of our momentum modes. Next, we want to imagine that each ϕ_k is a superposition of a left-moving and right-moving wave. These two waves have independent phases, $e^{i\theta_L}$ and $e^{i\theta_R}$. With this in mind, we can now rewrite Equation 4.30 as,

$$\varphi_{k,\mathrm{pr}} = \frac{1}{\sqrt{2}}\left(e^{i\theta_L}\sqrt{-W_{k,\mathrm{pr}}^2 \ln X_L} + e^{i\theta_R}\sqrt{-W_{k,\mathrm{pr}}^2 \ln X_R}\right) \tag{4.35}$$

As it is computationally impossible to deal with complex numbers, we separate the real and imaginary components of $\varphi_{k,\mathrm{pr}}$ and store each in its own array. We define the real part as,

$$\mathrm{Re}\,\varphi_{k,\mathrm{pr}} = \frac{1}{\sqrt{2}}\left(\cos\theta_L\sqrt{-W_{k,\mathrm{pr}}^2 \ln X_L} + \cos\theta_R\sqrt{-W_{k,\mathrm{pr}}^2 \ln X_R}\right) \tag{4.36}$$

and the imaginary as,

$$\mathrm{Im}\,\varphi_{k,\mathrm{pr}} = \frac{1}{\sqrt{2}}\left(\sin\theta_L\sqrt{-W_{k,\mathrm{pr}}^2\ln X_L} + \sin\theta_R\sqrt{-W_{k,\mathrm{pr}}^2\ln X_R}\right). \tag{4.37}$$

Now, we define the derivatives as they do in [100],

$$\mathrm{Re}\,\varphi'_{k,\mathrm{pr}} = \frac{\omega_{k,\mathrm{pr}}}{\sqrt{2}}\left(\sin\theta_L\sqrt{-W_{k,\mathrm{pr}}^2\ln X_L} + \sin\theta_R\sqrt{-W_{k,\mathrm{pr}}^2\ln X_R}\right) - H_0\mathrm{Im}\,\varphi_{k,\mathrm{pr}} \tag{4.38}$$

and

$$\mathrm{Im}\,\varphi'_{k,\mathrm{pr}} = \frac{\omega_{k,\mathrm{pr}}}{\sqrt{2}}\left(\cos\theta_L\sqrt{-W_{k,\mathrm{pr}}^2\ln X_L} + \cos\theta_R\sqrt{-W_{k,\mathrm{pr}}^2\ln X_R}\right) - H_0\mathrm{Re}\,\varphi_{k,\mathrm{pr}}. \tag{4.39}$$

and we have successfully mapped out the initial configuration of our field in momentum space. We must evolve our field in position space, however. We can take the inverse Fourier transform of our momentum space representation to obtain the position space representation of our field. Our field is a discrete object with grid resolution $dk = 2\pi/L$, and thus requires a discrete Fourier transform,

$$\varphi_x = \frac{(2\pi)^{3/2}}{L^3}\sum_k \varphi_k\, e^{i\vec{k}\cdot\vec{x}}. \tag{4.40}$$

There exists an algorithm, `FFTW`, that performs Fourier transforms and inverse Fourier transforms. The use of this makes calculating the position space representation of the initial field slice computationally very easy. And with that, we are finally done with the initialization of our scalar field.

CHAPTER 5

OBSERVATIONAL CONSTRAINTS ON THE EFFECTIVE FIELD THEORY OF DARK ENERGY

As we learned in Section 3.3, the EFTDE approach provides a framework to describe a large class of dark energy and modified gravity models. While this is a huge accomplishment, we are faced with a rather expansive landscape of models containing many free parameters and no good way to distinguish between them. Our goal in the following original work is to isolate which of these models can reproduce observation. This allows us to rule in or out large classes of EFTDE models. For the models we rule in, it will be important to identify any unique observational signatures. Namely, we look at where EFT models lie in a $w_0 - w_a$ plane, where w_0 and w_a are terms in the CPL parameterization of the equation of state parameter, defined by,

$$w_{\rm DE}(a) = w_0 + w_a(1-a). \tag{5.1}$$

Some models (like DGP and F(R) gravity) have been ruled out through lensing and large scale structure measurements. Hordeski models remain an intriguing (and preferred) model within the EFTDE framework because, among other things, the resulting equations of motion are second order in time and space derivatives. For this reason, we focus our study on Hordeski models. That is, models which satisfy the following relationship between EFT functions,

$$2\hat{M}^2 = \bar{M}_2^2 = -\bar{M}_3^2; \;\; m_2 = 0. \tag{5.2}$$

Part of the convenience of the EFTDE formalism is the ability to study the perturbations separate from the background. In order to stay consistent with data, we are interested in Horndeski models that differ only slightly from ΛCDM. We define the background to be strictly ΛCDM, $w = -1$, and study the perturbations about that background. All information about the perturbations is contained in the second-order and higher terms in

3.121.

5.1 Observational Quantities

These second-order and higher terms in Equation 3.121 are thought to have direct observable implications. For example, the cubic operators of the EFT of inflation formalism can be straightforwardly related to the observable three-point functions of the CMB. Coupled with the wealth of present and future CMB data, it behooves us to consider the effects EFTDE models may have on observables in the CMB.

The angular power spectrum of the CMB anisotropies measures amplitude as a function of wavelength. The fundamental quantity is always written in terms of the spherical harmonics, $Y_{\ell m}(\theta, \phi)$, which describe wave functions on a sphere. The spherical harmonics are therefore analogous to a complex exponential in flat space, $e^{ikx} \leftrightarrow Y_{\ell m}(\theta, \phi)$, employing the use of ℓ and m instead of wave number, k. ℓ is the number of waves along a meridian – the 'wavelength' of the mode. And, m is the number of modes along the equator – determining the 'shape' of the mode. The angular power spectrum can then be defined as an average over m for every ℓ,

$$\hat{C}_\ell = \frac{1}{2\ell + 1} \sum_{m=-\ell}^{+\ell} |a_{\ell m}|^2 \tag{5.3}$$

where the $a_{\ell m}$ are the expansion coefficients of the spherical harmonics and $\hat{C}_\ell$ is a three-vector of the form $\left(\hat{C}_\ell\right)^T = \left(C_\ell^{TT} \;\; C_\ell^{EE} \;\; C_\ell^{TE}\right)$. In the case of CMB observation, these are our data points, measuring the temperature variation, $\delta T/T$ [137]. Using the information provided by the angular power spectrum, we aim to fit EFTDE models to standard, ΛCDM parameters, thus reconciling theory with observation by creating the first map from the EFTDE functions to real data. A summary of the real data used in this work can be found in Table 5.1 [138; 139; 140]. Once this best fit is found, we can quantify how good of a fit it is by calculating the χ^2.

Probe	Experiment	Measurements	Details
CMB	Stage-4	angular power spectrum, C_ℓ	from $\ell = 2$ to $\ell = 2500$ TT, TE, and EE components
SNIa	WFIRST	apparent magnitude, $m(z)$	16 effective supernovae in redshift bins of size 0.1 from $z = 0.1$ to $z = 1.6$
BAO	DESI	angular diameter distance $D_A(z)$ Hubble parameter $H(z)$	13 redshift bins size 0.1 from $z = 0.65$ to $z = 1.85$

Table 5.1: A summary of the data sets used to calculate χ^2 for each observational probe.

For example, the χ^2 contribution from the CMB S-4 data can be calculated,

$$\chi^2 = \sum_{\ell=2}^{\ell=2500} \left(\hat{C}_\ell^{\rm emu} - \hat{C}_\ell^{\rm EFT}\right)^T {\rm Cov}_\ell^{-1} \left(\hat{\rm C}_\ell^{\rm emu} - \hat{\rm C}_\ell^{\rm EFT}\right) \tag{5.4}$$

where "emu" indicates the emulated angular power spectrum. The covariance matrix, Cov_ℓ, is defined to be,

$${\rm Cov}_\ell = \frac{2}{(2\ell+1){\rm f_{sky}}} \begin{pmatrix} \left(\bar{C}_\ell^{TT}\right)^2 & \left(\bar{C}_\ell^{TE}\right)^2 & \bar{C}_\ell^{TT}\bar{C}_\ell^{TE} \\ \left(\bar{C}_\ell^{TE}\right)^2 & \left(\bar{C}_\ell^{EE}\right)^2 & \bar{C}_\ell^{EE}\bar{C}_\ell^{TE} \\ \bar{C}_\ell^{TT}\bar{C}_\ell^{TE} & \bar{C}_\ell^{EE}\bar{C}_\ell^{TE} & \frac{1}{2}\left(\left(\bar{C}_\ell^{TE}\right)^2 + \bar{C}_\ell^{TT}\bar{C}_\ell^{EE}\right) \end{pmatrix}. \tag{5.5}$$

The entries in the covariance matrix,

$$\bar{C}_\ell^{TT} = C_\ell^{TT} + N_\ell^{TT} \tag{5.6}$$

$$\bar{C}_\ell^{EE} = C_\ell^{EE} + N_\ell^{EE} \tag{5.7}$$

$$\bar{C}_\ell^{TE} = C_\ell^{TE}, \tag{5.8}$$

contain noise terms,

$$N_\ell^{TT} = \Delta_T^2 \exp\left[\frac{\ell(\ell+1)\theta_{FWHM}^2}{8\ln 2}\right] \tag{5.9}$$

$$N_\ell^{EE} = 2 \times N_\ell^{TT}, \tag{5.10}$$

where $\Delta_T = 1\mu K$, $\theta_{FWHM} = 8.7 \times 10^{-4}$rad, and $f_{\rm sky} = 0.4$. Similar calculations for χ^2 are done for the data acquired in the WFIRST and DESI experiments, which probe supernovae and BAO data, respectively.

To accomplish our task of reconciling theory with data, we employ many different numerical tools. A summary of our computational methodology is explained in the following section.

5.2 Computational Tools

Our goal is to find some map from the EFT functions appearing in Hordeski theories of MG to standard, cosmological parameters. To do this, we first use `EFTCAMB` to generate angular power spectra for a large number of Horndeski models. Then, using an emulator to speed up `CAMB`-like output and a minimizer built into `python`, we fit the EFT model to 6 standard cosmological parameters and 2 dark energy parameters: $\Omega_b h^2$, $\Omega_c h^2$, A_s, H_0, n_s, τ, w_0, and w_a.

5.2.1 EFTCAMB

`CAMB`, the Code for Anisotropies in the Microwave Background, is an open-source Einstein-Boltzmann equation solver used to study the evolution of perturbations in the universe [101]. The code is rather robust and can produce many useful outputs. Most relevant to this project is the angular power spectrum of the CMB, C_ℓ, a plot that shows how the temperature pattern in the universe varied at the time of recombination. See Section 5.1 for

a more detailed discussion of this observational quantity and how it relates to the EFTDE.

`EFTCAMB` is a patch for `CAMB` which implements the EFTDE approach to cosmic acceleration [102; 103]. It provides all the conveniences of the original Einstein-Boltzmann solver, and allows its user to implement and study almost any DE/MG model. The user is able to specify a background (ΛCDM or other) and the code evolves the full perturbation equations on all linear scales without relying on any quasi static approximation. Additionally, the user can demand stability conditions be checked in order to ensure that the underlying gravitational theory is acceptable.

The code uses the EFTDE action, Equation 3.121, with the scalar degree of freedom, π, explicitly realized,

$$
\begin{aligned}
S &= \int d^4x\sqrt{-g}\Bigg\{\frac{m_0^2}{2}[1+\Omega(\tau+\pi)]R + \Lambda(\tau+\pi) - c(\tau+\pi)a^2\Bigg[\delta g^{00} - 2\frac{\dot{\pi}}{a^2} \\
&+ 2\mathcal{H}\pi\left(\delta g^{00} - \frac{1}{a^2} - 2\frac{\dot{\pi}}{a^2}\right) + 2\dot{\pi}\delta g^{00} + 2g^{0i}\partial_i\pi - \frac{\dot{\pi}^2}{a^2} + g^{ij}\partial_i\pi\partial_j\pi - (2\mathcal{H}^2+\dot{\mathcal{H}})\frac{\pi^2}{a^2} + ...\Bigg] \\
&+ \frac{M_2^4(\tau+\pi)}{2}a^4\left(\delta g^{00} - 2\frac{\dot{\pi}}{a^2} - 2\frac{\mathcal{H}\pi}{a^2} + ...\right)^2 \\
&- \frac{\bar{M}_1^3(\tau+\pi)}{2}a^2\left(\delta g^{00} - 2\frac{\dot{\pi}}{a^2} - 2\frac{\mathcal{H}\pi}{a^2} + ...\right)\left(\delta K_\mu^\mu + 3\frac{\dot{\mathcal{H}}}{a}\pi + \frac{\bar{\nabla}^2\pi}{a^2} + ...\right) \\
&- \frac{\bar{M}_2^2(\tau+\pi)}{2}\left(\delta K_\mu^\mu + 3\frac{\dot{\mathcal{H}}}{a}\pi + \frac{\bar{\nabla}^2\pi}{a^2} + ...\right)^2 \\
&- \frac{\bar{M}_3^2(\tau+\pi)}{2}\left(\delta K_j^i + \frac{\dot{\mathcal{H}}}{a}\pi\delta_j^i + \frac{1}{a^2}\bar{\nabla}^i\bar{\nabla}_j\pi + ...\right)\left(\delta K_j^i + \frac{\dot{\mathcal{H}}}{a}\pi\delta_j^i + \frac{1}{a^2}\bar{\nabla}^j\bar{\nabla}_i\pi + ...\right) \\
&+ \frac{\hat{M}^2(\tau+\pi)}{2}a^2\left(\delta g^{00} - 2\frac{\dot{\pi}}{a^2} - 2\frac{\mathcal{H}\pi}{a^2} + ...\right)\left(\delta R^{(3)} + 4\frac{\mathcal{H}}{a}\bar{\nabla}^2\pi + ...\right) \\
&+ m_2^2(\tau+\pi)(g^{\mu\nu}+n^\mu n^\nu)\partial_\mu(a^2g^{00} - 2\dot{\pi} - 2\mathcal{H}\pi + ...)\partial_\nu(a^2g^{00} - 2\dot{\pi} - 2\mathcal{H}\pi + ...) + ...\Bigg\} \\
&+ S_m[g_{\mu\nu}, \chi_i].
\end{aligned}
\tag{5.11}
$$

Note that instead of parameterizing the conformal coupling to gravity via Ω, as is done in

the original EFTDE, the code uses $1 + \Omega$, for reasons of numerical accuracy. Choosing a background sets the functions c and Λ in the code. The remaining background quantity, Ω, is free to be set by the user. For the purposes of this project, we are interested in studying perturbations around a ΛCDM background, so we will keep $\Omega = 1$. The theory of EFTDE in general, however, allows this parameter to differ from 1 and the `EFTCAMB` code allows for this as well.

The remaining second order EFT functions, $\{M_2,\, \bar{M}_1,\, \bar{M}_2,\, \bar{M}_3,\, \hat{M},\, m_2\}$, encode the dynamics of the linear scalar perturbations and are free to be set by the user. The rescaled, dimensionless functions appear in the code as γ_i and are defined to be,

$$\begin{aligned} \gamma_1 = \frac{M_2^4}{m_0^2 H_0^2}, \qquad \gamma_2 = \frac{\bar{M}_1^3}{m_0^2 H_0}, \qquad \gamma_3 = \frac{\bar{M}_2^2}{m_0^2}, \\ \gamma_4 = \frac{\bar{M}_3^2}{m_0^2}, \qquad \gamma_5 = \frac{\hat{M}^2}{m_0^2}, \qquad \gamma_6 = \frac{m_2^2}{m_0^2}. \end{aligned} \tag{5.12}$$

In the dimensionless program variables defined here and used in `EFTCAMB`, Horndeski gravity equates to

$$2\gamma_5 = \gamma_3 = -\gamma_4; \;\; \gamma_6 = 0. \tag{5.13}$$

Remember, these functions are time-dependent. There are a number of hard-coded parameterizations defined in the code,

Constant	$\gamma_i(a) = \gamma_{i,0}$
Linear	$\gamma_i(a) = \gamma_{i,0} a$
Power Law	$\gamma_i(a) = \gamma_{i,0} a^s$
Exponential	$\gamma_i(a) = \exp \gamma_{i,0} a^s - 1$

and there is also space for user-defined functions. Hypothetically, the user can create their own model with any crazy combinations of EFT functions. However, theoretical priors baked into the code might flag certain user-defined models as not viable. It is of note that the full

set of physical conditions for the general EFTDE action is a topic of ongoing work. The conditions included in `EFTCAMB` are the ghost and gradient stability for GLPV theories. This class of theories includes the Horndeski models of interest.

5.2.2 EFTCosmoMC

`EFTCosmoMC` allows `EFTCAMB` to interface with actual cosmological data [104; 105]. It uses a Monte-Carlo approach to explore cosmological parameter space and the user is able to import actual Planck data sets. For this work, we use it to calculate the likelihood of an EFTDE model compared to actual observational data.

5.2.3 Emulators

When dealing with physical systems as complicated as our universe, performing robust numerical simulations such as these can often turn out to be quite cumbersome and time-consuming – even on a supercomputer working as fast as it can. It is for this reason that there has been much work – both in the field of cosmology and elsewhere – towards *further* speeding up numerical processes. One result of this work is the creation of *emulators*.

For our purposes, the emulator functions as an interpolator. Given a set of grid points and corresponding outcomes evaluated at these grid points, the emulator can interpolate between these grid points. After training the emulator with the aforementioned grid points and outputs, the emulator can produce output from grid points it was not initially trained on. For example, the cosmic emulator we use in Chapter 5 (called `EGG`) was introduced as a way to generate accurate predictions for the nonlinear matter power spectrum from a restricted number of simulations [142]. In this way, the emulator greatly decreases computation time, as compared to something like `CAMB`, matching its output to an accuracy of 1%.

In order to train the emulator efficiently, we want to find a distribution of parameters that provides optimal coverage of the space all the while using a limited number of sampling

points. That is, to populate the parameter space in a more clever way than simply gridding it out – with a large number of model parameters, this grid would become very large very quickly. Therefore, a Latin hypercube is often used. LH designs are a kind of stratified sampling scheme where only one sampling point can exist in each "row" or "column" and their higher-dimensional equivalents. Formally,

> A **Latin hypercube** design is an $n \times m$ matrix in which each column is a unique random permutation of $1, ..., n$.

The use of an LH sampling scheme thus allows us to efficiently cover the whole parameter space with the smallest amount of training points possible. Additionally, LH designs are often combined with other design strategies in order to further optimize the parameter selection.

5.3 Methods

The cosmic emulator we use is called `EGG` [141; 142]. We train it on established grid points and their corresponding outcomes – in this case, the inputs are the aforementioned cosmological parameters and the output is the angular power spectrum created by `CAMB`. We select grid points from within a parameter range as seen in Table 5.2. We use an LH sampling method so as to not be biased toward any one section of the 8-dimensional parameter space and affect the emulator's training and eventually, results [143]. To do this, we use a package built into `python` called `pyDOE` [144].

Once training is completed, the emulator acts like `CAMB` in that it can provide angular power spectra output for any cosmological parameter input (as long as it is within the parameter range specified in Table 5.2). It differs from `CAMB`, however, in that it can do this *much* faster and without losing much accuracy. Next, we use an optimizer called iminuit to find combinations of cosmological (and dark energy) parameters that best fit the EFTDE model in question – in this case, a Horndeski model [145]. This part of the numerical pipeline,

Parameter	$\Omega_b h^2$	$\Omega_c h^2$	A_s	H_0	n_s	τ	w_0	w_a
Upper Bound	0.02297	0.1257	2.703×10^{-9}	70.2	0.9865	0.0965	-0.5	0.5
Fiducial Value	0.02222	0.1197	2.196×10^{-9}	67.5	0.9655	0.06	-1	0
Lower Bound	0.02147	0.1137	1.132×10^{-9}	64.8	0.9445	0.0235	-1.5	-0.5

Table 5.2: Parameter ranges used in training the emulator and their fiducial values. For the 6 cosmological parameters, we allowed the parameters to range within 5σ of their fiducial value as taken from Planck data [8]. We allowed the dark energy parameters to have an arbitrarily wide range.

the minimization, employs the emulator to iterate through many cosmological parameters configurations quickly (corresponding to different angular power spectra) in order to find one that looks like the power spectrum of the EFT model. Once the minimizer arrives at this best fit solution, we calculate the χ^2 value to quantify exactly how good the fit is. A summary of the data sets we used to calculate this χ^2 can be found in Table 5.1.

From the best-fit cosmological model, we can identify what values of w_0 and w_a each EFT model yields. Plots of this can be found in the results section, Section 5.5. Before this, we must isolate the interesting ranges of Horndeski parameter space. That is, the parameterizations of EFT functions and the values of their coefficients which produce angular power spectra which align most closely with data. To do this, we use a code we learned about in Section 5.2.2 called `EFTCosmoMC`.

5.4 Exploring Horndeski Parameter Space

As introduced in Section 5.2.2, `EFTCosmoMC` allows `EFTCAMB` to interface with cosmological data. The user can input any EFT model and `EFTCosmoMC` calculates, among other things, the likelihood of the model compared to real data. The likelihood, $\mathcal{L}$, is a quantity, like χ^2, which quantifies how much the model's output differs from real data,

$$\mathrm{L} \sim \mathrm{e}^{-\chi^2/2} \tag{5.14}$$

This step helps to identify which Horndeski models will yield successful fits when fed through our established computational pipeline. Figures 5.1, 5.2, and 5.3 show the results of these tests for the chosen parameterization of the EFT functions, $\gamma_i = \gamma_{i,0}\, a$.

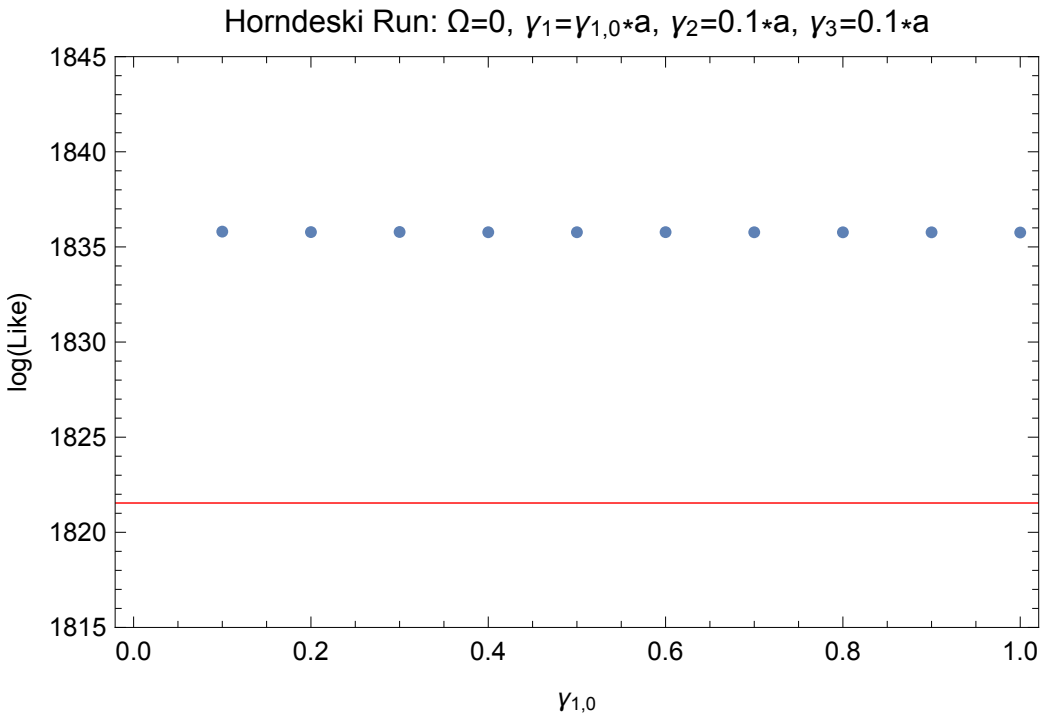

Figure 5.1: Likelihood comparison for ΛCDM background ($\Omega = 0$ in code parameters) with time-dependent parametrizations for the EFT functions in a Horndeski model. The red line denotes the expected likelihood for a ΛCDM model. Here, all parameters except $\gamma_{1,0}$ are held constant. We see that the value of $\gamma_{1,0}$ does not affect the likelihood significantly.

Based on what we learned through the use of `EFTCosmoMC` and the desire to keep our EFT models of interest close to observation, we proceed with our studies of Horndeski models with parameters randomly selected in the ranges: $\gamma_1 \leq 1$, $\gamma_2 \leq 0.1$ and $\gamma_3 \leq 0.1$, where we have dropped the $_{,0}$ subscript for convenience.

5.5 Results and Discussion

For the following summary of results, we used a linear parameterization for the EFT functions, Equation 5.1, and selected the parameters randomly based on parameter ranges deter-

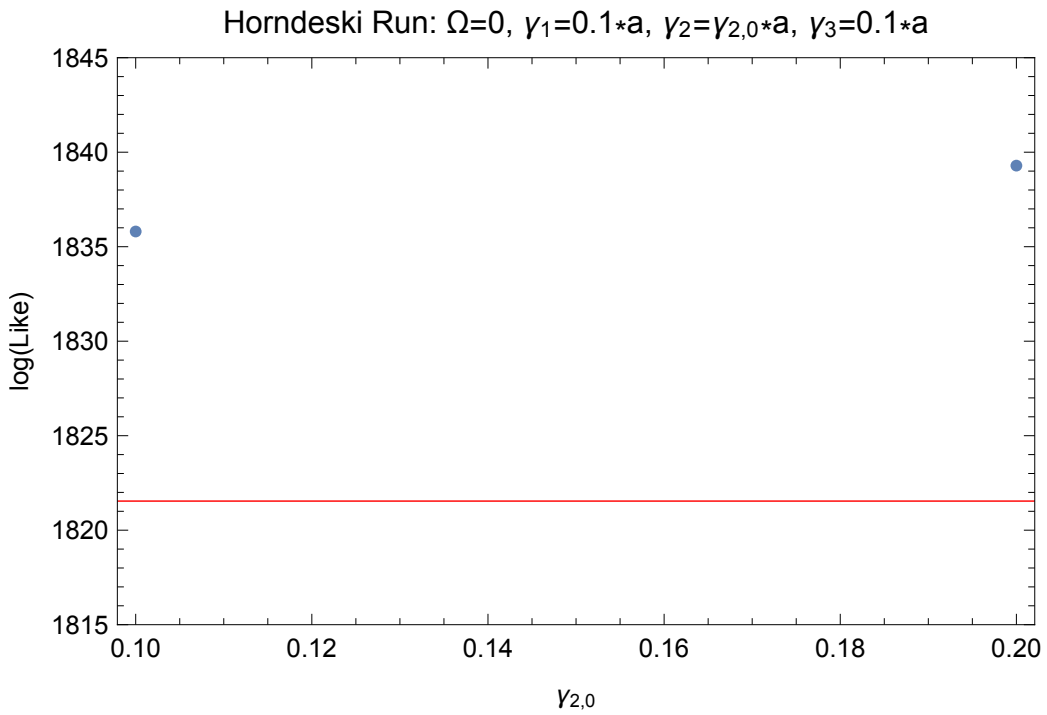

Figure 5.2: Likelihood comparison for ΛCDM background ($\Omega = 0$ in code parameters) with time-dependent parametrizations for the EFT functions in a Horndeski model. The red line denotes the expected likelihood for a ΛCDM model. Here, all parameters except $\gamma_{2,0}$ are held constant. When $\gamma_{2,0}$ takes on too large a value, the model no longer satisfies theoretical prior. We determined that $\gamma_{2,0} < 0.2$ is required for the model to remain theoretically stable.

mined in the trials with `EFTCosmoMC`, as described in Section 5.4. Additionally, we removed any run that returned a minimized χ^2 value of more than 5σ, or 650, as well as any run that hit a wall in our parameter space based on the upper and lower limits defined in Table 5.2. In this way, we make certain that we are reporting good fits as well as ones that lie somewhat close to observational data.

To arrive at the 5σ cutoff of $\chi^2 < 650$, we used the standard calculation of the standard deviation, σ,

$$\sigma = \sqrt{2 \times \text{d.o.f.}}\,, \tag{5.15}$$

where d.o.f. is the number of degree of freedom in the problem – approximately equal to the number of data points used. Our data consists of the angular power spectra (TT, TE,

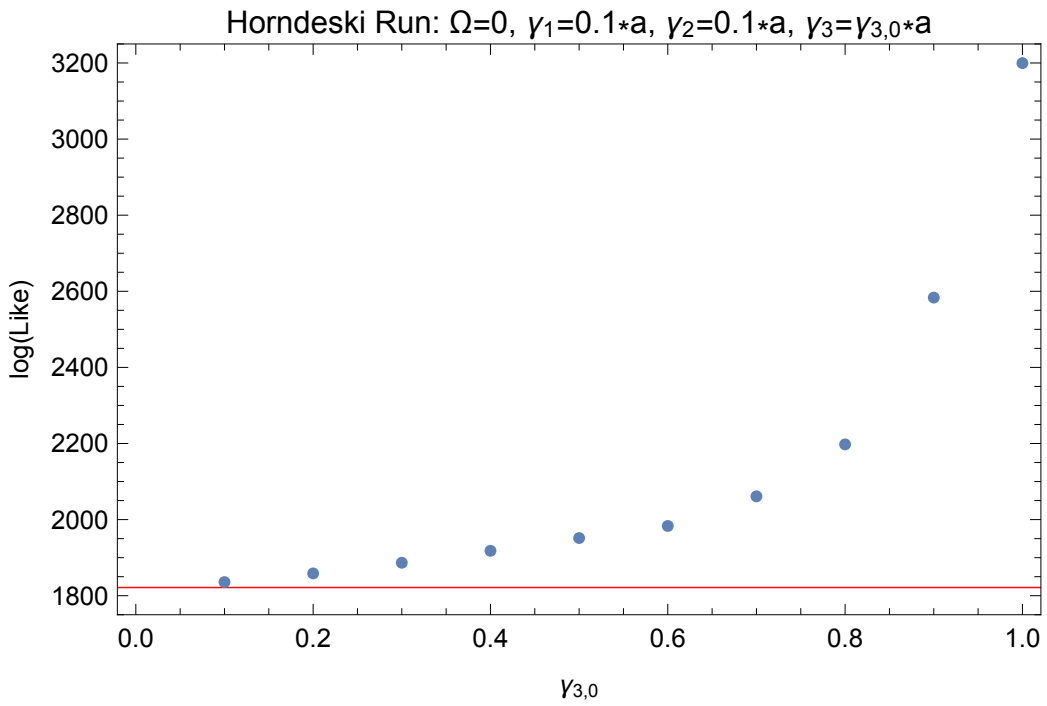

Figure 5.3: Likelihood comparison for ΛCDM background ($\Omega = 0$ in code parameters) with time-dependent parametrizations for the EFT functions in a Horndeski model. The red line denotes the expected likelihood for a ΛCDM model. Here, all parameters except $\gamma_{3,0}$ are held constant. We see that the likelihood increases exponentially as this parameter is turned up. Conversely, turning the parameter down results in a smooth, continuous approach to the expected output for the background.

and EE components), each of which has multipoles from $\ell = 2$ to $\ell = 2500$, leaving us with approximately 7500 data points and, thus, a 5σ cutoff of about 650 (rounding up).

Figure 5.4 shows the distribution of best-fit values of each cosmological and dark energy parameter for both ΛCDM and Horndeski runs. There is some noticeable scatter in the ΛCDM runs. This is due to an initial emulator error of about 1.2. In an ideal world, this initial emulator error would be zero. This is the price we pay for speed. The price is worth it in the end as the scatter in the EFT models is much greater than that in the ΛCDM models. We are able to identify features in the EFT fits that are not present in the ΛCDM fits. Such features are much more apparent when we isolate a 2D parameter plane of focus. For the purposes of this work, we are interested in the $w_0 - w_a$ plane.

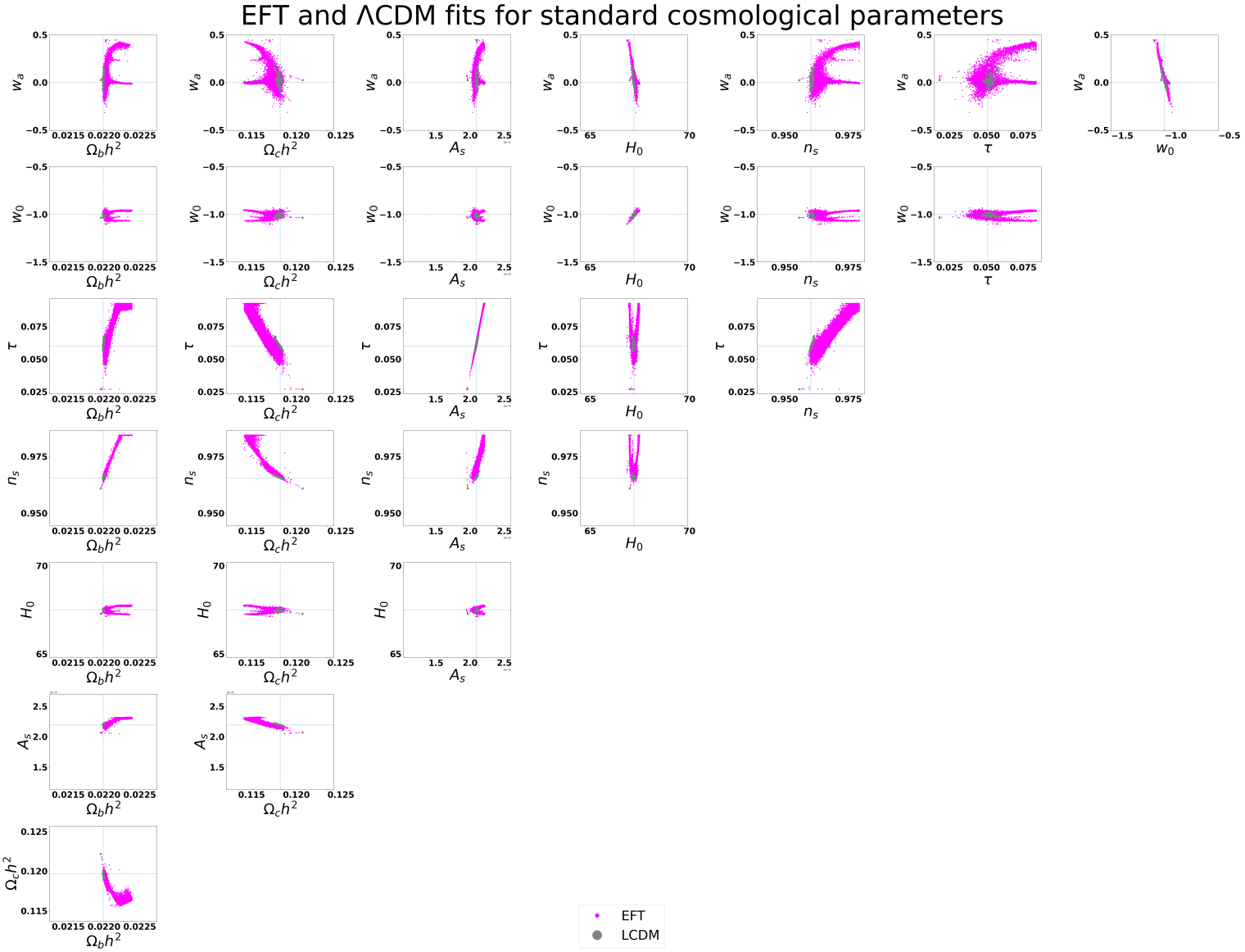

Figure 5.4: Triangular plot that shows the distribution of best-fit values of each parameter from both EFT (Horndeski) and fiducial (ΛCDM) realizations. This plot shows about 500 fiducial realizations and 20,000 realizations of EFT models with randomly selected values of $\gamma_1 < 1$, $\gamma_2 < 0.1$, and $\gamma_3 < 0.1$ and a linear parameterization for their associated functions, as described in Equation 5.1.

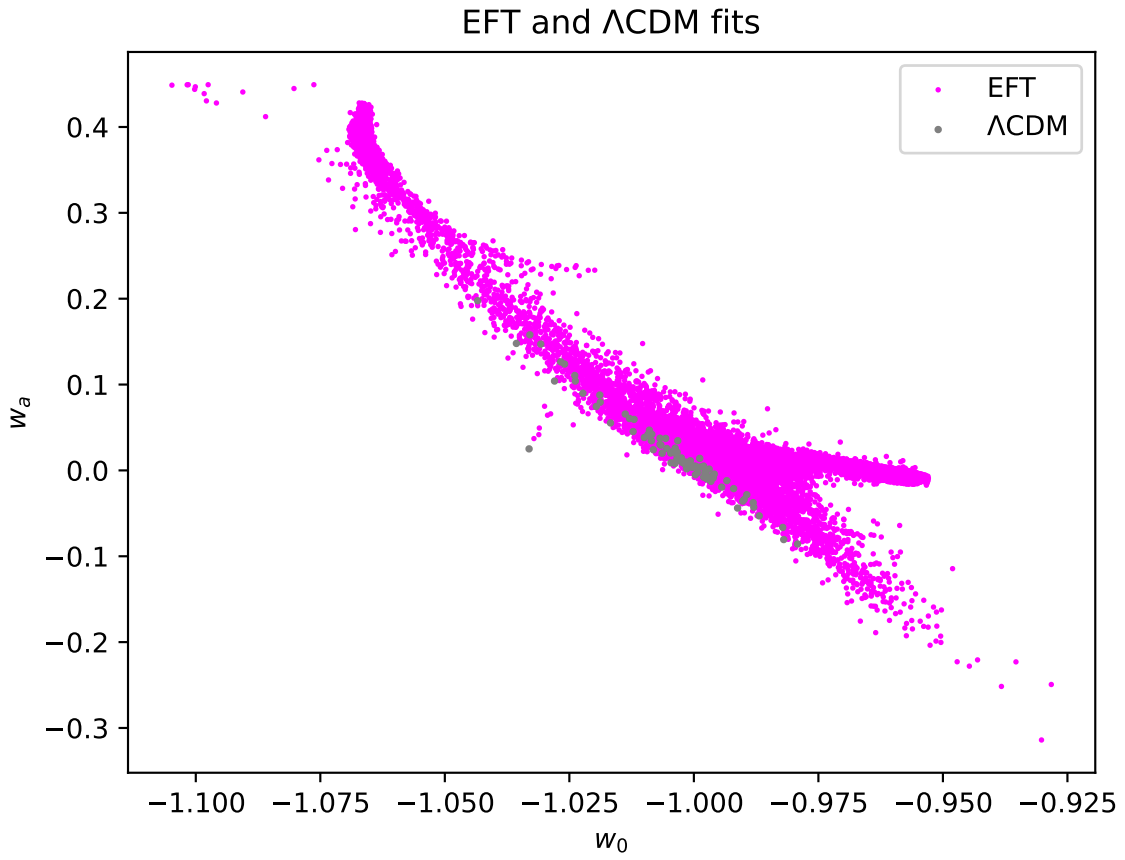

Figure 5.5: An enlarged plot of the $w_0 - w_a$ plane shown originally in Figure 5.4. The grey points show about 500 ΛCDM fits and the magenta points show about 20,000 EFT (Horndeski) fits to dark energy parameters w_0 and w_a. In an ideal world, we expect the ΛCDM model points to be at $w_0 = -1$ and $w_a = 0$. However, due to the imperfect accuracy of the emulator we see some scatter.

The magenta EFT points in Figure 5.5 exhibit a couple very distinct features as compared to the ΛCDM points. There is an obvious cluster of points off the diagonal created by the ΛCDM fits towards the bottom right of the plot. This group of points clearly picked a different line of constant w than the majority of the rest of the points in both ΛCDM and EFT realizations. Additionally, there is a small curve away from the diagonal in the top left of the plot. Both features become more pronounced as the values of γ_2 and γ_3 increase and seem to have no correlation with the value of γ_1. This jives with what we found in the

previous section, Section 5.4, which indicated that the value of γ_1 did not have much impact on the output (see Figure 5.1). Here, we see that as the values of γ_2 and γ_3 increase, the points in the $w_0 - w_a$ plane creep away from their ΛCDM background. Similarly, the value of χ^2 increases as γ_2 and γ_3 increase, as shown in Figure 5.6. So, the farther from ΛCDM we are, the worse our fits are. All fits plotted, however, are within the 5σ range of observation.

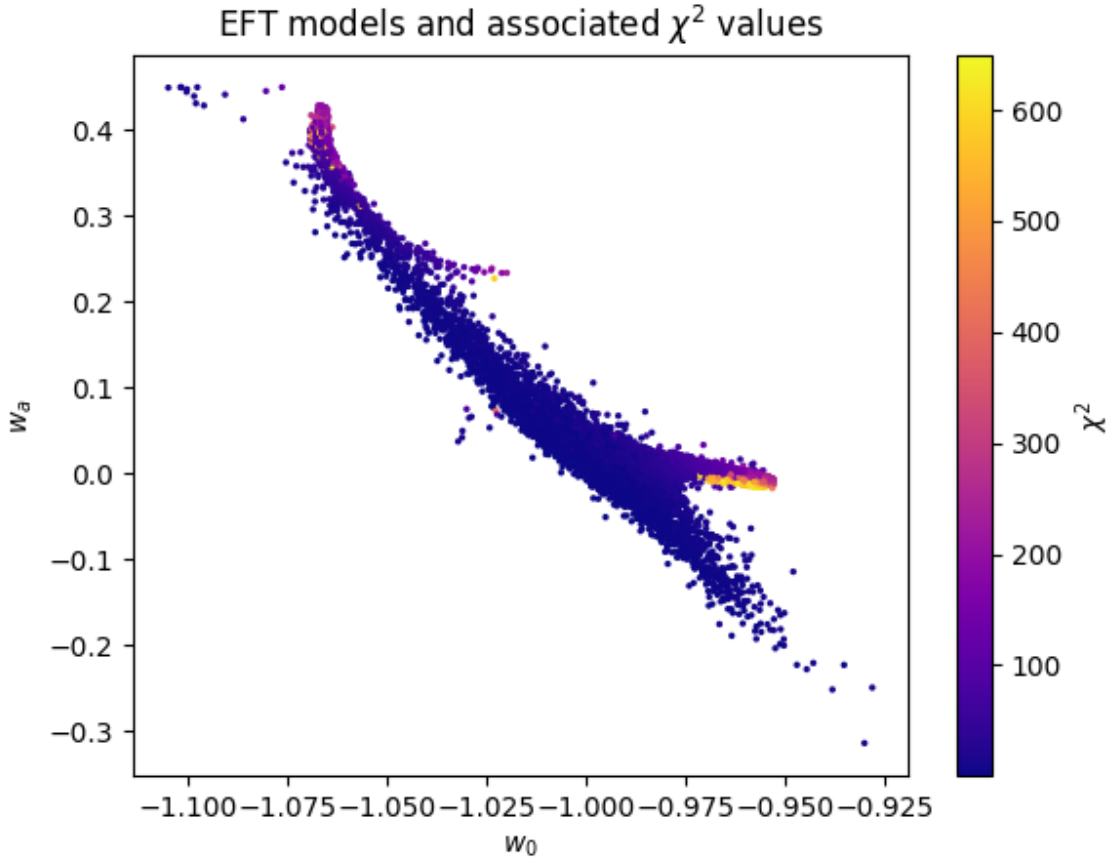

Figure 5.6: A plot of the same $w_0 - w_a$ plane shown in Figure 5.5. All points on this plot are randomly chosen Horndeski models within the parameter space determined to produce observation and with $\chi^2 < 650$. The gradient shows how the specific value of χ^2 changes for each region of the plot. In general, the farther the points are from ΛCDM, the higher the χ^2 value.

In conclusion, we see features unique to the Horndeski models in all parameter combinations. We have focused on the $w_0 - w_a$ plane, but other parameter combinations offer

interesting insight as well. There is a splitting in the w_0 parameter, seen in Figure 5.4, that is of particular interest. The EFT models seem to gravitate to two distinct w_0 values. Also of note is that there is very little scatter in the $w_0 - H_0$ plane. The EFT realizations cluster around the standard, fiducial value, overlapping the ΛCDM realizations fit to a $w_0 w_a$CDM universe almost exactly. Further analysis into this and more can be found in the forthcoming paper, expected on the Arxiv this summer.

CHAPTER 6

CONCLUSIONS

In this thesis, we have investigated multiple open questions in cosmology through the lens of Effective Field Theories. After acquainting ourselves with Weinberg and Cheung et. al.'s formulations of the EFT of Inflation, we introduced a generalized theory using EFT formalism for all models of (p)reheating: the EFT of Reheating. This novel work showed that, by extending Cheung et. al.'s EFT of Inflation to include the end of inflation and the beginning of reheating, we can describe most existing models of reheating as well as some new ones. This work exemplifies how useful the EFT framework is in studying cosmological phenomenology.

A good portion of the original research in this thesis focused on the application of the EFT formalism to the question of dark energy and modified gravity. The accelerated expansion we observe at present day is not so different from the expansion during the inflationary epoch (albeit at very different energy scales). Therefore, extending the EFT of Inflation to include matter terms is somewhat natural. We saw in Chapter 5 how this Effective Field Theory of Dark Energy can efficiently describe all models of dark energy and modified gravity containing one extra degree of freedom. The work in this thesis investigated the relationship between these EFTDE theories and observation. We determined that a Horndeski theory of gravity remains a plausible explanation for the observed accelerated expansion of the universe. However, the EFT parameters in the theory must remain rather small and close to standard ΛCDM values in order to reproduce observation. We left many EFTDE models unexplored and this represents an area for future research.

Additionally, as the field of cosmology continues to progress, the need for efficient numerical tools will only grow. This thesis utilized a few kinds of computational techniques to tackle big questions in cosmology. Namely, we used `CAMB` to train an emulator in tandem with `EFTCAMB` and a minimizer to complete the work done on the Effective Field Theory

of Dark Energy in Chapter 5. In Chapter 4, we used an open-source code called `GABE` to investigate the decay of moduli fields (fields generic to string theory) into gauge fields at the end of inflation. Ultimately, we found no strong resonance in the gauge fields and thus no significant decay of the moduli fields. The code, `GABE`, evolves scalar fields over an expanding background, making it a very useful tool for a cosmologist studying the evolution of the universe. It is possible to use `GABE` in the future to study other models of resonance and (p)reheating, as this remains an area of active study in cosmology.

REFERENCES

[1] A. Einstein, "Cosmological Considerations in the General Theory of Relativity," *Sitzungsber. Preuss. Akad. Wiss. Berlin (Math. Phys.)*, (1917).

[2] R. H. Brandenberger, [arXiv:hep-ph/9910410 [hep-ph]].

[3] A. Friedman, Z. Phys. **10**, 377-386 (1922) doi:10.1007/BF01332580

[4] J. P. Luminet, Gen. Rel. Grav. **45**, 1619-1633 (2013) doi:10.1007/s10714-013-1547-4 [arXiv:1305.6470 [physics.hist-ph]].

[5] H. P. Robertson, Astrophys. J. **83**, 257-271 (1936) doi:10.1086/143726

[6] A. G. Walker, "On riemannian spaces and spherical symmetry about a line and the conditions for isotropy in general relativity," Quart J. Math. Oxford 6 (1935).

[7] E. Hubble, National Academy of Sciences, **15**, 3, pp. 168-173 (1929) doi 10.1073/pnas.15.3.168

[8] N. Aghanim *et al.* [Planck], Astron. Astrophys. **641**, A6 (2020) doi:10.1051/0004-6361/201833910 [arXiv:1807.06209 [astro-ph.CO]].

[9] D. Camarena and V. Marra, Phys. Rev. Res. **2**, no.1, 013028 (2020) doi:10.1103/PhysRevResearch.2.013028 [arXiv:1906.11814 [astro-ph.CO]].

[10] S. Weinberg, Rev. Mod. Phys. **61**, 1-23 (1989) doi:10.1103/RevModPhys.61.1

[11] C. L. Bennett et al., Astrophys. J. Suppl. 208 (2013) doi:10.1088/0067-0049/208/2/20

[12] A. A. Penzias and R. W. Wilson, Astrophys. J. 142 (1965), pp. 419-421. doi: 10.1086/148307.

[13] A. H. Guth, Phys. Rev. D **23**, 347-356 (1981) doi:10.1103/PhysRevD.23.347

[14] A. Silvestri and M. Trodden, Rept. Prog. Phys. **72**, 096901 (2009) doi:10.1088/0034-4885/72/9/096901 [arXiv:0904.0024 [astro-ph.CO]].

[15] D. Baumann, "Effective Field Theory in Cosmology," Cargese Lectures, University of Amsterdam.

[16] S. Weinberg, "The Quantum Theory of Fields," Cambridge University Press, (1995).

[17] J. Polchinski, [arXiv:hep-th/9210046 [hep-th]].

[18] C. P. Burgess, [arXiv:hep-ph/9812470 [hep-ph]].

[19] H. Georgi, Annual Review of Nuclear and Particle Science **43**, 1 (1993) doi:10.1146/annurev.ns.43.120193.001233.

[20] A. V. Manohar, Lect. Notes Phys. **479**, 311-362 (1997) doi:10.1007/BFb0104294 [arXiv:hep-ph/9606222 [hep-ph]].

[21] D. B. Kaplan, [arXiv:nucl-th/0510023 [nucl-th]].

[22] O. Ozsoy, G. Sengor, K. Sinha and S. Watson, arXiv:1507.06651 [hep-th].

[23] L. F. Abbott, E. Farhi and M. B. Wise, Phys. Lett. **117B**, 29 (1982). doi:10.1016/0370-2693(82)90867-X

[24] A. Albrecht, P. J. Steinhardt, M. S. Turner and F. Wilczek, Phys. Rev. Lett. **48**, 1437 (1982). doi:10.1103/PhysRevLett.48.1437

[25] A. D. Dolgov and A. D. Linde, Phys. Lett. **116B**, 329 (1982). doi:10.1016/0370-2693(82)90292-1

[26] A. D. Dolgov and D. P. Kirilova, Sov. J. Nucl. Phys. **51**, 172 (1990) [Yad. Fiz. **51**, 273 (1990)].

[27] J. H. Traschen and R. H. Brandenberger, Phys. Rev. D **42**, 2491 (1990). doi:10.1103/PhysRevD.42.2491

[28] L. Kofman, A. D. Linde and A. A. Starobinsky, Phys. Rev. D **56**, 3258 (1997) doi:10.1103/PhysRevD.56.3258 [hep-ph/9704452].

[29] M. A. Amin, M. P. Hertzberg, D. I. Kaiser and J. Karouby, Int. J. Mod. Phys. D **24**, 1530003 (2014) doi:10.1142/S0218271815300037 [arXiv:1410.3808 [hep-ph]].

[30] R. Allahverdi, R. Brandenberger, F. Y. Cyr-Racine and A. Mazumdar, Ann. Rev. Nucl. Part. Sci. **60**, 27 (2010) doi:10.1146/annurev.nucl.012809.104511 [arXiv:1001.2600 [hep-th]].

[31] S. Y. Khlebnikov and I. I. Tkachev, Phys. Rev. Lett. **77**, 219 (1996) doi:10.1103/PhysRevLett.77.219 [hep-ph/9603378].

[32] R. Easther and E. A. Lim, JCAP **0604**, 010 (2006) doi:10.1088/1475-7516/2006/04/010 [astro-ph/0601617].

[33] J. Garcia-Bellido and A. D. Linde, Phys. Rev. D **57**, 6075 (1998) doi:10.1103/PhysRevD.57.6075 [hep-ph/9711360].

[34] G. N. Felder, J. Garcia-Bellido, P. B. Greene, L. Kofman, A. D. Linde and I. Tkachev, Phys. Rev. Lett. **87**, 011601 (2001) doi:10.1103/PhysRevLett.87.011601 [hep-ph/0012142].

[35] R. Easther, J. T. Giblin, Jr. and E. A. Lim, Phys. Rev. Lett. **99**, 221301 (2007) doi:10.1103/PhysRevLett.99.221301 [astro-ph/0612294].

[36] L. R. Price and X. Siemens, Phys. Rev. D **78**, 063541 (2008) doi:10.1103/PhysRevD.78.063541 [arXiv:0805.3570 [astro-ph]].

[37] R. Easther, H. Finkel and N. Roth, JCAP **1010**, 025 (2010) doi:10.1088/1475-7516/2010/10/025 [arXiv:1005.1921 [astro-ph.CO]].

[38] M. P. Hertzberg, J. Karouby, W. G. Spitzer, J. C. Becerra and L. Li, "Theory of self-resonance after inflation. I. Adiabatic and isocurvature Goldstone modes," Phys. Rev. D **90**, 123528 (2014) doi:10.1103/PhysRevD.90.123528 [arXiv:1408.1396 [hep-th]].

[39] M. A. Amin and D. Baumann, "From Wires to Cosmology," JCAP **1602**, no. 02, 045 (2016) doi:10.1088/1475-7516/2016/02/045 [arXiv:1512.02637 [astro-ph.CO]].

[40] S. Weinberg, Phys. Rev. D **77**, 123541 (2008) doi:10.1103/PhysRevD.77.123541 [arXiv:0804.4291 [hep-th]].

[41] M. Park, K. M. Zurek and S. Watson, Phys. Rev. D **81**, 124008 (2010) doi:10.1103/PhysRevD.81.124008 [arXiv:1003.1722 [hep-th]].

[42] P. Creminelli, M. A. Luty, A. Nicolis and L. Senatore, JHEP **0612**, 080 (2006) doi:10.1088/1126-6708/2006/12/080 [hep-th/0606090].

[43] C. Cheung, P. Creminelli, A. L. Fitzpatrick, J. Kaplan and L. Senatore, JHEP **0803**, 014 (2008) doi:10.1088/1126-6708/2008/03/014 [arXiv:0709.0293 [hep-th]].

[44] L. Senatore and M. Zaldarriaga, JHEP **1204**, 024 (2012) doi:10.1007/JHEP04(2012)024 [arXiv:1009.2093 [hep-th]].

[45] P. Creminelli, G. D'Amico, J. Norena and F. Vernizzi, JCAP **0902**, 018 (2009) doi:10.1088/1475-7516/2009/02/018 [arXiv:0811.0827 [astro-ph]].

[46] J. K. Bloomfield, É. É. Flanagan, M. Park and S. Watson, JCAP **1308**, 010 (2013) doi:10.1088/1475-7516/2013/08/010 [arXiv:1211.7054 [astro-ph.CO]].

[47] G. Gubitosi, F. Piazza and F. Vernizzi, JCAP **1302**, 032 (2013) [JCAP **1302**, 032 (2013)] doi:10.1088/1475-7516/2013/02/032 [arXiv:1210.0201 [hep-th]].

[48] M. Lewandowski, A. Maleknejad and L. Senatore, arXiv:1611.07966 [astro-ph.CO].

[49] D. Baumann, A. Nicolis, L. Senatore and M. Zaldarriaga, JCAP **1207**, 051 (2012) doi:10.1088/1475-7516/2012/07/051 [arXiv:1004.2488 [astro-ph.CO]].

[50] L. Kofman and P. Yi, Phys. Rev. D **72**, 106001 (2005) doi:10.1103/PhysRevD.72.106001 [hep-th/0507257].

[51] D. R. Green, Phys. Rev. D **76**, 103504 (2007) doi:10.1103/PhysRevD.76.103504 [arXiv:0707.3832 [hep-th]].

[52] G. N. Felder, L. Kofman and A. D. Linde, Phys. Rev. D **59**, 123523 (1999) doi:10.1103/PhysRevD.59.123523 [hep-ph/9812289].

[53] P. A. R. Ade *et al.* [Planck Collaboration], Astron. Astrophys. **594**, A20 (2016) doi:10.1051/0004-6361/201525898 [arXiv:1502.02114 [astro-ph.CO]].

[54] J. M. Maldacena, JHEP **0305**, 013 (2003) doi:10.1088/1126-6708/2003/05/013 [astro-ph/0210603].

[55] V. Assassi, D. Baumann, D. Green and L. McAllister, JCAP **1401**, 033 (2014) doi:10.1088/1475-7516/2014/01/033 [arXiv:1304.5226 [hep-th]].

[56] A. Adams, N. Arkani-Hamed, S. Dubovsky, A. Nicolis and R. Rattazzi, JHEP **0610**, 014 (2006) doi:10.1088/1126-6708/2006/10/014 [hep-th/0602178].

[57] D. A. Easson and A. Vikman, arXiv:1607.00996 [gr-qc].

[58] X. Chen and Y. Wang, JCAP **1004**, 027 (2010) doi:10.1088/1475-7516/2010/04/027 [arXiv:0911.3380 [hep-th]].

[59] S. Cremonini, Z. Lalak and K. Turzynski, JCAP **1103**, 016 (2011) doi:10.1088/1475-7516/2011/03/016 [arXiv:1010.3021 [hep-th]].

[60] A. Achucarro, J. O. Gong, S. Hardeman, G. A. Palma and S. P. Patil, JCAP **1101**, 030 (2011) doi:10.1088/1475-7516/2011/01/030 [arXiv:1010.3693 [hep-ph]].

[61] A. J. Tolley and M. Wyman, Phys. Rev. D **81**, 043502 (2010) doi:10.1103/PhysRevD.81.043502 [arXiv:0910.1853 [hep-th]].

[62] G. Shiu and J. Xu, Phys. Rev. D **84**, 103509 (2011) doi:10.1103/PhysRevD.84.103509 [arXiv:1108.0981 [hep-th]].

[63] A. Avgoustidis, S. Cremonini, A. C. Davis, R. H. Ribeiro, K. Turzynski and S. Watson, JCAP **1206**, 025 (2012) doi:10.1088/1475-7516/2012/06/025 [arXiv:1203.0016 [hep-th]].

[64] C. P. Burgess, M. W. Horbatsch and S. P. Patil, JHEP **1301**, 133 (2013) doi:10.1007/JHEP01(2013)133 [arXiv:1209.5701 [hep-th]].

[65] D. Baumann and D. Green, JCAP **1109**, 014 (2011) doi:10.1088/1475-7516/2011/09/014 [arXiv:1102.5343 [hep-th]].

[66] C. Armendariz-Picon, M. Trodden and E. J. West, JCAP **0804**, 036 (2008) doi:10.1088/1475-7516/2008/04/036 [arXiv:0707.2177 [hep-ph]].

[67] F. C. Adams, J. R. Bond, K. Freese, J. A. Frieman and A. V. Olinto, Phys. Rev. D **47**, 426 (1993) doi:10.1103/PhysRevD.47.426 [hep-ph/9207245].

[68] N. Arkani-Hamed, H. C. Cheng, P. Creminelli and L. Randall, JCAP **0307**, 003 (2003) doi:10.1088/1475-7516/2003/07/003 [hep-th/0302034].

[69] S. Dimopoulos, S. Kachru, J. McGreevy and J. G. Wacker, JCAP **0808**, 003 (2008) doi:10.1088/1475-7516/2008/08/003 [hep-th/0507205].

[70] N. Vogt-Nilsen, MURA-118, MURA-NVN-3.

[71] B. R. Greene, T. Prokopec and T. G. Roos, Phys. Rev. D **56**, 6484 (1997) doi:10.1103/PhysRevD.56.6484 [hep-ph/9705357].

[72] M. Amin, "FloqEx," [http://mustafa-amin.com/home/codes/].

[73] M. A. Amin, R. Easther, H. Finkel, R. Flauger and M. P. Hertzberg, Phys. Rev. Lett. **108**, 241302 (2012) doi:10.1103/PhysRevLett.108.241302 [arXiv:1106.3335 [astro-ph.CO]].

[74] P. Adshead, Y. Cui and J. Shelton, JHEP **1606**, 016 (2016) doi:10.1007/JHEP06(2016)016 [arXiv:1604.02458 [hep-ph]].

[75] E. V. Linder, G. Sengor and S. Watson, JCAP **1605**, no. 05, 053 (2016) doi:10.1088/1475-7516/2016/05/053 [arXiv:1512.06180 [astro-ph.CO]].

[76] C. Cheung, A. L. Fitzpatrick, J. Kaplan and L. Senatore, JCAP **0802**, 021 (2008) doi:10.1088/1475-7516/2008/02/021 [arXiv:0709.0295 [hep-th]].

[77] S. Weinberg, Phys. Rev. D **67**, 123504 (2003) doi:10.1103/PhysRevD.67.123504 [astro-ph/0302326].

[78] F. Piazza and F. Vernizzi, Class. Quant. Grav. **30**, 214007 (2013) doi:10.1088/0264-9381/30/21/214007 [arXiv:1307.4350 [hep-th]].

[79] T. Noumi, M. Yamaguchi and D. Yokoyama, JHEP **1306**, 051 (2013) doi:10.1007/JHEP06(2013)051 [arXiv:1211.1624 [hep-th]].

[80] H. L. Child, J. T. Giblin, Jr, R. H. Ribeiro and D. Seery, Phys. Rev. Lett. **111**, 051301 (2013) doi:10.1103/PhysRevLett.111.051301 [arXiv:1305.0561 [astro-ph.CO]].

[81] C. de Rham, Living Rev. Rel. **17**, 7 (2014) doi:10.12942/lrr-2014-7 [arXiv:1401.4173 [hep-th]].

[82] M. C. Johnson and M. Kamionkowski, Phys. Rev. D **78**, 063010 (2008) doi:10.1103/PhysRevD.78.063010 [arXiv:0805.1748 [astro-ph]].

[83] M. S. Turner, Phys. Rev. D **28**, 1243 (1983). doi:10.1103/PhysRevD.28.1243

[84] J. S. Bains, M. P. Hertzberg and F. Wilczek, arXiv:1512.02304 [hep-th].

[85] S. R. Behbahani, A. Dymarsky, M. Mirbabayi and L. Senatore, JCAP **1212**, 036 (2012) doi:10.1088/1475-7516/2012/12/036 [arXiv:1111.3373 [hep-th]].

[86] C. P. Burgess, Living Rev. Rel. **7**, 5 (2004) doi:10.12942/lrr-2004-5 [gr-qc/0311082].

[87] V. Mukhanov, "Physical Foundations of Cosmology,"

[88] R. Easther, R. Flauger and J. B. Gilmore, JCAP **1104**, 027 (2011) doi:10.1088/1475-7516/2011/04/027 [arXiv:1003.3011 [astro-ph.CO]].

[89] K. Jedamzik, M. Lemoine and J. Martin, JCAP **1004**, 021 (2010) doi:10.1088/1475-7516/2010/04/021 [arXiv:1002.3278 [astro-ph.CO]].

[90] J. F. Dufaux, G. N. Felder, L. Kofman, M. Peloso and D. Podolsky, JCAP **0607**, 006 (2006) doi:10.1088/1475-7516/2006/07/006 [hep-ph/0602144].

[91] B. A. Bassett, S. Tsujikawa and D. Wands, Rev. Mod. Phys. **78**, 537 (2006) doi:10.1103/RevModPhys.78.537 [astro-ph/0507632].

[92] J. F. Dufaux, A. Bergman, G. N. Felder, L. Kofman and J. P. Uzan, Phys. Rev. D **76**, 123517 (2007) doi:10.1103/PhysRevD.76.123517 [arXiv:0707.0875 [astro-ph]].

[93] J. T. Giblin and E. Thrane, Phys. Rev. D **90**, no. 10, 107502 (2014) doi:10.1103/PhysRevD.90.107502 [arXiv:1410.4779 [gr-qc]].

[94] D. G. Figueroa and F. Torrenti, arXiv:1609.05197 [astro-ph.CO].

[95] K. D. Lozanov and M. A. Amin, doi:10.1103/PhysRevLett.119.061301 arXiv:1608.01213 [astro-ph.CO].

[96] D. Lopez Nacir, R. A. Porto, L. Senatore and M. Zaldarriaga, JHEP **1201**, 075 (2012) doi:10.1007/JHEP01(2012)075 [arXiv:1109.4192 [hep-th]].

[97] D. Green, JCAP **1503**, no. 03, 020 (2015) doi:10.1088/1475-7516/2015/03/020 [arXiv:1409.6698 [hep-th]].

[98] `http://cosmo.kenyon.edu/gabe.html`

[99] T. S. Bunch and P. C. W. Davies, Proc. Roy. Soc. Lond. A **360**, 117-134 (1978) doi:10.1098/rspa.1978.0060

[100] G. N. Felder and I. Tkachev, Comput. Phys. Commun. **178**, 929-932 (2008) doi:10.1016/j.cpc.2008.02.009 [arXiv:hep-ph/0011159 [hep-ph]].

[101] A. Lewis, "CAMB Notes," `https://cosmologist.info/notes/CAMB.pdf`.

[102] B. Hu, M. Raveri, N. Frusciante and A. Silvestri, [arXiv:1405.3590 [astro-ph.IM]].

[103] `http://www.eftcamb.org`.

[104] `https://github.com/EFTCAMB/EFTCosmoMC`

[105] A. Lewis and S. Bridle, Phys. Rev. D **66**, 103511 (2002) doi:10.1103/PhysRevD.66.103511 [arXiv:astro-ph/0205436 [astro-ph]].

[106] G. Kane, K. Sinha and S. Watson, Int. J. Mod. Phys. D **24**, no.08, 1530022 (2015) doi:10.1142/S0218271815300220 [arXiv:1502.07746 [hep-th]].

[107] D. Baumann and L. McAllister, doi:10.1017/CBO9781316105733 [arXiv:1404.2601 [hep-th]].

[108] T. Banks, D. B. Kaplan and A. E. Nelson, Phys. Rev. D **49**, 779-787 (1994) doi:10.1103/PhysRevD.49.779 [arXiv:hep-ph/9308292 [hep-ph]].

[109] B. de Carlos, J. A. Casas, F. Quevedo and E. Roulet, Phys. Lett. B **318**, 447-456 (1993) doi:10.1016/0370-2693(93)91538-X [arXiv:hep-ph/9308325 [hep-ph]].

[110] G. D. Coughlan, W. Fischler, E. W. Kolb, S. Raby and G. G. Ross, Phys. Lett. B **131**, 59-64 (1983) doi:10.1016/0370-2693(83)91091-2

[111] T. Banks, M. Berkooz and P. J. Steinhardt, Phys. Rev. D **52**, 705-716 (1995) doi:10.1103/PhysRevD.52.705 [arXiv:hep-th/9501053 [hep-th]].

[112] T. Banks, M. Berkooz, S. H. Shenker, G. W. Moore and P. J. Steinhardt, Phys. Rev. D **52**, 3548-3562 (1995) doi:10.1103/PhysRevD.52.3548 [arXiv:hep-th/9503114 [hep-th]].

[113] A. L. Erickcek and K. Sigurdson, Phys. Rev. D **84**, 083503 (2011) doi:10.1103/PhysRevD.84.083503 [arXiv:1106.0536 [astro-ph.CO]].

[114] J. Fan, O. Özsoy and S. Watson, Phys. Rev. D **90**, no.4, 043536 (2014) doi:10.1103/PhysRevD.90.043536 [arXiv:1405.7373 [hep-ph]].

[115] A. L. Erickcek, K. Sinha and S. Watson, Phys. Rev. D **94**, no.6, 063502 (2016) doi:10.1103/PhysRevD.94.063502 [arXiv:1510.04291 [hep-ph]].

[116] R. Easther, R. Galvez, O. Ozsoy and S. Watson, Phys. Rev. D **89**, no.2, 023522 (2014) doi:10.1103/PhysRevD.89.023522 [arXiv:1307.2453 [hep-ph]].

[117] J. Georg, G. Şengör and S. Watson, Phys. Rev. D **93**, no.12, 123523 (2016) doi:10.1103/PhysRevD.93.123523 [arXiv:1603.00023 [hep-ph]].

[118] J. Georg and S. Watson, JHEP **09**, 138 (2017) doi:10.1007/JHEP09(2017)138 [arXiv:1703.04825 [astro-ph.CO]].

[119] L. Kofman, A. D. Linde, X. Liu, A. Maloney, L. McAllister and E. Silverstein, JHEP **05**, 030 (2004) doi:10.1088/1126-6708/2004/05/030 [arXiv:hep-th/0403001 [hep-th]].

[120] S. Watson, Phys. Rev. D **70**, 066005 (2004) doi:10.1103/PhysRevD.70.066005 [arXiv:hep-th/0404177 [hep-th]].

[121] B. Greene, S. Judes, J. Levin, S. Watson and A. Weltman, JHEP **07**, 060 (2007) doi:10.1088/1126-6708/2007/07/060 [arXiv:hep-th/0702220 [hep-th]].

[122] S. Cremonini and S. Watson, Phys. Rev. D **73**, 086007 (2006) doi:10.1103/PhysRevD.73.086007 [arXiv:hep-th/0601082 [hep-th]].

[123] S. Kachru, R. Kallosh, A. D. Linde and S. P. Trivedi, Phys. Rev. D **68**, 046005 (2003) doi:10.1103/PhysRevD.68.046005 [arXiv:hep-th/0301240 [hep-th]].

[124] J. P. Conlon, F. Quevedo and K. Suruliz, JHEP **08**, 007 (2005) doi:10.1088/1126-6708/2005/08/007 [arXiv:hep-th/0505076 [hep-th]].

[125] B. S. Acharya, K. Bobkov, G. L. Kane, J. Shao and P. Kumar, Phys. Rev. D **78**, 065038 (2008) doi:10.1103/PhysRevD.78.065038 [arXiv:0801.0478 [hep-ph]].

[126] J. T. Deskins, J. T. Giblin and R. R. Caldwell, Phys. Rev. D **88**, no.6, 063530 (2013) doi:10.1103/PhysRevD.88.063530 [arXiv:1305.7226 [astro-ph.CO]].

[127] P. Adshead, J. T. Giblin, T. R. Scully and E. I. Sfakianakis, JCAP **12**, 034 (2015) doi:10.1088/1475-7516/2015/12/034 [arXiv:1502.06506 [astro-ph.CO]].

[128] P. Adshead, J. T. Giblin, T. R. Scully and E. I. Sfakianakis, JCAP **10**, 039 (2016) doi:10.1088/1475-7516/2016/10/039 [arXiv:1606.08474 [astro-ph.CO]].

[129] D. Green and T. Kobayashi, JCAP **03**, 010 (2016) doi:10.1088/1475-7516/2016/03/010 [arXiv:1511.08793 [astro-ph.CO]].

[130] O. Özsoy, J. T. Giblin, E. Nesbit, G. Şengör and S. Watson, Phys. Rev. D **96**, no.12, 123524 (2017) doi:10.1103/PhysRevD.96.123524 [arXiv:1701.01455 [hep-th]].

[131] L. Iliesiu, D. J. E. Marsh, K. Moodley and S. Watson, Phys. Rev. D **89**, no.10, 103513 (2014) doi:10.1103/PhysRevD.89.103513 [arXiv:1312.3636 [astro-ph.CO]].

[132] V. Demozzi, V. Mukhanov and H. Rubinstein, JCAP **08**, 025 (2009) doi:10.1088/1475-7516/2009/08/025 [arXiv:0907.1030 [astro-ph.CO]].

[133] N. Shuhmaher, JHEP **12**, 094 (2008) doi:10.1088/1126-6708/2008/12/094 [arXiv:hep-ph/0703319 [hep-ph]].

[134] N. Shuhmaher and R. Brandenberger, Phys. Rev. D **73**, 043519 (2006) doi:10.1103/PhysRevD.73.043519 [arXiv:hep-th/0507103 [hep-th]].

[135] T. Banks and M. Dine, Phys. Rev. D **50**, 7454-7466 (1994) doi:10.1103/PhysRevD.50.7454 [arXiv:hep-th/9406132 [hep-th]].

[136] M. Del Zotto, J. J. Heckman, P. Kumar, A. Malekian and B. Wecht, Phys. Rev. D **95**, no.1, 016007 (2017) doi:10.1103/PhysRevD.95.016007 [arXiv:1608.06635 [hep-ph]].

[137] V. F. Mukhanov, Int. J. Theor. Phys. **43**, 623-668 (2004) doi:10.1023/B:IJTP.0000048168.90282.db [arXiv:astro-ph/0303072 [astro-ph]].

[138] X. Li, N. Weaverdyck, S. Adhikari, D. Huterer, J. Muir and H. Y. Wu, Astrophys. J. **862**, no.2, 137 (2018) doi:10.3847/1538-4357/aacaf7 [arXiv:1806.02515 [astro-ph.CO]].

[139] R. Hounsell, et al., Astrophys. J. **867** (2018) doi:10.3847/1538-4357/aac08b [https://arxiv.org/abs/1702.01747]].

[140] A. Aghamousa *et al.* [DESI], [arXiv:1611.00036 [astro-ph.IM]].

[141] `https://github.com/lanl/EGG`

[142] K. Heitmann, M. White, C. Wagner, S. Habib and D. Higdon, Astrophys. J. **715**, 104 (2010) doi:10.1088/0004-637X/715/1/104 [arXiv:0812.1052 [astro-ph]].

[143] K. Heitmann, D. Higdon, M. White, S. Habib, B. J. Williams and C. Wagner, Astrophys. J. **705**, 156 (2009) doi:10.1088/0004-637X/705/1/156 [arXiv:0902.0429 [astro-ph.CO]].

[144] `https://pythonhosted.org/pyDOE/randomized.html#latin-hypercube`

[145] `https://iminuit.readthedocs.io/en/stable/`

EVA NESBIT

Syracuse University Department of Physics
ehnesbit@syr.edu

EDUCATION

Syracuse University *August 2016 - July 2021 (expected)*
PhD Candidate, Department of Physics Thesis Topic: Effective Computational Cosmology

Kenyon College *August 2012 - May 2016*
B.A. Major: Physics with Scientific Computing Concentration

PROFESSIONAL EXPERIENCE

Volunteer in Research and Development September 2019 - Present
Museum of Science and Technology

· Helped in the design, development, and execution of an engineering camp for middle school aged children at the local science museum.

Graduate Teaching Assistantship August 2016 - May 2019
Syracuse University

· Served as the lab instructor for multiple sections of both introductory physics labs.

Director of Girls' Science Saturdays May 2014 - May 2016
Kenyon College

· Served as the director of a science outreach program designated for middle school-aged girls in the central Ohio area. Oversaw two programs a year. This role entailed designing programs and lesson plans, organizing and ordering materials, and training staff.

Physics Homework Grader August 2013 - May 2016
Kenyon College

· Served as the primary grader for introductory physics courses over numerous semesters.

AWARDS AND HONORS

Recipient of Syracuse University Graduate Fellowship September 2020 - May 2021
Syracuse University

· The most prestigious graduate student fellowship at Syracuse, awarded to those with exceeding competence and dedication to their research.

Recipient of Syracuse Summer Dissertation Fellowship May 2020 - August 2020
Syracuse University

· This is awarded to a select group of outstanding doctoral students to facilitate progress towards completion of the dissertation.

Recipient of REDF Graduate Fellowship August 2019 - May 2020
Syracuse University

· The Research Excellence Doctoral Funding (REDF) fellowship is awarded to those who have exhibited promise and excellence in their area of research based on publications as well as recommendations by their advisor and department.

Recipient of Department of Physics Award for Outstanding Teaching June 2017
Syracuse University

· I received this award after my first year teaching based upon student reviews of courses I taught and consultations with instructors.

High Honors in Physics August 2015 - May 2016
Kenyon College

· A continuation of work done over the summer; employed lattice-evolution software to evolve nonlinear equations of motion over an expanding background, simulating the evolution of the Universe. This work is used to study physics beyond the standard model, specifically, effective field theories.

NSF Graduate Research Fellowship Honorable Mention April 2016
Kenyon College

· I was awarded this distinction for the research I completed for my honors thesis on the Effective Field Theory of Reheating during my senior year of undergrad.

NSF Summer Science Scholar Summer 2015
Kenyon College

· Studied non-canonical cosmology; A set of coupled nonlinear equations of motion derived from the implementation of nonlinear terms to the Lagrangian (comprising an effective field theory) was implemented onto lattice-evolution software and subsequently investigated.

APPOINTMENTS AND PRESENTATIONS

Participant at ACT Data School April 2021
University of Toronto

· Participated in the data school, held remotely. I learned how to analyze CMB and ACT data using computational tools like Docker, Anaconda, and Jupyter Notebooks.

Participant at KITP-UCSB Inflation 2020 Conference March 2020
Kavali Institute for Theoretical Physics

· Participated in a conference held at the Kavali Institute for Theoretical Physics at UC Santa Barbara, "From Inflation to the Hot Big Bang." Attended lectures and discussions groups.

Research Assistantship June 2019 - August 2019
Syracuse University

· Focused on the study dark energy phenomenology and theory as it relates to and constrains observational data. Additionally, I study oscillon formation in the early universe via string cosmology models. My work on both of these projects allowed me to become a more self-directed researcher and developed my ability to problem-solve and employ creative solutions.

Nonlinear Physics at the End of Inflation August 2016
University of Michigan

· Gave a poster presentation at the COSMO 2016 conference held at University of Michigan. The poster reviewed my Senior Honors work in computational cosmology and early universe dynamics.

An Effective Field Theory Approach to Reheating August 2015
MIT

· Gave a talk at the Kenyon-MIT-Dartmouth Undergraduate Cosmology Research Conference on the beginnings of my Senior Honors work. This focused on numerical solutions to non-cononical models for reheating the universe (populating it with the first matter particles).

Gravitational Waves from Reheating August 2014
MIT

· Gave a talk at the Kenyon-MIT-Dartmouth Undergraduate Cosmology Research Conference on the work I completed over the summer. This focused on the study of gravitational wave production from a two-minima model of inflation with a time-dependent tunneling rate using code that evolves scalar fields over an expanding background.

Summer Science Scholar Summer 2014
Kenyon College

· Used lattice evolution software to study the production of gravitational waves via a first order phase transition that ends inflation. A time-dependent tunneling rate is added to the theory of old inflation in order to facilitate the phase transition. Results from this research are used to put constraints on observational endeavors at observatories like LIGO, etc.

PUBLICATIONS

· O.Özsoy, J. T. Giblin, E. Nesbit, G. Şengör and S. Watson, "Toward an Effective Field Theory Approach to Reheating," Phys. Rev. D **96**, no. 12, 123524 (January 2017).

· J. T. Giblin, G. Kane, E. Nesbit, S. Watson, Y. Zhao, "Was the Universe Actually Radiation Dominated Prior to Nucleosynthesis?" Phys. Rev. D. **96**, no. 4, 043525 (June 2017).

· E. Nesbit, J. T. Giblin, S. Watson, "Resonance and Oscillon Formation in Fibre Inflation Models" (To Appear).

· D. Huterer, Y. Wen, E. Nesbit, S. Watson, "Observational Constraints on the Effective Field Theory of Dark Energy" (To Appear).